Role of cGMP Phosphodiesterases in Idiopathic Pulmonary Fibrosis

Inaugural Dissertation
submitted to the
Faculty of Medicine
in partial fulfillment of the requirements
for the PhD-Degree
of the Faculties of Veterinary Medicine and Medicine
of the Justus Liebig University Giessen

by
Nikolova, Sevdalina Vaskova
of
Varna, Bulgaria

Giessen 2009

From the Department of Medicine
Director / Chairman: Prof. Dr. Werner Seeger
of Medicine of the Justus Liebig University Giessen

First Supervisor and Committee Member: Prof. Dr. Ralph Schermuly

Second Supervisor and Committee Member: Priv.-Doz. Dr. Stephan Rosenkranz

Committee members: Prof. Dr. Ernst Petzinger and Prof. Dr. Susanne Rohrbach

Date of Doctoral Defense: 16th of March 2009

Table of content

Table of content I
List of figures IV
List of tables V
List of abbreviations VI
Summary X
Zusammenfassung XI
I. Introduction 1
1. Idiopathic pulmonary fibrosis (IPF). 2
1.1. Classification. 3
1.2. Definition. 4
1.3. Histopathology. 4
1.4. Pathogenesis. 5
1.5. Role of AECs in IPF pathogenesis. 10
1.5.1. Morphological characteristics of the alveolar epithelium. 10
1.5.2. ATII cells: stem cells of the alveolar epithelium. 10
1.5.3. ATII cells and alveolar re-epithealization. 12
1.5.4. Growth factor control of ATII cell proliferation. 13
1.6. Diagnosis and evaluation. 14
1.6.1. Clinical presentation. 14
1.6.2. Diagnosis. 14
1.7. Treatment. 15
1.7.1. Phosphodiesterase (PDE) inhibitors. 15
2. PDEs. 15
2.1. Cyclic nucleotide specificity. 16
2.2. cGMP. 17
2.3. cGMP PDEs. 19
2.4. cGMP PDEs in the lung. 21
2.5. PDE6. 21
2.5.1. Phototransduction. 22
2.5.2. The PDE6D subunit. 24
II. Aims of the study. 25

III. Materials and Methods. ····· 27
3.1. Materials. ····· 28
3.1.1. Instruments, consumables, chemicals and enzymes. ····· 28
3.1.2. Cloning reagents. ····· 31
3.1.3. Cell culture materials. ····· 32
3.1.4. Antibodies, blocking peptides and siRNA targeting sequences. ····· 33
3.1.5. Kits. ····· 34
3.1.6. Buffers and solutions. ····· 34
3.2. Methods. ····· 36
3.2.1. Human lung tissue. ····· 36
3.2.2. RNA isolation. ····· 36
3.2.3. cDNA synthesis. ····· 37
3.2.4. PCR. ····· 38
3.2.5. RT-PCR. ····· 38
3.2.6. Agarose gel electrophoresis and PCR product purification. ····· 39
3.2.7. Western blotting. ····· 40
3.2.8. Densitometry. ····· 41
3.2.9. Immunohistochemical staining. ····· 41
3.2.10. Cloning. ····· 42
3.2.10.1. PCR amplification of complete gene sequence. ····· 42
3.2.10.2. Generating ‘A-tailing’ to blunt-ended PCR fragments. ····· 43
3.2.10.3. Ligation of A-tailed DNA Fragment into PGEMT-easy vector. ····· 44
3.2.10.4. Heat shock transformation. ····· 44
3.2.10.5. pGEMT easy recombinant clone selection. ····· 45
3.2.10.6. Small scale plasmid DNA purification. ····· 45
3.2.10.7. Directional TOPO cloning in pcDNA 3.1 vector. ····· 45
3.2.10.8. TOPO cloning reaction. ····· 46
3.2.10.9. pcDNA 3.1 clone analysis. ····· 46
3.2.10.10. Large scale endotoxin free plasmid extraction. ····· 46
3.2.10.11. Glycerol stock. ····· 47
3.2.11. siRNA ····· 47
3.2.12. Cell culture. ····· 47
3.2.12.1. Cryopreservation and thawing of cell cultures. ····· 48
3.2.13. Transient transfection. ····· 49

3.2.13.1. Transient transfection efficiency assessment. ····· 49
3.2.14. Measurement of cell proliferation. ····· 49
3.2.14.1. MTT cell proliferation assays. ····· 50
3.2.14.2. (^{3}H)-Thymidine incorporation assay. ····· 50
3.2.15. Statistical analysis. ····· 50
IV. Results. ····· 51
4.1. mRNA expression profile of cGMP PDEs in IPF lungs. ····· 52
4.2. mRNA detection of the PDE6 enzyme subunits in lung tissue samples of donors and IPF patients. ····· 54
4.3. Protein expression of the PDE6 enzyme subunits in lung tissue samples of donors and IPF patients. ····· 56
4.4. Cellular localization of the PDE6 enzyme subunits in lung tissue samples of donors and IPF patients. ····· 57
4.5. The PDE6 enzyme subunits are expressed in human ATII cells. ····· 58
4.6. Effects of PDE6D modulations on A549 cell proliferation. ····· 60
4.7. PDE6D knockdown inhibits ERK phosphorylation. ····· 62
V. Discussion ····· 64
5.1. mRNA profile of cGMP PDEs in lung tissue samples of donors and IPF patients. ····· 65
5.2. Detection of PDE6 enzyme subunits in lung tissue samples of donors and IPF patients. ····· 65
5.3. PDE6 enzyme subunits expression in human AECs. ····· 66
5.4. Functionality of PDE6. ····· 67
5.5. Individual functional capacity of PDE6D. ····· 68
5.6. Summary points. ····· 69
5.7. Future issues. ····· 70
VI. Appendix ····· 79
VII. Declaration ····· 87
VIII. Curriculum vitae ····· 89
IX. Acknowledgements ····· 95
X. References ····· 98

List of figures

Figure 1. Histopathology of IPF. ····· 4
Figure 2. Hypothetical models of IPF pathogenesis..····· 9
Figure 3. Progenitor cells of the alveolar epithelium. ····· 12
Figure 4. Representative model of the alveolar epithelial repair process.····· 12
Figure 5. HRCT abnormalities in IPF. ····· 15
Figure 6. Chemical basis of PDE enzymatic activity. ····· 16
Figure 7. cGMP metabolism. ····· 18
Figure 8. Schematic representation of catalytic and GAF domains arrangement in cGMP PDEs. ····· 20
Figure 9. Schematic subunit composition and structure of rod and cone PDE6 enzymes. ····· 22
Figure 10. Vertabrate visual phototransduction cascade. ····· 23
Figure 11. mRNA profile of cGMP PDEs in lung tissue samples of donors and IPF patients. ····· 53
Figure 12. PDE6 mRNA detection in lung tissues from donors and IPF patients. · 55
Figure 13. PDE6 immunoreactivity in lung tissues from donors and IPF patients.· 57
Figure 14. Immunohistochemical localization of PDE6 in lung sections from donors and IPF patients.····· 58
Figure 15. The PDE6 enzyme subunits are expressed in human ATII cells. ····· 59
Figure 16. Knockdown of endogenous PDE6D expression decelerates the proliferation rate of human A549 AECs. ····· 61
Figure 17. Overexpression of PDE6D accelerates the proliferation rate of human A549 AECs. ····· 62
Figure 18. PDE6D siRNA knockdown inhibits serum stimulated ERK phosphoprylation. ····· 63
Figure 19. Schematic presentation of the major strategies used to purify rod PDE6 and cone PDE6 enzymes from retina. ····· 71
Figure A1. pGEM-T vector circle map and sequence reference points.····· 85
Figure A2. Structure of pcDNA3.1/V5-His-TOPO expression vector and sequence reference points. ····· 86
Figure A3. Principle of directional TOPO cloning protocol. ····· 86

List of tables

Table I. Classification and contrasting histological features of IIPs. ····· 80
Table II. Properties of cyclic nucleotide PDE families. ····· 81
Table III. Gene specific primer sequences and RT-PCR conditions. ····· 83
Table IV. Primers used for cloning. ····· 84
Table V. Characteristics of IPF patients with UIP pattern. ····· 84
Table VI. Approaches for inducing pulmonary fibrosis in animal models. ····· 73
Table VII. Efficacy and selectivity of PDE inhibitors to inhibit purified, activated bovine rod and cone PDE6. ····· 74

List of abbreviations

AECs	alveolar-epithelial cells
AEC kit	3-Amino-9-ethyl carbazole
AIP	acute interstitial pneumonia
ANP	atrial natriuretic peptide
ATI	alveolar epithelial type I
ATII	alveolar epithelial type II
A U	arbitary units
BAL	bronchoalveolar lavage
BNP	B-type natriuretic peptide
BSA	Bovine serum albumin
cAMP	cyclic adenosine monophosphate
cDNA	Complementary deoxyribonucleic acid
CFA	cryptogenic fibrosing alveolitis
cGMP	cyclic guanosine monophosphate
CMV	cytomegalovirus
CNP	C-type natriuretic. peptide
COP	and cryptogenic organizing pneumonia
DIP	desquamative interstitial pneumonia
dNTP	Deoxynucleoside triphosphate
EBV	Epstein-Barr virus

ECL	Enhanced chemiluminescence
ECM	Extracellular matrix
EGF	Epidermal Growth Factor
EGF-R	Epidermal Growth Factor-Receptors
EGTA	Ethylene glycol-bis (2-amino-ethylether)-N,N,N',N', -tetraacetic-acid
EMSA	electrophoretic mobility shift assay
ET	endothelin
FasL	Fas ligand,
FBS	fetal bovine serum
FGF	fibroblast growth factor
GAPDH	glyseraldehyde-3-phosphate dehydrogenase
GC	guanylyl cyclase
GCAP	gyanylate cyclase activating protein
GDI	guanine nucleotide dissociation inhibitor
GM-CSF	Granulocyte macrophage-colony stimulating factor
GRK2	G-protein coupled receptor kinase 2
GTP	guanosine triphosphate
GVA	glycerol-vinyl-alcohol
HB-EGF	Heparin Binding-Epidermal Growth Factor
HBSS	Hanks' Buffered Salt Solution
HGF	Hepatocyte Growth Factor
HRCT	high-resolution computer tomography
HRP	Horseradish peroxidase

IFN	interferon
IIPs	idiopathic interstitial pneumonias
IL	interleukin
IPF	Idiopathic pulmonary fibrosis
IPTG	Isopropyl β-D-1-thiogalactopyranoside
KGF	Keratinocyte Growth Factor
LB	Luria Broth
LIP	lymphoid interstitial pneumonia
mRNA	messenger Ribonucleic Acid
MAPK	mitogen-activated ptotein kinase
MTT	3-[4,5-dimethylthiazol-2-yl]-2,5-diphenyl-tetrazolium bromide
NAC	N-acetyl cysteine
NEAA	non-essential amino acids
NO	nitric oxide
NSIP	non-specific interstitial pneumonia
PAA	polyacrylamide
PAGE	Polyacrylamide Gel Electrophoresis
PBS	phosphate-buffered saline solution
PBS	Phosphate buffered saline
PCR	polymerase chain reaction
PDE	phosphodiesterase
PDGF	platelet-derived growth factor
PGE	prostaglandin E
PKA	Protein kinase A

PKG	cGMP-dependent protein kinase G
proSP-C	pro-surfactant protein-C
PVDF	Ployvinylidene difluoride
RB-ILD	respiratory bronchiolitis-associated interstitial lung disease
rd	retinal degeneration
RNA	Ribonucleic acid
RT-PCR	Reverse Transcription-Polymerase Chain Reaction
SDS	Sodium Dodecyl Sulfate
SEM	Standard error of means
sGC	soluble guanylyl cyclase
TAE	Tris-Acetate EDTA
TBS	Tris-buffered saline
TE	Tris-EDTA
TGF	transforming growth factor
Th	T helper cells
TLB	transbronchial lung biopsy
TNF	tumor necrosis factor
UIP	usual interstitial pneumonia
VEGF	vascular endothelial growth factor

SUMMARY

Summary

Idiopathic Pulmonary Fibrosis (IPF) is a progressive interstitial lung disease of unknown etiology associated with high morbidity and mortality, and further characterized by abnormal alveolar epithelial and fibro-proliferative responses, excessive extra-cellular matrix deposition, patchy inflammatory infiltrations and progressive loss of normal lung structure. At present there is no demonstrably effective therapy for blocking or reversing the progression of the disease. This situation demands a better understanding of the molecular and cellular mechanisms involved in the pathogenesis of IPF.

Current evidence suggests a role of cyclic guanosine monophosphate phosphodiesterases (cGMP-PDEs) in the pathogenesis of various proliferative lung diseases, including IPF. Lung PDE6 expression and function has received little or no attention. The present study aimed to characterize (i) cGMP PDEs profile in IPF, (ii) PDE6 subunits expression in human lung, (iii) PDE6 subunits expression and alteration in IPF and (iv) functionality of the specific PDE6D subunit. The experiments were carried out with human lung samples from donors and IPF patients. RT-PCR analyses from donor and IPF human lungs revealed up-regulation of PDE1A, PDE10A and PDE11A in the IPF lungs and expression of PDE6 subunits mRNA transcripts in human lungs. Westernblot analysis showed 2-fold up-regulation of PDE6A and PDE6B, and 2-fold down-regulation of PDE6D and membrane localization of PDE6G in the IPF lungs as compared to the donor lungs. Immunohistochemical analysis showed alveolar epithelial localization of the PDE6 subunits. RT-PCR analysis from donor and IPF-derived human primary alveolar type (AT) II cells confirmed the cellular localization of the PDE6 subunits and the down-regulation pattern of PDE6D. Further, siRNA-mediated PDE6D knockdown and an ectopic PDE6D expression in A549 cells demonstrated the modulatory effects of PDE6D on alveolar epithelial cell (AEC) proliferation. Additionally, we showed that these effects specifically involve ERK phosphorylation. Collectively, we report (i) mRNA expression profile of cGMP PDEs in IPF, (ii) previously unrecognized PDE6 expression in human lungs, (iii) pronounced alterations of PDE6 subunits in IPF-derived lungs and (iv) characterize the functional role of PDE6D in AEC proliferation.

ZUSAMMENFASSUNG

Zusammenfassung

Die idiopathische pulmonale Fibrose (IPF) ist eine progressive interstitielle Lungenerkrankung unbekannter Ätiologie, assoziiert mit hoher Morbidität und Mortalität. IPF charakterisiert sich weiterhin durch abnormale epitheliale und fibro-proliferative Reaktionen, exzessive Ablagerung extrazellulärer Matrix, ungleichmäßige inflammatorische Infiltrate und einen progressiven Verlust der normalen Lungenstruktur. Gegenwärtig existiert keine nachweislich effektive Therapie zur Beeinflussung des Krankheitsverlaufs. Diese Tatsache unterstreicht die Notwendigkeit für ein besseres Verständnis der molekularen und zellulären Mechanismen, die in der Pathogenese der IPF involviert sind.

Neue Studien weisen auf eine Rolle der Phosphodiesterasen des zyklischen Guanosinmonophosphats (cGMP-PDEs) an der Pathogenese von unterschiedlichen Lungenerkrankungen, einschließlich IPF. Allerdings wurden die Expression und Funktion der Lungen-Phosphodiesterase 6 (PDE6) bisher wenig untersucht. Die vorliegende Studie hat sich Folgendes zum Ziel gesetzt: (i) die Charakterisierung der Expressionsprofile der cGMP-PDEs bei IPF in der Lunge, (iii) die Charakterisierung der Expression der PDE6-Untereinheiten in der Lunge, (iii) die Untersuchung der Expressen der PDE6-Untereinheiten bei IPF und (iv) charakterisierung der Funktion der PDE6D-Untereinheit.

Untersucht wurde Lungenmaterial von gesunden Probanden und IPF-Patienten. Durch RT-PCR wurde eine Hochregulation der Gen-Transkription von PDE1A, PDE10A und PDE11A in IPF-Proben sowie eine Basis-Transkription der PDE6-Untereinheiten nachgewiesen. Western-Blot-Experimente zeigten eine Hochregulation von PDE6A und PDE6B ums Zweifache und eine gleichstarke Abschwächung von PDE6D bei IPF im Vergleich zu gesunden Probanden. Darüber hinaus wurde eine Membranlokalisation der PDE6G bei IPF festgestellt. Die immunhistochemischen Untersuchungen zeigten die Lokalisation der PDE6-Untereiheiten im alveolaren Epithel. RT-PCR-Analysen von primären Typ II alveolaren Zellen (ATII) von Probanden und IPF-Patienten bestätigten die Anwesenheit der PDE6-Untereinheiten und die Herunterregulation von PDE6D bei IPF. Durch siRNA-Knockdown von PDE6D und ektopische Expression von PDE6D in der A549 Zellinie wurden die modulierenden Effekte dieser Untereinheit auf die Proliferation von alveolaren Epithelzellen (AEC) demonstriert. Es konnte auch

gezeigt werden, daß diese Effekte spezifisch die Phosphorylierung von ERK beeinflussen.

Zusammenfassend, wurden in dieser Arbeit (i) die Expressionsprofile der Phosphodiesterasen des zyklischen Guanosinmonophosphats (cGMP-PDEs) in IPF-Lungengewebe erstellt. (ii) eine bis dato nicht beschriebene Expression von PDE6 in der humanen Lunge konnte nachgewiesen werden. (iii) die Veränderung der PDE6-Espression in IPF-Lungenproben und (iv) die Rolle der PDE6D-Untereinheit bei der Proliferation von AEC wurden analysiert.

CHAPTER 1: INTRODUCTION

I. Introduction

1. IPF.

IPF, also known as cryptogenic fibrosing alveolitis (CFA) is a distinct subgroup of idiopathic interstitial pneumonias (IIPs). It is a terminal condition in most patients, characterized by aberrant scarring of the lung tissue and dramatic loss of respiratory function secondary to AEC damage, aberrant fibroblast accumulation, excessive collagen deposition, and matrix remodeling [1-3]. As the name implies IPF is a disease of unknown origin (from the Greek words "idio"- peculiar or unusual, "pathy"–illness, and “kryptos”-hidden). Significant numbers of factors, however, are reported to consistently increase the risk for IPF:

Occupational and environmental exposures: such as mineral dust (silica/silicates), metal dust (steel, brass, and lead), wood dust (specifically pine), stone or sand dust, farming, cattle or livestock handling and use of wood fires are considered substantial risk factors for IPF development [4-7].

Cigarette smoking: is identified as a potent risk factor with an odds ratio increasing with the pack/year of smoking [8, 9].

Asymptomatic gastroesophageal reflux: a small study produced evidence that asymptomatic gastroesophageal reflux occurs more frequently in patients with IPF than in patients with other interstitial lung diseases and thus deserves to be considered as a possible etiological feature of IPF [10].

Chemotherapeutic agents and radiation: are considered to induce high incidence of pulmonary complications, pulmonary fibrosis being one of them [11-14]

Infectious agents: a high incidence of Epstein-Barr virus (EBV) [15, 16], influenza [17-20], cytomegalovirus (CMV) [21], and hepatitis C [22, 23] infections is reported in patients with IPF. The etiologic relevance of these reports, however, remains elusive [24, 25].

Heredity factors: familial cases of IPF are reported as well and are considered to be inherited as an autosomal dominant trait with variable penetrances [26-29]. Several investigators have reported an association between IPF and α1 -antitrypsin inhibition (Pi) alleles present on chromosome 14 [30-32]. Thomas *et al.* have identified a mutation in the prosurfactant protein-C (proSPC) gene

(leucine→glutamine) in a kindred of patients with familial IPF, resulting in an improper proSP-C folding and processing in ATII cells [33]. A recent and intriguing report described polymorphisms of *hTERT* and *hTR* genes regulating telomere length in a cohort of patients with familial IPF. These genes have a pivotal role in controlling cell death and aging and therefore are of particular importance [34].

IPF is a devastating disease with a very poor prognosis and currently unavailable drug therapy. The average survival rate of IPF patients is approximately three to five years from the onset of the symptoms [35-37]. Some predominance in males is observed [5, 35]. Eventhough IPF is considered a disease of the elderly people; cases are reported in young children and infants as well [36-38]. Recent reports suggest that IPF is substantially more prevalent than previously considered [39-41]. The notably malignant pattern of IPF compared to the other subgroups of IIPs, demands a better understanding of what constitutes IPF.

1.1. Classification.

Hamman and Rich [42] are often credited for the first description of unexplained interstitial pneumonia in 1944. Nevertheless, it was Scadding and Hinson, in 1967, who actually defined IPF for what it is known today [43]. The growing body of information on IIPs was first systematized by Liebow and Carrington on the basis of specific histologic patterns [44]. Subsequently, the Liebow-Carrington classification scheme has undergone numerous revisions [43, 45-50]. The morphological spectrum of IPF in these revised classification schemes, however, still encompassed several histological patterns. There was a need IPF to be more narrowly defined as a distinct clinical entity. In 2002, an international consensus statement [51] has proposed the classification of IIPs into seven distinct subtypes: usual interstitial pneumonia (UIP), non-specific interstitial pneumonia (NSIP), respiratory bronchiolitis-associated interstitial lung disease (RB-ILD), desquamative interstitial pneumonia (DIP), acute interstitial pneumonia (AIP), lymphoid interstitial pneumonia (LIP) and cryptogenic organizing pneumonia (COP). The classification and the most contrasting histological features of the seven distinct IIPs categories are given in Table I (appendix).

1.2. Definition.

Of these IIPs entities, IPF is defined as a specific form of chronic fibrosing interstitial pneumonia, limited to the lung, and associated with the histopathological pattern of UIP on open or thoracoscopic surgical lung biopsy [51]. Henceforth, the two terms IPF and UIP are often used in an analogus manner.

1.3. Histopathology.

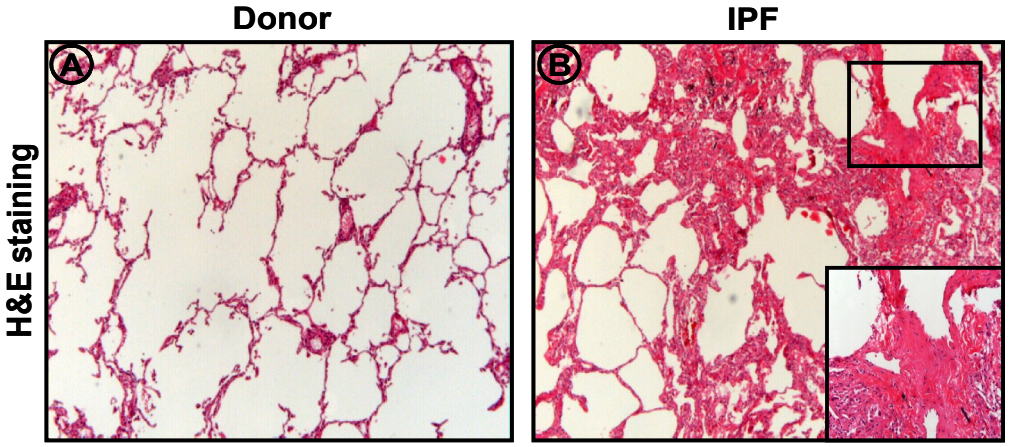

Figure 1. Histopathology of IPF.

a) Hematoxylin&Eosin (H&E) staining showing the normal lung structure in a donor subject, b) H&E staining showing the distorted lung structure in a IPF patient, magnification 50x. Author's slide.

The cardinal features of UIP are temporal heterogeneity, fibrosis with variable numbers of fibroblastic foci, honeycomb changing, interstitial inflammation and vascular remodeling [52]. These histopathologic changes affect mostly the peripheral subpleural parenchyma.

Heterogeneity: is the most striking histological feature of UIP. Areas of normal lung structure (lower left quadrant in Figure 1b) contrast with areas of extensive fibrosis honeycomb changes, interstitial inflammation and vascular remodeling (right quadrant in Figure 1b) [1].

Fibrosis: areas of active fibrosis are characterized by clusters of fibroblasts/ myofibroblasts observed at the border between fibrotic and normal lung, termed fibroblastic foci (square box, Figure 1b) [2]. Alveolar epithelial injury with hyperplastic type II pneumocytes is often seen in these areas [53]. The fibrotic

zone usually shows temporal heterogeneity with dense acellular collagen bundles ("old fibrosis") and scattered fibroblastic foci, signifying a progressive process.

Honeycomb changes: these are enlarged cystic airspaces, filled with mucin and lined by bronchiolar and bronchial epithelium type II pneumocytes and occasionally metaplastic squamous epithelium (Figure 5b) [54]. The honeycomb cysts are separated by thick walls, which contain collagen with varying degrees of inflammation. Smooth muscle cell hyperplasia is commonly seen in the zones of honeycombing [47].

Inflammation: the inflammatory component is typically mild to moderate, patchy and consists primary of lymphocytes, plasma cells, and macrophages. Other inflammatory cells such as neutrophils and eosinophils may be present at low abundance. The inflammation occurs mainly in areas of collagen deposition or honeycomb lesions, and rarely in otherwise unaltered alveolar septa [2].

Vascular remodeling: shows a heterogeneous pattern with both areas of vessel ablation and other areas of neovascularization. Vessel ablation is detected within the fibroblastic foci and in the areas of honeycombing [55-61].

It should be mentioned, however, that the histological features of UIP described above overlap with the histological features observed in asbestosis, chronic hypersensitivity pneumonitis and collagen vascular disorders [2]. Accumulating evidence suggests as well coexistence of UIP and other IIPs like NSIP and DIP in lung biopsies and lung explants from IPF patients [62-65].

1.4. Pathogenesis.

The exact mechanisms underlying the pathogenesis of IPF remain enigmatic. For the past three decades, a substantial body of research has been conducted in understanding the triggering mechanisms of fibrosis in IPF. From these attempts, three major hypotheses have emerged.

The inflammation hypothesis: is based on the idea that injury/inflammation precedes the fibrotic response in IPF (Figure 2a) [66, 67]. A support to this hypothesis was suggested by the presence of interstitial and alveolar inflammatory cells as well as the super-physiological expression of pro-inflammatory cytokines such as interleukin (IL)-1, transforming growth factor (TGF)-β and tumor necrosis factor (TNF)-α in the lungs of patients with IPF [66, 68]. In addition, immune

deviation towards a T-helper type 2 (Th 2) cytokine profile (IL-4, IL-5, IL-10, IL-13), favouring a fibroproliferative response has been shown to predominate in the lungs of patients with IPF [69, 70]. Along with that, Kolb *et al*. have demonstrated that at least in animal model inflammation induced by transient over-expression of IL-1β is followed by remodeling and fibrosis [71]. It has become evident, from multiple sources, however, that inflammation may not be a key feature in IPF [1]. Inflammatory cells and intra-alveolar macrophage accumulation do not depict the major histological findings in IPF. A mild-to-moderate alveolitis is found either in early or late disease stages [47]. Experimental models and some human diseases showed that inflammation is not required for the development of a fibrotic response [72-74]. Clinical measurements of inflammation markers, either cellular or acellular, either in blood or in bronchoalveolar lavage (BAL) fluid, fail to correlate with stage and/or outcome of the disease [75, 76]. And mostly, potent and long-term anti-inflammatory and/or immunosuppressive therapies do not improve disease outcome [1]. Henceforth, an alternative hypothesis has been advocated.

The abnormal wound healing hypothesis: is suggested by Selman *et al.* through an extensive study of the literature. It states that IPF represents a form of abnormal wound healing process in the lung and brings into focus the epithelial-mesenchymal interplay. According to this hypothesis repetitive episodes of acute lung injuries result in an AECs damage and activation. AECs secrete multiple cytokines and growth factors such as platelet-derived growth factor (PDGF), TNF-α, TGF-β, endothelin-1 that provoke fibroblast migration, proliferation, and transdifferentiation into myofibroblasts. The myofibroblasts in return induce: (i) epithelial cell apoptosis (Fas ligands); (ii) angiogenesis [vascular endothelial growth factor (VEGF), fibroblast growth factor (FGF)]; (iii) basement membrane disruption (gelatinases A and B). This signaling interplay results in excessive and disordered collagen matrix remodeling, impaired fibrinogenesis/ fibrinolysis, failure of re-epithelialization and culminates in aberrant remodeling of the lung parenchyma (Figure 2b) [3, 77].

The multiple hit hypothesis: is proposed in the literature most recently. It presents an attractive unified hypothesis, postulating that IPF develops as a consequence of abnormalities occurring in multiple biological pathways that affect both wound repair and inflammation (Figure 3c). This hypothesis is evidenced by oligonucleotide microarray data, showing an IPF-gene specific pattern,

characterized by up-regulation of genes indicative of ongoing both tissue remodeling and inflammatory processes: smooth muscle markers, extracellular matrix proteins, proinflammatory cytokines and antioxidants, and immunoglobulins [78]. In line, a recent multicenter high-resolution computer tomography (HRCT) study revealed that architecture distortion (lower-lung honeycombing, upper-lung irregular lines) and inflammation (significant mediastinal adenopathy) are the most prominent radiological abnormalities in IPF [79]. The speculated redundancy in IPF aetiology (aforementioned) is of further support to this notion.

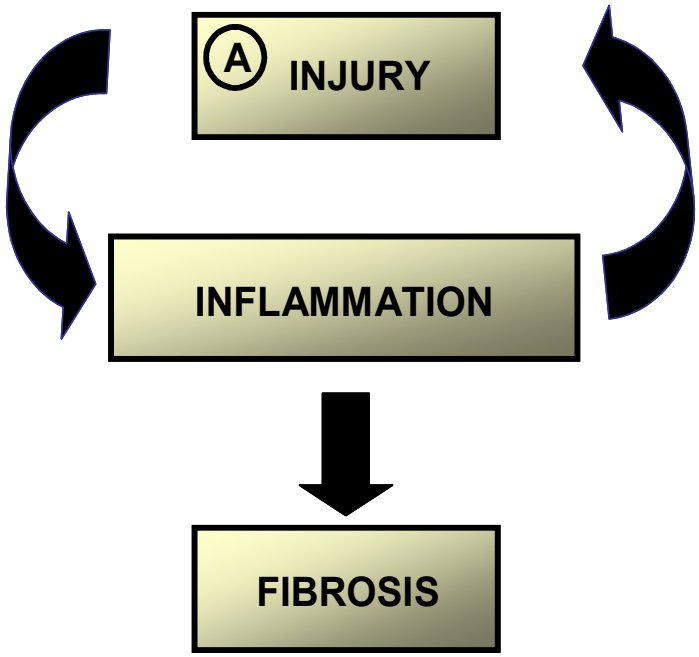

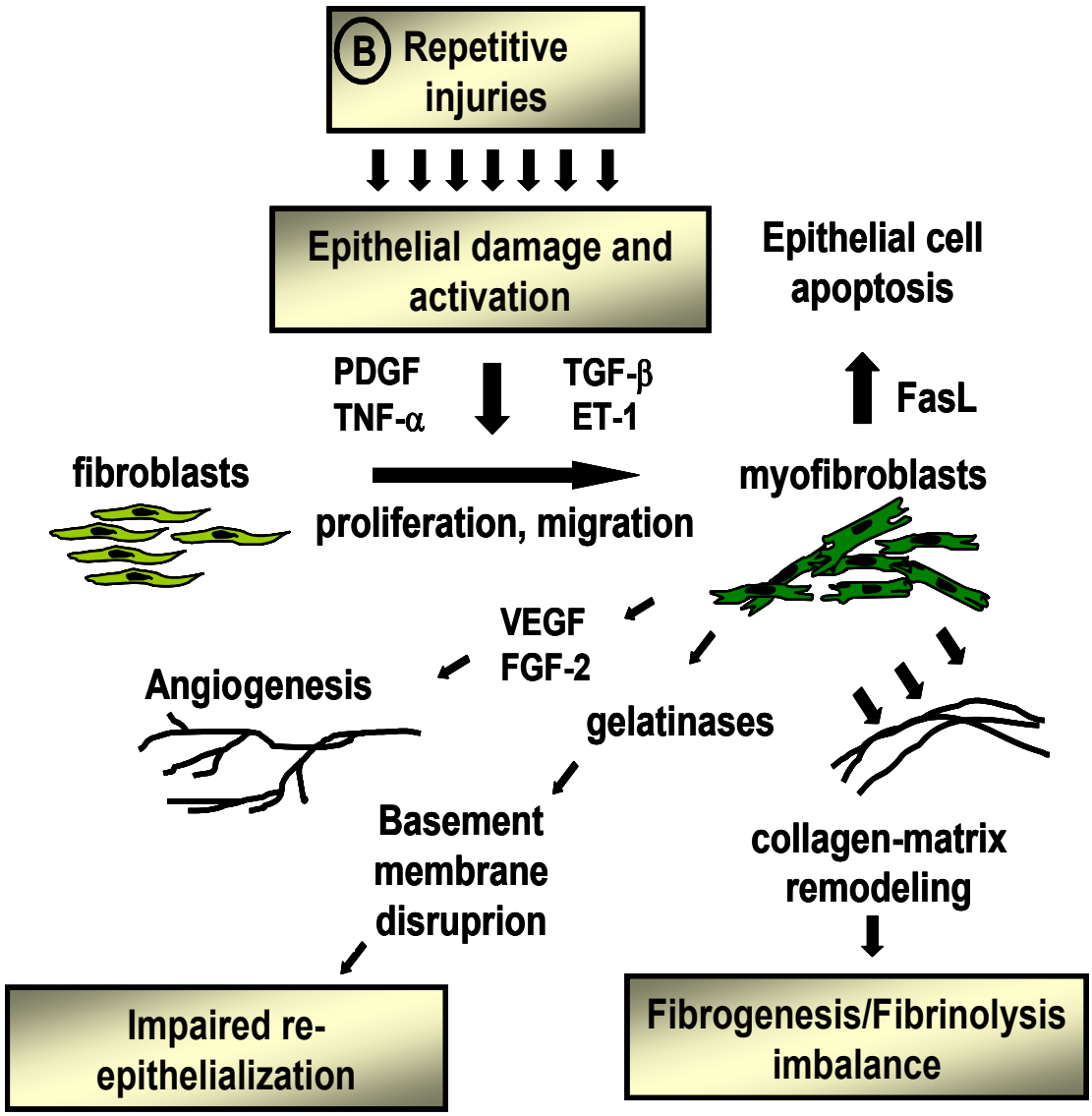
B Repetitive injuries
Epithelial damage and activation
Epithelial cell apoptosis
PDGF
TNF-α
TGF-β
ET-1
FasL
fibroblasts
proliferation, migration
myofibroblasts
VEGF
FGF-2
Angiogenesis
gelatinases
Basement membrane disruprion
collagen-matrix remodeling
Impaired re-epithelialization
Fibrogenesis/Fibrinolysis imbalance

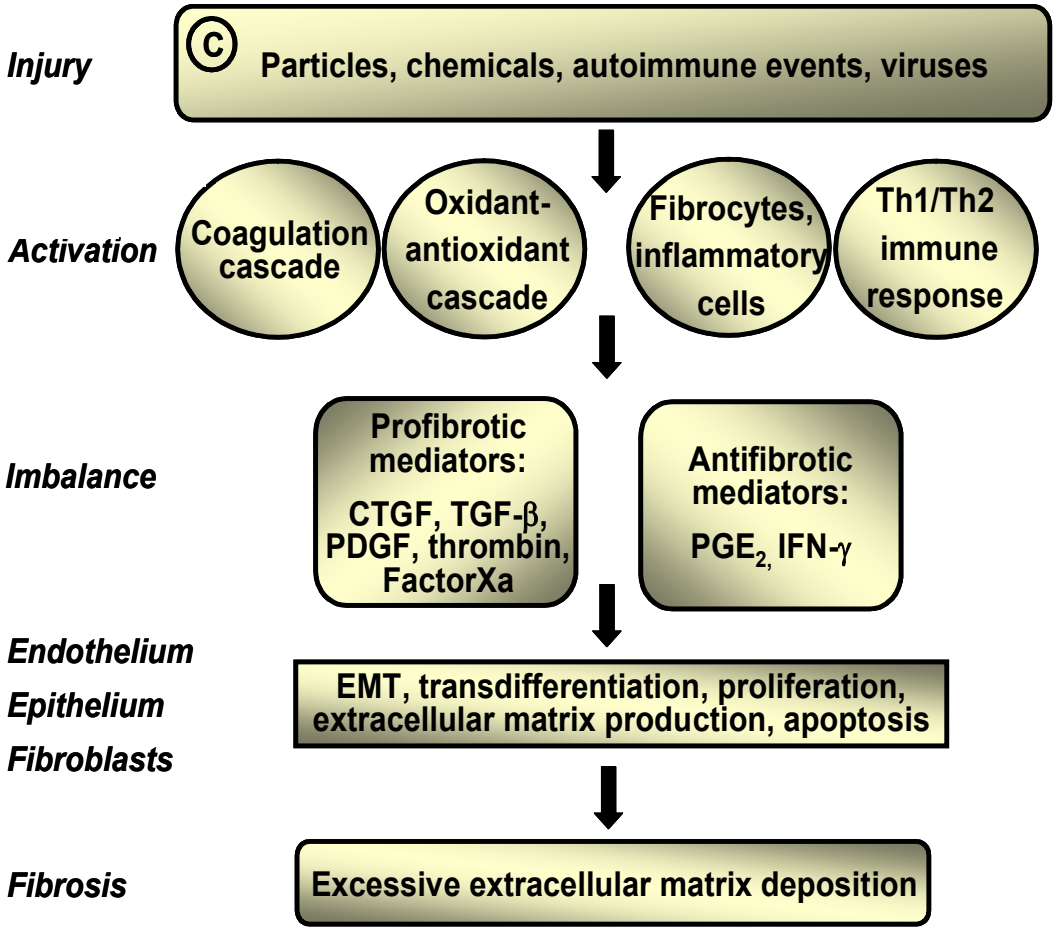

Figure 2. Hypothetical models of IPF pathogenesis.

a) Inflammation hypothesis, b) Aberrant wound healing hypothesis, c) Multiple hit hypothesis, *PDGF* platelet-derived growth factor, *TNF-α* tumor necrosis factor- α, *TGF-β* transforming growth factor -β, *ET-1* endothelin-1, *FasL* Fas ligand, *VEGF* vascular endothelial growth factor, *FGF-2* fibroblast growth factor, *CTGF* connective tissue growth factor, *Th1/2* T helper cells 1/2, PGE_2 prostaglandin E2, *IFN-γ* interferon-γ, summarized from [3, 80, 81]. The figure is author's design.

1.5. Role of AECs in IPF pathogenesis.

Several lines of evidence suggest the role of AECs in the pathogenesis of IPF. Namely, upon injury (associated with fibrosis) AECs display (i) marked ultrastructural alterations: hyperthrophy and hyperplasia, aberrant cuboidalization, occurance of intermediate cells (ii) marked phenotypic alterations: expression of cytokeratin epitopes usually not present in the alveolar epithelium [82], altered cytoskeletal dynamics, altered morphoregulatory proten expression (adhesion molecules) [83], enhanced secretion of proteases, cytokines and soluble factors etc., (iii) redundant physiological processes: proliferation [84, 85], bronchiolar and squamous metaplasia, [86-88], apoptosis [89-91] and mesenchymal transdifferentiation [92, 93].

1.5.1. Morphological characteristics of the alveolar epithelium.

The alveolar epithelium is composed of two morphologically distinct cell types, ATI and ATII cells. ATI cells are large flattened cells that cover 95% of the lungs' surface area [94], form the barrier to gas exchange and regulate lung liquid homeostasis [95, 96]. ATII cells cover the remaining 5% of the lungs' surface area. These are cuboidal cells with rounded nuclei and short microvilli along their apical surface. ATII cells have numerous cytoplasmic organelles, including lamellar bodies. ATII cells reside in alveolar corners and have many functions [97]. They produce, secrete and reuptake surfactant proteins [98-102], transport electrolytes from the apical surface into the interstitium [103, 104], synthesize components of the basement membrane [105], and contribute to the lung innate immune response [106-111].

1.5.2. ATII cells: stem cells of the alveolar epithelium.

However, the most remarkable feature of ATII cells is their ability to proliferate and differentiate (stem cells characteristics). It is generally accepted that a putative subpopulation of ATII cells, hyperplasic ATII cells, give rise to both ATII cells by division and ATI cells by transdifferentiation during normal lung growth and repair following lung injury [112-115]. The transdifferentiation of ATII cells into ATI cells is proposed to progress through an intermediate cell type that exhibits both ATII specific and ATI-specific characteristics. Reports show that this transition may be

influenced by soluble factors and the extracellular matrix [116] and may be partially reversible [117-119].

The turnover time of ATII cells under normal and pathological conditions is significantly different. The turnover time of ATII cells in normal lung is reported to elapse between 2-3 weeks [120, 121]. The proliferation kinetics of ATII cells upon injury, however, is drastically accelerated. The study of Kauffman SL has demonstrated that in urethane-injured adult mice the duration of a complete ATII cell cycle is 22 hours [122]. Evans *et al.* have shown that in NO_2-injured rats the completeion of ATII cell cycle takes 2-3 days [123].

Bone marrow and nonciliated bronchiolar epithelial cells are also considered stem cells of the alveolar epithelium [124, 125]. The plasticity of ATI cells is still speculative. Despite of the presumption that ATI cells are terminally differentiated cells [113]. Reports suggest self repair features of ATI cells [126] and capability to transdifferentiate into ATII cells as well [127]. Figure 3 depicts the role of ATII, ATI, bone marrow and airway cells in repopulating the lung alveolar epithelium.

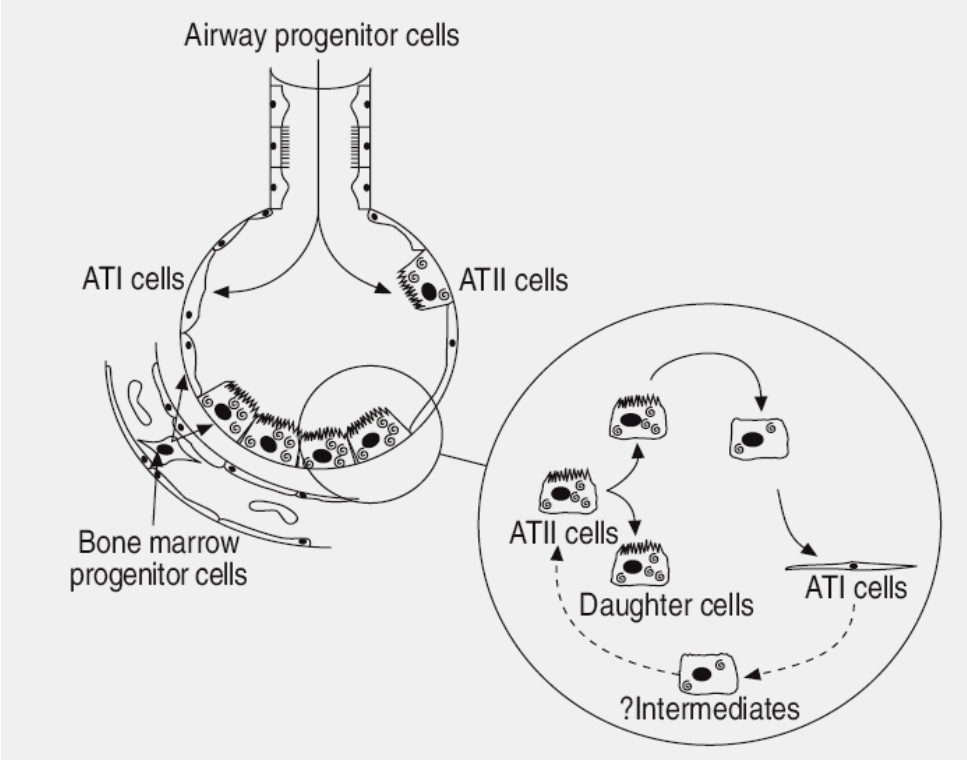

Figure 3. Progenitor cells of the alveolar epithelium.

ATII cells are pointed out in the above picture as the major proliferative cells of the alveolar epithelium, capable of (trans)differentiation. The plasticiity of ATI cells, bone marrow and airway epithelial cells are also depicted in this cartoon, adapted from [128].

1.5.3. ATII cells and alveolar re-epithealization.

ATII cells proliferation is an essential step in the normal alveolar re-epithealization process. Upon injury, the highly vulnerable ATI cells (cell morphology) are primary damaged (necrosis/apoptosis). This “drop out” of ATI cells results in denudation of the basement membrane. The repopulation of the denuded basement membrane comprises the following sequence of events: (i) proliferation of ATII cells; (ii) migration of the ATII cells along the surface of the alveolar epithelial basement membrane; and (iii) differentiation of ATII cells (hyperplastic subpopulation) into ATI cells (Figure 4)

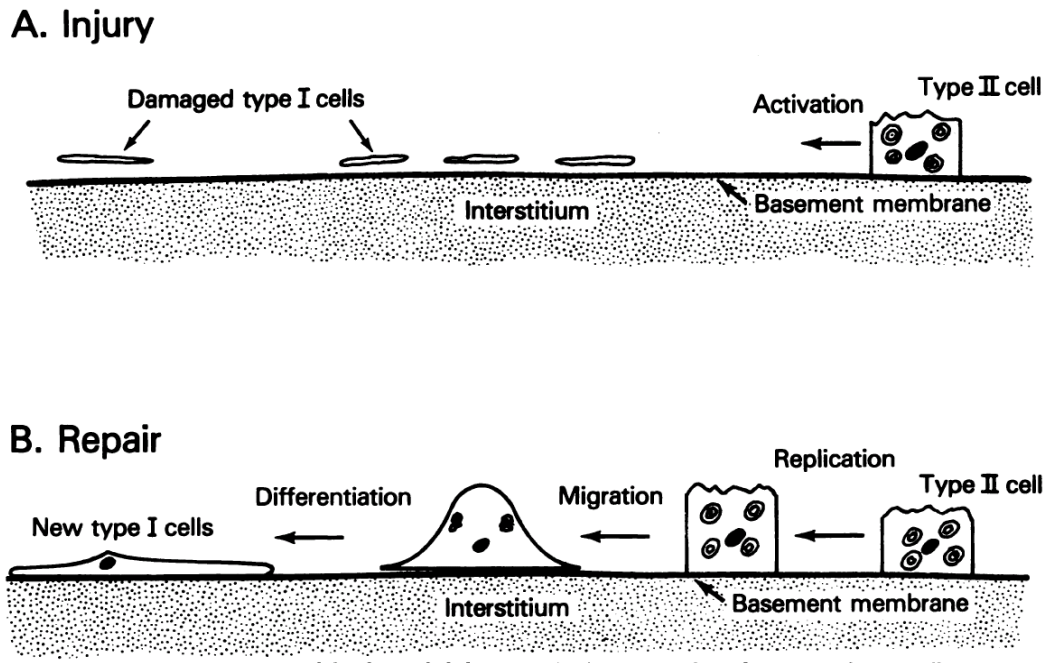

Figure 4. Representative model of the alveolar epithelial repair process.

a) Upon injury ATI cells show detached flat processes and blebbing as a typical feature of denudation, b) In response the activated ATII cells proliferate, migrate

across the basement membrane, and differentiate into ATI cells, repopulating the alveolar epithelium, adapted from [129].

In IPF, the ability of ATII cells to carry out proliferation, migration and differentiation appears seriously compromised [130]. At a comprehensive look the proliferative phenotype of AECs in IPF appears to be significantly heterogeneous. Higher rates of AEC proliferation have been observed at the broncho-alveolar junction in IPF lungs [86]. Multiple studies have reported rapid proliferation of ATII cells following injury [131-134]. Conversely, reduced proliferative capacity of ATII cells and/or the inability to differentiate into ATI cells have also been reported in IPF [130] and in explant lung models of fibrosis [72].

1.5.4. Growth factor control of ATII cell proliferation.

ATII cells proliferation appears to be highly regulable. Various growth factors and cytokines have been found to influence the proliferative phenotype of ATII cell. Some of these regulatory signals have paracrine and autocrine mechanism of action. Some exirt effects in a juxtacrine fashion and many are bound to the extracellular matrix and potentially available without the need for any local production. Growth factors known to stimulate ATII cell proliferation are FGF, hepatocyte growth factor (HGF) and epidermal growth factor (EGF). KGF, a member of the FGF family, also known as FGF-7, has been shown to be a potent mitogen of ATII cells *in vivo* [135-137]. HGF has been reported to have mitogenic and fibrinolytic activities [138]. KGF and HGF are paracrine growth factors. Their expression is confined to the mesenchyme, whereas their receptor expression is confined to the epithelium [139, 140]. The EGF family of growth factors acts via autocrine and juxtacrine pathways. EGF ligands (EGF, TGFα, HB-EGF, etc.) bind several subtypes of EGF-R, erbB1 (HER1), erbB2 (HER2), erbB3 and/or erbB4. Both the ligands and the receptors are expressed at the cell surface of pulmonary epithelial cell [141-143]. Activated EGF receptors induce mitogenic and morphogenic cellular responses, which are crucial in the airway and alveoli epithelial repair process [144-146]. Conversely, growth factors known to inhibit ATII cell proliferation are TGF-β, parathyroid hormone-like growth factor and components of the IGF system. TGF-β can completely inhibit the stimulating effect of KGF *in vitro* [147]. Increased expression of IGFBP-2, type-2 IGF receptor and

IGF-II, is associated with ATII cell growth arrest [148].

1.6. Diagnosis and evaluation.

1.6.1. Clinical presentation.

IPF presents insidiously with gradual onset of progressive dyspnoea on exertion and a nonproductive cough. The most frequent clinical symptoms are (i) bibasilar, end-inspiratory fine crackles on auscultation, predominantly in the lower posterior lung zones (typically “dry” and “Velcro” in quality), (ii) abnormal enlargement of the fingernail bases (clubbing), (iii) loss of appetite and weight, fatigue, weakness, and vague chest pains (iv) blue-colored skin (cyanosis) around the mouth or in the fingernails due to low oxygen (advanced disease) [51]. Importantly, the presenting clinical symptoms of IPF are non-specific and are often attributed to other diseases. Thus, definite diagnosis is frequently delayed with several years from the onset of the symptoms.

1.6.2. Diagnosis.

The accuracy of IPF diagnosis depends on the utilization of the following criteria: (i) exclusion of other known causes of IIPs, like drug toxicities, environmental exposures and connective tissue disorders with no features to support an alternative diagnosis from transbronchial lung biopsy (TLB) or bronchoalveolar lavage (BAL) samples, (ii) abnormalities of lung function, which include restricted and/or impaired lung gas exchange at rest or exercise or decreased diffuse lung capacity for carbon monooxide; and (iii) bibasilar reticular abnormalities (fine network of lines) and honeycombing (one or more rows of clustered cysts) and architectural distortion on HRCT scans [51] (Figure 5b).

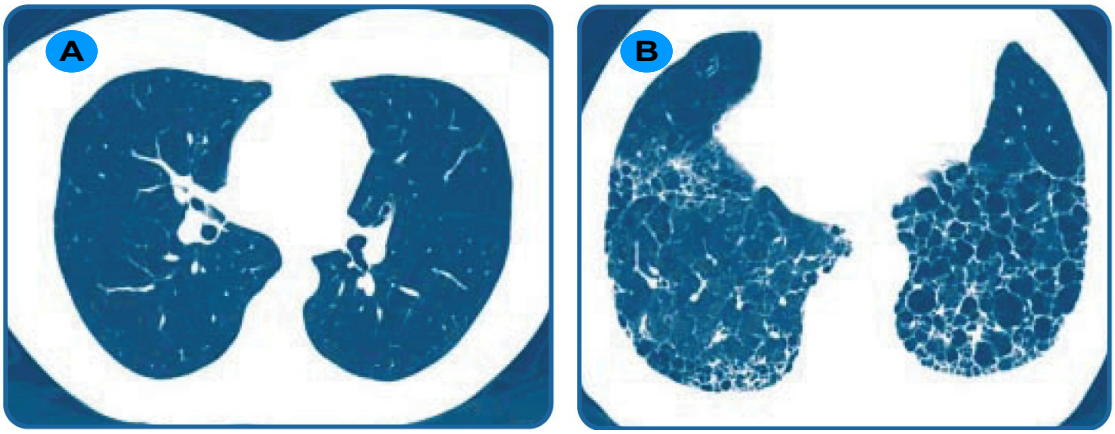

Figure 5. HRCT abnormalities in IPF. a) HRCT of normal lung, b) HRCT of IPF lung, adapted from [149].

1.7. Treatment.

IPF is a unresolved clinical issue. Treatment options include oxygen therapy and pulmonary rehabilitation to improve the breathing of the patients. Lung transplantation is a feasible treatment option for selected patients with IPF. Convential drug therapies (corticosteroids, IFN-γ_{1b}, N-acetyl cysteine (NAC), bosentan, imatinib mesylate etc.) [150] provide only marginal effects. In the light of poor prognosis and lack of available drug therapy alternative therapeutic strategies should be persued. New treatment approaches for IPF patients should include agents that inhibit alveolar epithelial injury or enhance alveolar epithelial repair, anti-inflammatory and anti-oxidant approaches, agents that inhibit fibroblast proliferation or induce fibroblast apoptosis.

1.7.1. Phosphodiesterase (PDE) inhibitors.

In the recent years it had become readily apperant that PDE inhibitors might serve as effective and specific therapeutic agents. Of interest, effective PDE inhibitor therapies have been demonstrated for a variety of proliferative pulmonary disorders: pulmonary arterial hypertension [151-153], cancer [154-156], asthma and chronic obstructive pulmonary disease [157, 158]. Most importantly, a particular PDE inhibitor (sildenefil) had shown beneficial effects in experimental models of pulmonary fibrosis and IPF secondary to PAH [159-161]. Hence forth, PDEs and PDE inhibitor strategy in IPF of specific need to be investigated.

2. PDEs.

PDEs form a large superfamily of enzymes that metabolize the ubiquitious second messenger molecules cyclic guanosine monophosphate (cGMP) and cyclic adenosine monophosphate (cAMP) to their respective inactive 5' monophosphates GMP and AMP (Figure 6). To date, 11 families of PDEs with varying selectivities for cGMP and cAMP have been identified in mammalian tissues. Each of the PDE families contain multiple isoforms, expressed either as products of different genes or as products of the same gene through alternative promoter initiation and/or

alternative mRNA splicing. Thus, the mammalian PDE superfamily (class I PDEs) is composed of more than 50 isoenzyme variants [162-166]. Notably, the individual PDE families have unique tissue, cellular, and sometime subcellular distributions [166], thus contributing to the compartmentalization of the cyclic nucleotide signaling. The unique characteristics of each PDE family and their pharmacological inhibitory profiles are summarized in Table II (appendix).

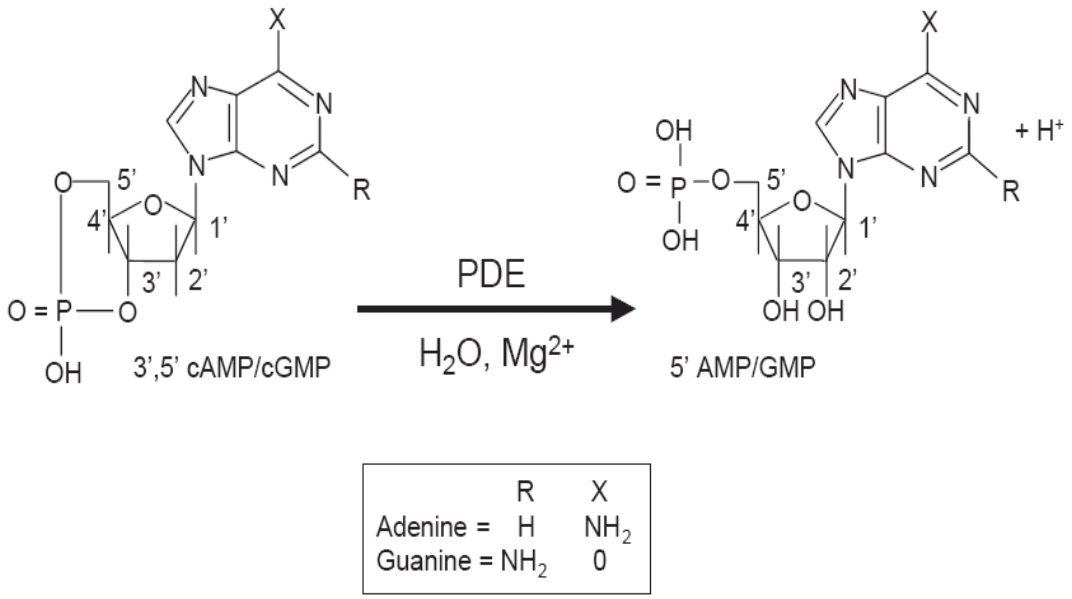

Figure 6. Chemical basis of PDE enzymatic activity.

The cartoon shows PDEs as enzymes that hydrolyze the 3' cyclic phosphate bond in the ribose ring of cAMP and cGMP, adapted from [167].

2.1. Cyclic nucleotide specificity.

Of the 11 PDE families, 3 families specifically hydrolyze cGMP (PDE5, PDE6 and PDE9), 3 families specifically hydrolyze cAMP (PDE4, PDE7 and PDE8) and 5 families hydrolyze both cyclic nucleotides with varying efficiency (PDE1, PDE2, PDE3, PDE10 and PDE11). The substrate specificity of the PDE enzymes is defined by the hydrogen-bonding network properties of their catalytic domain. In the catalytic pocket of PDEs 5, 6 and 9 invarient glutamine is fixed by neighbouring residues into a position that favours cGMP binding. Conversly, for PDEs 4, 7 and 8 this gutamine is constrained by neighbouring residues into a position that favours cAMP binding. Consistently, for bisubstrate specific PDEs the glutamine is able to

rotate freely, thus allowing hydrogen-bonding network formation for both cyclic nucleotide molecules [168].

2.2. cGMP.

cGMP controls a diverse array of physiological processes, including vascular smooth muscle relaxation, natriuresis, platelet function, neutrophil adhesion, sperm motility, neuronal signaling, and sensory transduction. cGMP is a common regulator of ion channel conductance, glycogenolysis, and cellular apoptosis [169]. cGMP play a key role in controlling epithelial cell functions such as ciliary motility and cytokine production [170-172]. Moreover, cGMP hemodynamics are of great essentiality for the phototransduction responses in the mammalian eye [173].

cGMP exerts its biological responses via activation of cGMP-dependent protein kinases, cyclic nucleotide-gated channels and cGMP binding proteins. Cytoplasmic levels of cGMP may be modulated non enzymatically by sequestering proteins [174], and/or by transport mechanisms that cause cGMP efflux from the cells [175]. However, the amplitude and the duration of cGMP signaling are mainly regulated enzymatically by the balanced activities of guanylyl cyclases (GCs) and the competing action of cGMP PDEs.

GCs are a family of enzymes that catalyzes the conversion of guanosine triphosphate (GTP) to cGMP. GCs exist in two forms: a soluble form and a membrane-bound (particulate) form [176-178]. The soluble GC (sGC) is a heme-containing heterodimer, consisting of α and β subunits, which make up the active enzyme. The sGC is activated upon NO and NO donors binding. The particulate GC is a plasma membrane receptor for the natriuretic peptides: BNP (B-type natriuretic peptide), ANP (atrial natriuretic peptide), CNP (C-type natriuretic. peptide) and related hormones [176, 178] (Figure 7).

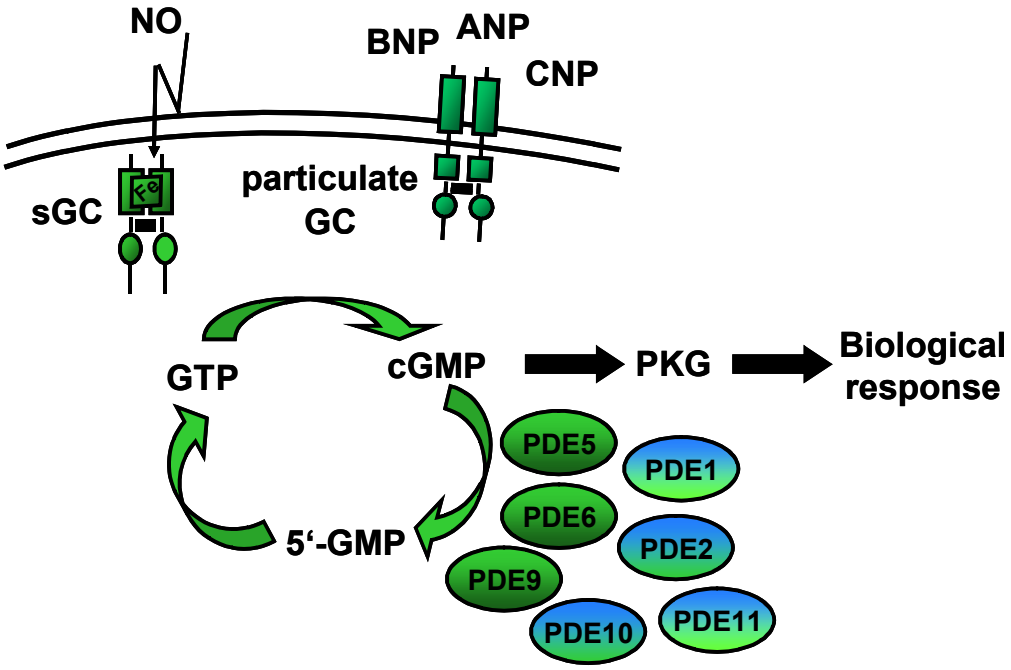

Figure 7. cGMP metabolism.

The metabolism of cGMP is controlled by the synthetic enzymes: sGC and particulate GC and the hydrolytic enzymes: PDEs. cGMP elicits diverse biological reponses via activation of PKG, adapted from [179]. *NO* nitric oxide, *sGC* soluble guanylyl cyclase, *BNP* B-type natriuretic peptide, *ANP* atrial natriuretic peptide, *CNP* C-type natriuretic. peptide, *GS* guanylyl cyclase, *GTP* guanosine triphosphate, *cGMP* cyclic guanosine monophosphate, *PKG* cGMP-dependent protein kinase G, *PDE* phosphodiesterase. Author's slide.

2.3. cGMP PDEs.

cGMP PDEs are categorized in three major subgroups: cGMP-stimulated cyclic nucleotide PDEs [180], photoreceptor cGMP-specific PDEs [181, 182], and cGMP-binding cGMP specific PDEs described in lung and platelets [183, 184].

The cGMP degrading PDE enzymes are notable for the presence of tandem GAFa/GAFb motifs in their regulatory region. The GAF acronym is derived from the names of the first three classes of proteins recognized to contain this domain: mammalian cGMP-binding PDEs, *Anabaena* adenylyl cyclases, and *Escherichia coli* FhlA [185]. GAF domains in PDEs provide for dimerization, cyclic nucleotide binding and allosteric regulation [186, 187]. Three of the five GAF domain-containing PDEs (PDE2, PDE5, and PDE6) serve as feedback regulation sides of cyclic nucleotide signaling by virtue of cAMP/cGMP binding to one of the tandem GAF domains. The GAF domains in PDE10 and PDE11 are poorly characterized. There is no clear report on allosteric regulation of PDE10 and PDE11 by cGMP [188-190].

cAMP/cGMP binding to the regulatory GAF domains in PDE2, PDE5 and PDE6 have differential effect on their enzymatic activities. Binding of cGMP to the GAFb domain of PDE2 is responsible for a direct allosteric stimulation (approximately 10-fold) of enzymatic activity [191-194]. Additionally, binding of cAMP to the GAFb domain of PDE2 also stimulates enzymatic activity [187, 192]. For PDE5, cGMP binding to the GAFa domain increases PDE5 catalytic activity directly [195, 196]. Moreover, cGMP binding to the GAFa domain of PDE5 induces conformational changes that exposes a serine residue (Ser102 in human PDE5 enzyme and Ser92 in bovine PDE5 enzyme) for phosphorylation by either PKG or the catalytic subunit of protein kinase A (PKA), which in turn activates both catalytic and allosteric cGMP-binding activities of PDE5 [197]. Unlike PDE2 and PDE5, cGMP occupancy of the GAFa domain of PDE6 reduces the basal activity of the enzyme. An effect related to enhanced affinity of the inhibitory PDE6G/H subunit for the catalytic dimer of the PDE6 enzymes [198, 199]. Reciprocally, binding of the inhibitory PDE6G/H subunit to the catalytic core of the enzyme enhances cGMP binding to the PDE6 GAFa domain [200, 201]. The arrangement of the catalytic and GAF domains in PDE2, PDE5, PDE6, PDE10 and PDE11 is given in Figure 8.

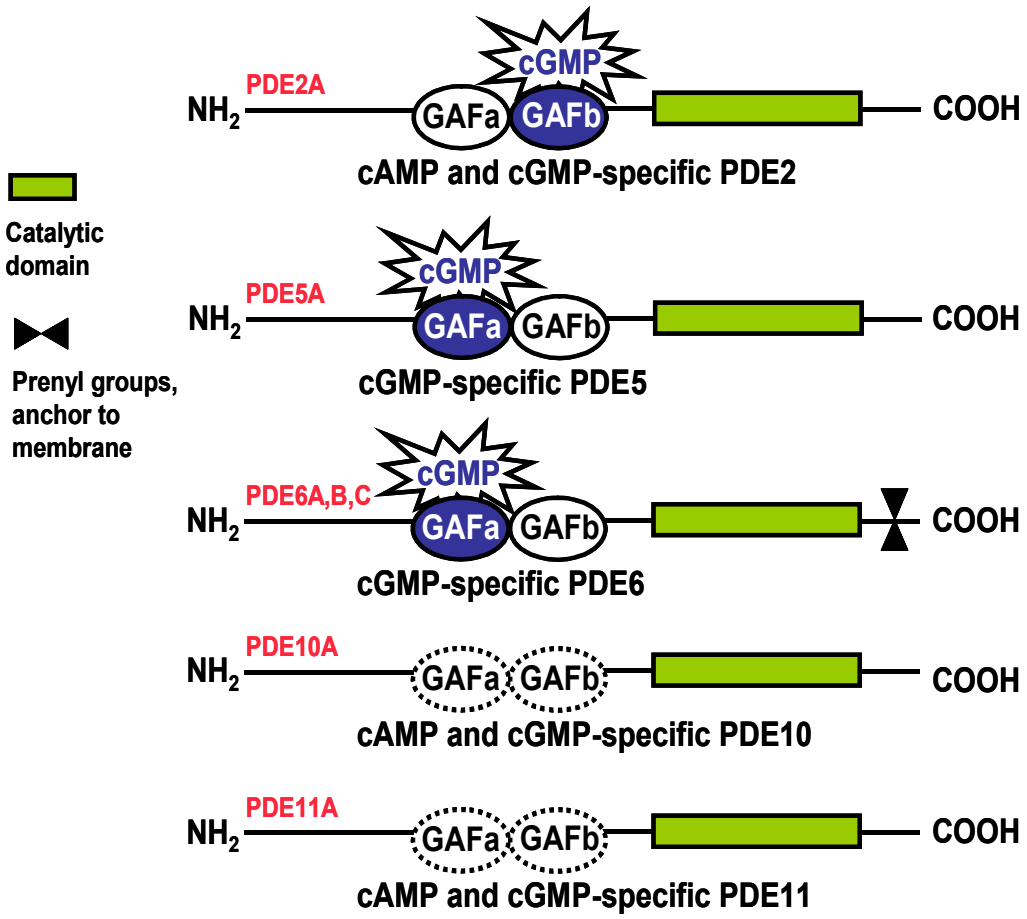

Figure 8. Schematic representation of catalytic and GAF domains arrangement in cGMP PDEs.

GAF domains with delineated regulatory properties are represented with solid line. GAF domains with currently unknown regulatory properties are represented with dotted line, adapted from [166, 202]. Author's slide.

2.4. cGMP PDEs in the lung.

Of the major cGMP degrading PDEs (PDE5, 6 and 9), PDE5 is considered the most abundant cGMP metabolizing enzyme in the lung [203-205]. PDE5 activity is ascribed mainly to pulmonary smooth muscle cells [206, 207] and is thought to limit the vasodilator and antiproliferative effects of cGMP-mediated vasoactive factors, such as NO and the natriuretic peptides on the pulmonary vasculature. Besides minor PDE5 activity is reported in bronchial epithelial cells [208] with speculated role in inflammation and remodeling processes [209].

Lung expression of PDE9 is reported as well [210]. The biological role of PDE9A is currently not well characterized. The high affinity of PDE9A for cGMP, 20 folds higher than that of PDE5, suggests its critical importance in cGMP-driven processes [183].

2.5. PDE6.

Until now, there are no reports regarding lung expression of PDE6. This enzyme is thought to be primary localized in the rod and cone photoreceptive cells of the mammalian retina [211]. The rod PDE6 enzyme is composed of two catalytic subunits PDE6α and PDE6β, encoded by PDE6A and PDE6B genes respectively, two identical inhibitory subunits PDE6γ, encoded by PDE6G [212, 213] and one regulatory subunit PDE6δ, encoded by the PDE6D gene [214]. The cone PDE6 enzyme represents two identical catalytic subunits PDE6α', encoded by PDE6C gene and two identical cone-specific inhibitory subunits PDE6γ', encoded by PDE6H gene [182] (Figure 9).

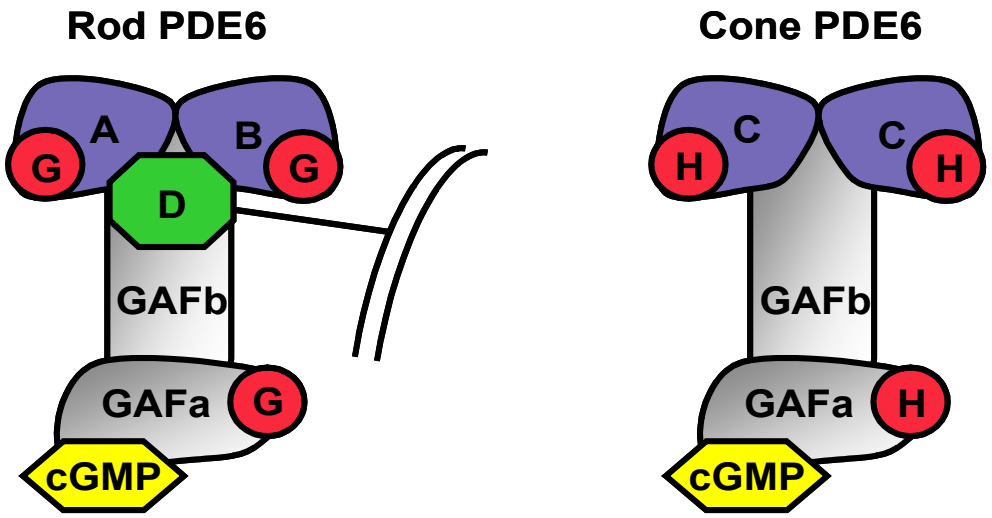

Figure 9. Schematic subunit composition and structure of rod and cone PDE6 enzymes.

The catalytic core of rod PDE6 enzyme is represented by PDE6A and PDE6B subunits. The catalytic core of cone PDE6 is represented by two identical PDE6C subunits. The regulatory domains of both rod and cone PDE6 are represented by tandem GAF domains (GAFa and GAFb). Both enzymes contain regions at their catalytic and GAF domains that interact with the respective inhibitory subunit PDE6G and PDE6H. The PDE6D subunit, which is unique to the rod PDE6 enzyme, is also shown in the picture. PDE6D interacts with the catalytic core (PDE6A and PDE6B) of the rod PDE6 enzyme and defines enzyme solubilization from the plasma membrane, adapted from [211, 215]. Author's slide.

2.5.1. Phototransduction.

PDE6 is known for its pivotal role in the phototransduction process [216-218]. It is considered the primary regulator of cytoplasmic cGMP concentration in the eye. In dark, PDE6 exists in an inactive form. The relatively high cGMP levels (several μM) permit a fraction of the cGMP-gated ion channels in the plasma membrane to remain open, allowing a current to circulate through the photoreceptor cells. Photoexcitation of a visual pigmen (rhodopsin in rod photoreceptive cells and iodopsin in cone photoreceptive cells) activates a photoreceptor G-protein, transducin. The activated α subunit of transducin interacts with the PDE6 holoenzyme, causing its activation by removal of the inhibitory PDE6G/H subunit. The activated PDE rapidly hydrolyzes cGMP. Fast depletion of cGMP in the outher segments of the photoreceptors results in a closure of cGMP-gated cation channels and a drastic Na^+ and Ca^{2+} depletion in the photoreceptive cells (blockage of Na^+ and Ca^{2+} entry and continuous work of Na^+/Ca^{2+}-K^+ exchangers). The ensuing hyperpolarization initiates the photoresponse of the photoreceptor neuron. Low intracellular Ca^{2+} levels promote activation of GC by gyanylate cyclase activating protein (GCAP), boosting up the cGMP leveles and closing up the circle of photoreceptors activation/deactivation [215, 219] (Figure 10).

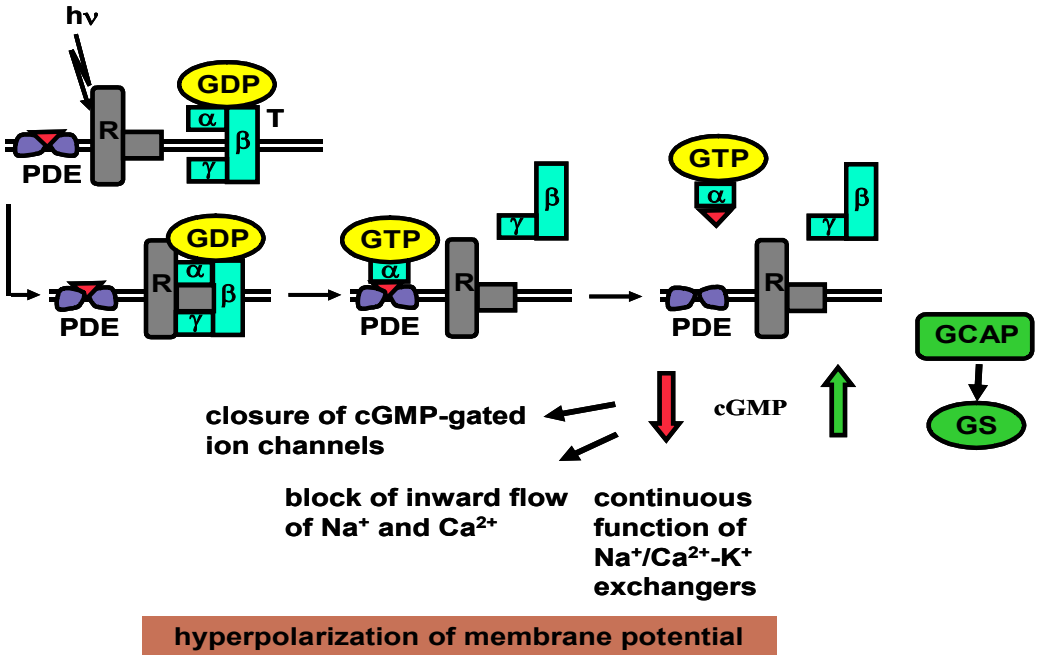

Figure 10. Vertabrate visual phototransduction cascade.

Shown in the picture is the visual excitation pathway in rod photoreceptors. Photoactivation of rhodopsin results in a GDP to GTP exchange at the α subunit of transducin. The activated α subunit of transducin (T_{α}-GTP) de-represses the blockade of the inhibitory PDE6G subunit from the catalytic core of the rod PDE6 enzyme, making the ezyme active and capable of degrading cGMP. The drop in cGMP levels in the outher segment causes dissociation of cGMP from the cGMP-gated ion channels in the plasma membrane, causing their closure. The reduced entry of cations (Na^+ and Ca^{2+}) in the outher segment causes membrane hyperpolarization and ultimate generation of the receptor potential at the photoreceptor synapse. Reactions involved in the recovery of the photoresponse (elevation of cGMP levels through activation of GCAP) are also schemed above, adapted from [211, 215]. *R* rhodopsin, *T* transducin, *PDE* rod phosphodiesterase 6, *GCAP* gyanylate cyclase activating protein, *GC* guanylyl cyclase. Author's slide.

Recently, an interaction between the PDE6 and Wnt/Ras signaling cascades has been reported in non-retinal tissues. Wang H *et al.* have postulated that the atypical Wnt/Ca^{2+}/cGMP pathway implicated in development involves PDE6 [220]. Nancy *et al*. have demonstrated that the PDE6D subunit regulates the membrane association of Ras and Rap GTPases [221]. This suggests functionality of PDE6 in non-retinal tissues and brings up the question of PDE6 expression in human lung in general, along with a plausible role for PDE6 in IPF.

Analysis of PDE6 functional assembly and activity in retinal and non-retinal tissues, however, is hampered by the unique characteristics of this enzyme: (i) functional assembly of the PDE6 complex requires at a minimum all subunits, (ii) enzyme activity is determined by various posttranslational modifications: N-terminal acetylation, C-terminal isoprenylation and carboxylmethylation, (iii) functional PDE6 expression pre-requests additional chaperon proteins [222]. Thus, we opted to characterize a complex independent function of the specific PDE6D subunit.

2.5.2. The PDE6D subunit.

In the context of phototransduction the PDE6D subunit defines the solubilization of the PDE6 enzyme from the plasma membrane and consequently the uncoupling from its effector transducin via interaction with the isoprenylated C-termini $\alpha\beta$ catalytic core of the enzyme [223]. However, the role of PDE6D extends beyond retinal tissue and the phototransduction cascade. This highly conserved protein sequence [224] has been detected in a variety of non-retinal tissues, including, heart, placenta, lung, brain, skeletal muscles and liver [223, 225]. A substantial body of information has been reported on the individual functional capacity for PDE6D apart from its role in the rod PDE6 enzyme complex [226]. PDE6D is reported to regulate the membrane association of Ras and Rap GTPases in a manner similar to guanine nucleotide dissociation inhibitor (GDI), but independent of the nucleotide-bound state (GDP/ GTP) of the small GTPase [221]. PDE6D has also been proposed to play a role in vesicular transport as an effector for, or via forming a complex with, Arl1, Arl2 and Arl3 [227, 228] and Rab13 [229]. Furthermore, PDE6D has been shown to be instrumental for the internalization and recycling of the human prostacyclin receptors [230]. In the present study, we asked whether PDE6D modulates the proliferation rate of AECs and specifically what are the signaling mechanisms accounting for PDE6D effects on AECs proliferation.

CHAPTER 2: AIMS

II. Aims of the study.

IPF is a progressive interstitial lung disorder associated with high morbidity and mortality. At present there is no demonstrably effective therapy for blocking or reversing the progression of the disease. Current evidences suggest that a possible therapeutic approach may include the use of sildenafil, a cGMP PDE5 inhibitor [159, 231]. However, the plausible contribution of other cGMP PDE isoforms to the pathogenesis of IPF has received relatively little attention. Thus, the present study was designed to analyze the expression profile of cGMP PDEs in lung tissues from donors and IPF patients. And consequently, focused on the characterization of PDE6, a previously unexplored cGMP degrading enzyme in the context of human pulmonary system and pulmonary disorders. In that respect the study design included the following aspects:

1. to characterize mRNA expression profile of cGMP PDEs in lung tissues from IPF patients as compared to donor lung tissues.

2. to evaluate PDE6 mRNA expression in human lung and the corresponding mRNA alterations in lung tissues from IPF patients.

3. to evaluate PDE6 protein expression in human lung and the corresponding protein alterations in lung tissues from IPF patients.

4. to assess the cellular and subcellular distribution of PDE6 subunits in lung tissues from donors and IPF patients.

5. to explore functional capacity of the specific PDE6D subunit in terms of AEC proliferation.

6. to delineate signaling pathways accounting for PDE6D effects on AEC proliferation.

CHAPTER 3: MATERIALS AND METHODS

"Though this be madness, yet there is method in it"
William Shakespeare, 1564 - 1616

III. Materials and Methods.

3.1. Materials.

3.1.1. Instruments, consumables, chemicals and enzymes.

Instruments, consumables, chemicals and general reagents commonly used in the experimental protocols of this thesis are listed below:

Instrument	Company name
Autoclave	Tuttnauer systec
Beta counter	Canberra Packard
BioDoc Analyzer	Biometra
Cell culture incubator	Heraeus
Cell culture microscope	Hund Wetzlar
counter plate reader (Type LP 400)	TECAN
Culture Hood (HB2448)	Heraeus
Developing machine Curix 60	AGFA
Electrophoresis apparatus system	Biometra, Bio-Rad
Film cassette	Amersham Biosciences
Fine scale (Mettler PM460)	Scaltec
Freezer, -20 °C	Bosch
Freezer, -80 °C	Sanyo
Heat block (TM 130-6)	HCL
Light microscope	Leica
Liquid nitrogen tank	Arpege 40
Lysis&Homogenization automated equipment	PeqLab
Magnetic stirrer	Bibby Stuard
Mega centrifuge (J-TB-024D)	Beckman
Microwave oven	Lotus
Mikrofuge	Hettlich
Mini spin centrifuge	Biofuge fresco, Heraeus
NonoDrop Spectophotometer	PeqLab
PCR-termocycler	Biometra

pH meter	InoLab
Pipettes: P10, P20, P100, P200, P1000	Eppendorf
Pipetus	Hirsschmann Laborgerate
SDS-PAGE gel system	Biometra, Bio-Rad
Shaker (WT 17)	Biometra
Spectrophotometer	Eppendorf
Temperature chamber	Binder
UV-Transilluminator	Biometra
Vortex	Scientific Industries
Water bath	Medingen
Water filter unit	Millipore
Western-Blot chamber	Bio-Rad

Consumable	**Company name**
Barrier food wrap	Saran
Blotting papper (3 mm)	Whatman
Cover slips	RL
Cryogenic vials	Corning
Eppendorf tubes, (1.5ml, 2ml)	Bio-Rad
Falcon centrifuge tubes (15 ml, 50ml)	Falcon
Hyper-sensitive X ray film	Amersham
Low-sensitive X ray film	AGFA
Nitrocellulose membrane (0.2 µm)	Bio-Rad
Scintillation vials	SGE
Tissue culture dishes (30 mm, 60 mm, 100 mm)	Cell Star
Tissue culture flasks (75 cm^2)	Cell Star
Tissue culture suspension plates (6, 12, 24, 48 wells)	Cell Star

Chemical or Enzyme	**Company name**
3-4,5-dimethylthiazol-2,5 diphenyl tetrabromide (MTT)	Sigma

Agarose, for routine use	Sigma
Ammonium persulfate (APS)	Sigma
Aqua B Braun	B Braun
β-mercaptoethanol	Sigma
Bovine serum albumin (BSA)	Serva
Bradford reagent	Biorad
Bromophenol blue	Merck
Calcium Chloride ($CaCl_2$)	Sigma
Chloroform, minimum 99%	Sigma
Citrate buffer 20x	Zymed lab
Complete Mini, EDTA-free protease inhibitor cocktail	Roche Diagnostics GmbH
DEPC-treated water	Fermentas
Dimethylsulfoxid (DMSO)	Sigma
Di-Sodium hydrogen phosphate anhydrous (Na_2HPO_4)	Merck
Disodium Phosphate (Na_2HPO_4)	Sigma
Ethanol (absolute)	Roth
Ethidium bromide (EtBr), 0.025%	Roth
Ethylene glycol-bis-(2-aminoethyl)-N,N,N', N'-tetraacetic acid (EGTA)	Serva
Ethylenedioxy-diethylene-dinitrilo-tetraacetic acid (EDTA)	Fluka
GeneRuler 100bp DNA Ladder (1 kb)	Fermentas
GeneRuler DNA Ladder Mix (10 kb)	Fermentas
Glacial acetic acid, minimum 99%	Sigma
Glucose	Sigma
Glycerol	Sigma
Glycine	Sigma
Hydrochloric acid fuming, 37%	Merck
Hydrochloride (HCl)	Roth
Iso-propyl alcohol (isopropanol)	Roth
Magnesium chloride ($MgCl_2$)	Merck

Magnesium sulfate ($MgSO_4$)	Sigma
Methanol (MeOH)	Fluka
Methyl-[^3H]-Thymidine, 250μCi	Amersham
N-2-Hydroxyethylpiperazine N'-2-Ethinesulfonic Acid (HEPES), minimum 99.5%	Sigma
Nonidet-P40 (NP-40) Substitute	Fluka
Pfu DNA polymerase	Promega
Phenymethanesulfonyl fluoride (PMSF) (0.1M)	Fluka
Potassium chloride (KCl)	Roth
Potassium dihydrogen phosphate (KH_2PO_4)	Roth
Rainbow marker	Amersham
Scintillation liquid (Rotiszint eco plus)	Roth
Sodium chloride (NaCl)	Sigma Aldrich
Sodium dodecyl sulfate (SDS)	Merck
Sodium hydrogen carbonate ($NaHCO_3$)	Fluka
Sodium hydroxide (NaOH)	Merck
Sodium orthovanadate (Na_3VO_4)	Sigma
Taq Polymerase	Promega
TEMED (N,N,N',N'-Tetramethyl-ethylene diamine)	Serva
Trichloroacetic acid (TCA), minimum 99%	Sigma Aldrich
Triton X-100 (t-Octylphenoxypolyethoxyethanol)	Sigma
Trizma base, minimum 99.9% titrationTris HCl	Sigma
Trizol reagent	Invitrogen
Tween 20	Sigma Aldrich
Xylol	Merck

3.1.2. Cloning reagents.

Reagent	Company name
Ampicilin	Invitrogen
dATP	Promega
IPTG	Promega
LB agar	Invitrogen

LB base	Invitrogen
Soc medium	Sigma
X-gal	Promega

LB agar medium (50 μg/ml ampicillin)	25 g LB broth dissolved in 1 l of double distilled water, sterile autoclaved (121°C, 15 min), 1ml of 50 mg/ml ampicillin stock solution addeded when the medium cooled down

LB agar plates **1.5% agar** **50 μg/ml ampicillin** **100 μM IPTG** **50 μg/ml X-gal**	32 mg LB agar dissolved in 1 l of distilled water, sterile autoclaved (121°C, 15 min), 1 ml of 50 mg/ml ampicillin, 1 ml of 100 mM IPTG, 1 ml of 50 mg/ml X-gal addeded when the medium cooled down, LB agar poored into petri dishes and let harden at room temperature

E. coli strain utilized in the cloning procedure:

JM 109 competent cells (>10^8 cfu/ μg)	**Promega**

3.1.3. Cell culture materials.

Cell culture and transfection reagents	**Company name**
DMSO	Sigma
DMEM F12	Invitrogen
FBS	PAA Laboratories
L-glutamine	PAN
Lipofectamine-2000	Invitrogen
MEM NEAA (100x)	Gibco
MEM vitamins	Gibco
Opti MEM-I +glutaMax-I	Gibco
PBS	PAN
Penicillin-streptomycin solution (100x)	PAA Laboratories

Trypsin-EDTA (10x)	PAN

Complete DMEM F12 medium	10% FBS, 1% MEM vitamin solution, 2 mM glutamate 1% MEM non-essential amino acids

Cell line utilized in the cell culture experiments:

A549 (human alveoar epithelial cells)	**American Type Culture Collection (Manassas, VA)**

3.1.4. Antibodies, blocking peptides and siRNA targeting sequences.

Antibody	**Company name**
anti-PDE6A rabbit polyclonal IgG	FabGennix, Abcam
anti-PDE6B rabbit polyclonal IgG	FabGennix, Proteintech
anti-PDE6D rabbit polyclonal IgG	FabGennix, Abcam
anti-PDE6G rabbit polyclonal IgG	FabGennix, Abcam
anti-total AKT rabbit polyclonal IgG	Santa Cruz
anti-phospho AKT (Ser 473) rabbit polyclonal IgG	Santa Cruz
anti-total ERK rabbit polyclonal IgG	Santa Cruz
anti-phospho ERK (Tyr 204) rabbit polyclonal IgG	Santa Cruz
anti-GAPDH mouse IgG	Novus Biologicals
anti-β-actin mouse IgG	Abcam
HRP conjugated rabbit anti-mouse IgG	Sigma Aldrich
HRP conjugated goat anti-rabbit IgG	Pierce

Immunizing peptide	**Company name**
anti-PDE6A immunizing peptide M(1)GEVTAEEVEKFLDSN(16)C	Abcam
anti-PDE6B immunizing peptide H(20)QYFG(K/R)KLSPENVAGAC(36)	Abcam

PDE6D siRNA target sequence	
Sense	5'-GGC-AGU-GUC-UCG-AGA-ACU-U-3'
Antisense	5'-AAG-UUC-UCG-AGA-CAC-UGC-C-3

3.1.5. Kits.

Kit	Company name
AEC staining kit	Zymed Laborotories
ECL chemiluminescence kit	Amersham
Endofree plasmid maxi kit	Qiagen
ECL solution kit	Amersham
Gel extraction kit	Qiagen
Improm II Reverse Transcription system	Promega
Miniprep kit	Qiagen
pcDNA3.1 directional TOPO cloning kit	Invitrogen
pGEM-T easy vector system II	Promega

3.1.6. Buffers and solutions.

Buffer or Solution (1 l)	Composition
Blocking solution	5 % skim milk powder in wash buffer
Buffer EB (elution buffer)	10 mM Tris-Cl, pH 8.5
Buffer ER (endotoxins removing buffer)	Proprietary formulation (Qiagen)
Buffer N3 (neutrallization buffer)	Proprietary formulation (Qiagen)
Buffer P1 (resuspension buffer)	50 mM Tris-Cl, pH 8.0, 10 mM EDTA
Buffer P2 (lysis buffer)	200 mM NaOH, 1% SDS
Buffer P3 (neutrallization buffer)	3.0 M Potassium acetate, pH 5.5
Buffer PB (binding buffer)	Proprietary formulation (Qiagen)
Buffer PE (wash buffer)	Proprietary formulation (Qiagen)
Buffer QBT (equilibration buffer)	750 mM NaCl, 50 mM MOPS, pH 7.0, 15% Isopropanol, 0.15% Triton
Buffer QC (wash buffer)	1.0 M NaCl, 50 mM MOPS, pH 7.0, 15%

	Iopropanol
Buffer QG (solubilization and binding buffer)	Contains guanidine isothiocyanate, pH 7.5
Buffer QN (elution buffer)	1.6 M Nacl, 50 mM MOPS, pH 7.0, 15% Isopropanol
Buffer TE (solubilization buffer)	10 mM Tris, pH 8.0, 1 mM EDTA
Citrate buffer (20x)	Zymed Laboratories
DNA loading dye (6x)	40% glycerol, 50 mM EDTA, 0.03% bromophenol blue, 0.4% orange G, 0.03% xylene cyanol
Freeze medium	70% complete DMEM-F12, 20% FBS, 10% DMSO
Gel loading buffer (6x)	40% glycerol, 50 mM EDTA, 0.03% bromophenol blue, 0.03% xylene cyanol
HBSS (1x) (Gibco)	0.137 M NaCl, 5.4 mM KCl, 0.25 mM Na_2HPO_4, 0.44 mM KH_2PO_4, 1.3 mM $CaCl_2$, 1.0 mM $MgSO_4$, 4.2 mM $NaHCO_3$
Hypotonic lysis buffer (1x)	10 mM HEPES, 10 mM NaCl, 1 mM KH_2PO_4, 5 mM $NaHCO_3$, 1 mM $CaCl_2$, 0.5 mM $MgCl_2$, 5 mM EDTA pH 7.5, 1 mM PMSF and 1x complete mini protease inhibitor cocktail
Laemmli buffer (5x)	10% SDS, 50% Glycerol, 25% β -mercaptoethanol, 300 mM Tris-Cl pH 6.8. 0,04% bromophenol blue
PBS (1x)	1.3 mM KCl, 0.5 mM KH_2PO_4, 135 mM NaCl, 3.2 mM Na_2HPO_4
Protein lysis buffer (1x)	150 mM NaCl, 1% Nonidet P-40, 0.1% SDS, 20 mM Tris-HCl pH 7.6, 5 mM EDTA, 1 mM EGTA, 1 mM PMSF, 1x Roche complete mini protease inhibitor cocktail
Running buffer (1x)	25 mM Tris, 192 mM glycine, 0.1 % SDS
Stripping buffer	12.5 ml 0.5 M Tris-HCl (pH 6.8), 0.7 ml ß-

	mercaptoethanol, 20 ml 10% SDS
TAE (50x)	2 M Tris, 5.5% acetic acid, 1.25 M EDTA (pH 8.8)
TBS (20x)	25 mM Tris, 2.75 mM NaCl, adjust to pH 8.0
Transfer buffer (1x)	20 mM Tris, 40 mM glycine, 20% methanol
Wash buffer	1/5 volume of 20x TBS, 0.1% Tween-20

SDS-PAGE stacking gel (4%) (ml)	0.89 ml ddH_2O, 0.375 ml 0.5 M Tris HCl, pH 6.8, 0.015 ml 10% SDS, 0.2 ml 30% PAA, 0.015 ml 10% APS, 0.0015 ml TEMED

SDS-PAGE resolving gel (10%) (ml)	1.78 ml ddH_2O, 1.13 ml 1.5 M Tris HCl, pH 8.8, 0.045 ml 10% SDS, 1.5 ml 30% polyacrylamide (PAA), 0.045 ml 10% APS, 0.002 ml TEMED

3.2. Methods.

3.2.1. Human lung tissue.

Lung tissue biopsies were obtained from 10 IPF patients with histological UIP pattern (4 females, 6 males, mean age = 56 $\pm$ 4). Detailed patients characteristics are listed in Table V (appendix). The study protocol for tissue donation was approved by the Ethik-Kommission am Fachbereich Humanmedizin der Justus-Liebig-Universitaet Giessen of the University Hospital Giessen (Germany) in accordance with national law and with Good Clinical Practice/International Conference on Harmonisation guidelines. Informed consent was obtained from each individual patient or the patient's next of kin.

3.2.2. RNA isolation.

Total RNA was isolated from exponentially growing cells and animal tissues using TRIzol reagent. Whole cell pellets were resuspended and animal tissues homogenised using Lysis&Homogenization automated equipment (PeqLab).

Briefly, 100 mg of lung tissues were homogenized in 1.0 ml TRIzol reagent, incubated for 10 min and spinned to get rid from the debris. The supernatant was mixed with 0.2

ml of chloroform. Samples were shaken vigorously by hand for 15 sec and incubated at room temperature for 2-3 min. Following centrifugation (12,000 x g, 15 min, 4°C), the aqueous phase was transferred into a fresh tube and mixed with 0.2 ml of isopropanol. After a further 10 min incubation the samples were centrifuged (12,000 x g, 10 min, 4°C), the supernatant removed and the RNA pellet washed in 75% RNA-graded ethanol. RNA pellets were resuspended in DEPC-treated water and stored at -70°C. RNA concentration and purity were measured spectroscopically (Nanodrop) by its absorbance at 260 nm and 280 nm. RNA purity was considered good when the A_{260}/A_{280} ratio was between 1.7 and 2.1. For the estimation of RNA concentration the below formula was employed:

$$\text{RNA concentration}=A_{260} \text{ x dlution factor x } 40 \text{ (g/mlRNA)}$$

3.2.3. cDNA synthesis.

Isolated total RNA was used to synthesize complementary DNA (cDNA) using Improm II reverse transcription system (Promega, Germany). The PCR cycles were performed in T 3000 Thermocycler (Biometra). Briefly, 5 µg of total RNA was combined with 0.5 µg of Oligo$(dT)_{15}$ in nuclease-free water for a final volume of 5 µl per RT reaction.This mixture was thermally denatured at 70°C for 5 min and rapidly chilled on ice. After a short spin, the reverse transcription reaction mix (see below) was added and incubated at 25°C for 5 min followed by incubation at 42°C for 1 h. Subsequently, the reaction mix was incubated at 70°C for 15 min for thermal inactivation of the reverse transcriptase. After synthesis, cDNA samples were either used immediately for PCR, or stored at -20°C.

Reverse Transcriptase reaction mix

Reagent	Reaction volume (µl)
ImProm-II Reaction buffer (5x)	4.0
$MgCl_2$ (25 mM)*	2.0
dNTP mix (10 mM)	1.0
RNasin® Ribonuclease Inhibitor	1.0
Nuclease-Free Water	X

ImProm-II Reverse Transcriptase	1.0
Final volume	**15.0**

*optimal Mg^{2+} concentration range is 1.5-8.0 mM

3.2.4. PCR.

To check for the presence of the gene of interest either in the animal tissue or cells, PCR was performed. PCR signal was amplified using the gene specific primers designed from the sequence available in the Genbank. For standard PCR, 20-23 bp long primers were designed, AT and GC content was checked and the difference in the melting temperature (Tm) between the forward and reverse primers was kept not more then 2-4ºC. The primer sequence was checked using the NCBI BLAST search for probable similarity with unrelated genes. PCR reaction was done in 0.2 ml thin wall tubes in T 3000 Thermocycler (Biometra). PCR for cDNA without reverse transcriptase was also done to check for genomic DNA contamination. Each primer pair was checked with several annealing temperatures depending on the Tm of the primer pair to get a single and specific PCR band. Gene specific primer sequences and RT-PCR conditions are given in Table III (appendix).

3.2.5. RT-PCR.

Semi quantitative RT-PCR was performed on cDNA samples by use of Taq DNA polymerase. The reaction mixture included:

PCR reaction mix

Reagent	Reaction volume (μl)	Final concentration
10x buffer	2.5	1x
$MgCl_2$ (25 mM)	1.5	1.5 mM
10 pmole/ μl FORWARD primer	1.25	0.5 μM
10 pmole/ μl FORWARD primer	1.25	0.5 μM
dNTP mix (10 mM)	0.5	0.2 mM
5 U/ μl *Taq* DNA polymerase	0.1	0.5 U/ 25 μl
ddH_2O_2	X	
cDNA template	X	0.1-0.2 μg/ 25 μl

Final volume	**25.0**

The tubes were flicked to mix and microfuged briefly before taking to the PCR machine. The thermal cycler's program was as follows:

Initial denaturation	**94°C**	**5 min**
Denaturation	**94°C**	**45 s**
Annealing	**variable**	**45 s**
Extension	**72°C**	**1 min**
Final extension	**72°C**	**10 min**
Cycles	**30-35**	

3.2.6. Agarose gel electrophoresis and PCR product purification.

PCR reactions were analyzed on appropriate % agarose gels in 1X TAE buffer, containing 0.5 µg/ml ethidium bromide. Samples were diluted in 6:1 ratio with DNA loading buffer (6x). Gel was run in 1X TAE buffer for 60 min at 80 V. Depending on the fragment size either GeneRuler 100 bp DNA Ladder (1 kb) or GeneRuler DNA Ladder Mix (10 kb) (Fermentas) were used. DNA bands were visualised under UV-Transilluminator of Biometra system. For semi-quantitative analysis of the PCR product, 10 – 20 µl of each reaction was used for electrophoresis. PCR signals were quantified in arbitary units (A.U) from optical density x band area. PCR signals were normalized to the GAPDH signal of the corresponding RT product to get a semi-quantitative estimate of the gene expression. The PCR product was purified with the QIAGEN gel extraction kit. Briefly, samples were loaded onto the gel. After gel run the corresponding bands were excised and placed in 1.5 ml eppendorf tubes. Then add 300 µl of buffer QG for every 100 mg of gel. Incubate the gel slices in buffer QG at 50°C for minimum 15 min. Then add 100 µl of isopropanol and placed in a QIAquick column. Centrifuge for 1 min at maximum speed. Then add 500 µl of buffer QG to the column and centrifuge again. After add 700 µl of buffer PE (containing ethanol) to the column and incubated for 5 min at room temperature. After centrifugation, place the column into a fresh 1.5 ml recovery tube and added 30 µl of prewarmed buffer EB directly to the center of the column. Incubated for 10 min at room temperature and then centrifuged for 2 min at 12,000 rpm. Discard the column and store the DNA at -20°C.

Further identities of transcripts were confirmed by DNA sequencing (AGOWA, Germany), where necessary.

3.2.7. Western blotting.

Total protein was isolated from exponentially growing cells and animal tissues using 1x protein lysis buffer. Whole cell pellets were resuspended and animal tissues homogenised using Lysis&Homogenization automated equipment (PeqLab). Briefly, lysates were centrifuged at 12,000 x g for 30 min at 4°C. Subcellular fractination was carried out in hypotonic lysis buffer at 110,000 x g for 1 h at 4°C (ultracentrifugation) to separate cytosolic proteins (supernatant) and crude plasma membrane proteins (pellet). Protein concentration was estimated using Bradford assay with a bovine serum albumin (BSA) standard. Equal amounts of protein in equal volumes of 1x protein lysis buffer were diluted in 5:1 ratio with 5 x Laemmli buffer and boiled for 5 min at 95°C. Subsequently, 20-50 µg proteins were run on appropriate % of SDS-polyacrylamide (SDS-PAGE) gel at a constant voltage of 130 V for 1-1.5 h in 1x running buffer. Upon completion of electrophoresis, the gel was carefully removed from glass plates. Gels were blotted onto nitrocellulose membrane using a wet tank transfer technique. Firstly, gel, whatman filter paper and nitrocellulose membrane were pre-soak in 1x transfer buffer for 5 min. The transfer sandwich (from cathode to anode (-/+)) was assembled as followes: two layers of whatman filter paper, gel, nitrocellulose membrane and two layers of whatman paper. Special attention was paid to eliminate all air bubbles trapped between the layers. Electroblotting was carried out in 1x transfer buffer for 1-1.5 h at 150 mA per two gels. Afterwards, membranes were incubated in blocking solution for 1 h at room temperature. Immunostaining was carried out overnight at 4°C with anti-PDE6A, anti-PDE6B, anti-PDE6D, anti-PDE6G antibodies (FabGennix), anti-total AKT, anti-phospho AKT, anti-total ERK, anti-phospho ERK (Santa Cruz) antibodies. The antibodies were diluted 1:1,000 in blocking solution. Later the membranes were washed (3x10 min) with wash buffer and incubated with the respective HRP (horse radish peroxidase) conjugated polyclonal secondary antibodies for 1 h at room temperature. After three final washing steps, antibodies bound to the proteins on the membrane were detected using enhanced chemiluminescence kit (GE Healthcare), according to the manufacturer's instructions.

Anti-GAPDH (Novus Biologicals) and anti-β-actin (Abcam) antibodies, diluted at 1:4,

000 in blocking solution, were used as internal controls for equal protein loading. For this the membrane was striped in preheated 1x stripping buffer. Otherwise when the kDa difference between the protein of interest and the internal control allowed, the membrane was cut into two parts and processed in parallel for the antibody of interest and the internal control antibody.

When necessary, the specificity of the primary antibody was verified by pre-treating with blocking peptide. Briefly, antibody was pre-reacted with defined fold excess of blocking peptide or PBS (sham). The reactions were vortexed to mix, microfuged briefly and incubated overnight at 4°C. Subsequently, the reactions were diluted (1:1, 000) in blocking buffer. One and the same sample was subjected twice to SDS-PAGE gel and parallel immunostaining was carried out with the blocking peptide pre-reacted antibody and sham pre-reacted antibody. The band(s) that were competed by the blocking peptide pre-reacted antibody, but not sham pre-treated antibody were considered specific. Equal protein loading was cross checked with internal control antibody (GAPDH) immunostaining.

3.2.8. Densitometry.

A densitometric analysis was performed to quantify the intensities of each band produced from PCR, RT-PCR analysis and immunoblotting. The band intensities were quantified using BioDoc analyze 2.1 software (Biometra). The relative intensities of target bands were expressed as a proportion of the β-actin or GAPDH bands intensities.

3.2.9. Immunohistochemical staining.

Immunohistochemical staining was carried out with AEC kit (Zymed Laborotories). Briefly, serial sections of paraffin-embedded lung tissue slides (3 μm in thickness) were pre-warmed at 55°C, dewaxed in xylene and rehydrated through an ethanol series. For antigen retrieval the slides were boiled in 1x citrate buffer (pH 6.0) for 20 min and 3% H_2O_2 methanol solution was used to quench the endogenous peroxidase activity. The slides were then incubated for 1 h in 10% non-immune goat serum to block non-specific binding sites. Subsequently, the serial sections were co-stained with anti-PDE6A (Abcam, 1:200 dilution), anti-PDE6B (Proteintech Group Inc., 1:200 dilution), anti-PDE6D (Abcam, 1:200 dilution), anti-PDE6G antibodies (Abcam, 1:200 dilution)

and anti-pro-SPC antibody (Chemicon International Inc., 1:1000 dilution). Immunohistochemical staining was performed overnight at 4°C. Biotinylated anti-rabbit secondary antibody and HRP-streptavidin enzyme conjugate were applied according to the manufacturer's instructions. After each incubation step, sections were washed briefly in PBS. Development of the reaction was carried out with AEC substrate (red color) for HRP for 10 min. Finally, sections were counterstained with hematoxylin (blue color), mounted in aqueous mounting media (GVA mount) and cover slipped. The sections were allowed to dry overnight before examined under a light microscope (Leica).

3.2.10. Cloning.

Complete gene sequence was RT-PCR-amplified from cDNA, using *Pfu* DNA polymerase. The *Pfu* DNA polymerase enzyme has 3'-5' exonuclease proof reading activity hence reduces the errors in nucleotide incorporation during PCR amplification. All PCR products were first cloned into pGEMT-easy cloning vector (Promega) by TA-cloning. Recombinant clones were selected by blue-white screening and thereafter the sequence of the clones was confirmed by sequencing using T7 and SP6 vector primers, Table IV (appendix). The pGEMT clones confirmed for the insert were subcloned into pcDNA3.1/V5-His expression vector (Invitrogen), utilizing the advantages of TOPO directional cloning.

3.2.10.1. PCR amplification of complete gene sequence.

Primer sequences used for cloning are listed in Table IV (appendix). PCR amplification was carried on cDNA samples by use of *Pfu* DNA polymerase. The reaction mixture included:

PCR reaction mix

Reagent	Reaction volume (μl)	Final concentration
Pfu DNA Polymerase 10x buffer with $MgCl_2$ (20 mM)	5.0	1x
10 pmole/ μl FORWARD primer	2.5	1.0 μM
10 pmole/ μl FORWARD primer	2.5	1.0 μM

dNTP mix (10 mM)	1.0	0.4 mM
Pfu DNA polymerase (2-3 U/ μl)	1.0	2.0-3.0 U/ 50 μl
ddH_2O_2	X	
DNA template	X	<0.5 μg/ 50 μl
Final volume	**50**	

The following PCR profile was used:

Initial denaturation	**94°C**	**5 min**
Denaturation	**94°C**	**1 min**
Annealing	**variable**	**3 min**
Extension	**72°C**	**1 min**
Final extension	**72°C**	**10 min**
Cycles	**30-35**	

3.2.10.2. Generating 'A-tailing' to blunt-ended PCR fragments.

Pfu polymerase enzyme has 3'-5' exonuclease activity hence generates blunt-ended PCR fragments. dATP was added at the 3' end of the gel purified PCR product (section 3.2.10.3) in order to enable TA-cloning of the PCR product into the pGEMT-easy vector.

A tailing reaction

Reagent	**Reaction volume (μl)**	**Final concentration**
10x buffer	1.0	1x
$MgCl_2$ (25 mM)	0.5	1.5 mM
dATP (2mM)	1.0	0.2 mM
5 U/ μl *Taq* DNA polymerase	1.0	5 U/ 10 μl
PCR product (template)	6.5	
Final volume	**10**	

After incubating the reaction mixture for 30 min at 72°C, the polymerase enzyme was inactivated by freezing the reaction mixture.

3.2.10.3. Ligation of A-tailed DNA Fragment into PGEMT-easy vector.

The isert vector molar ratio was optimized, using the following equation:

ng of vector x kb size of insert x insert:vector molar ration = ng of insert
kb size of vector

The ligation reaction was set up as described below:

Ligation reaction mix

Reagent	Reaction volume (μl)	Final Concentration
2x Rapid ligation buffer	5	1x
pGEM-T Easy vector	1	**1:3**
PCR product	X	**vector:insert**
T4 DNA ligase (3 Weiss U/ μl)	1	3 Weiss U/ 10 μl
ddH_2O_2	X	
Final volume	**10**	

The reaction mixture was mixed by pipetting, centrifuged briefly and incubated 1 h at room temperature. Then T4 DNA ligase in the ligation mix was heat inactivated for 20 min at 65°C.

3.2.10.4. Heat shock transformation.

Chemocompetent JM109 cells (Promega) were thawn on ice for 5-10 min. For a single transformation 1 aliquot (50 µl) of JM109 cells suspension was added to 3-5 µl of the ligation reaction mix in an eppendorf tube, equalling approximately 1-10 ng of circular plasmid DNA. Immediately after heat shock (45 s at 42°C) the tube was placed on ice for 2 min. After adding 450 µl of SOC medium, the tubes were incubated at 37°C for 1.5 h with shaking (150 rpm). The transformation reaction was spread in 100 µl volumes onto selective bacterial agar plates (50 µg/ml ampicillin, 100 μM IPTG, 50 μg/ml X-gal). An ethanol flamed glass-hockey stick was used for even distribution of

bacterial cultures. Plates were incubated overnight at 37°C.

3.2.10.5. pGEMT easy recombinant clone selection.

Successful cloning of an insert into pGEMT- easy vector interrupts the coding sequence (lacZ) of β-galactosidase (Figure A1 (appendix)). White colonies are indicative for vector containing insert and were subjected to a colony screen.

3.2.10.6. Small scale plasmid DNA purification.

Plasmid DNA was prepared in small scale using Qiagen spin miniprep kit. The principle of this kit is based on alkaline lysis of bacteria cells followed by adsorption of DNA onto a silica column.

Briefly, pick a single white colony using a sterile toothpick and use to innoculate 2-5 ml selective LB medium (50 µg/ml ampicillin). Grow bacterial cultures overnight in a 37°C incubator with shaking (220-300 rpm). Then collect bacteria by centrifugation at 6000 x g for 1 min at 4°C. Resuspend the bacterial pellet in 250 µl buffer P1 (containing RNase A). Then add 240 µl buffer P2 and gently invert the tube 4-6 times to mix. Then add 350 µl Buffer N3 and invert the tube immediately but gently 4-6 times. Centrifuge for 10 min at maximum speed. Then add the supernatant to the QIAprep spin column and centrifuge again. After add 500 µl buffer PB and centrifuge. Wash QIAprep spin colum by adding 750 µl buffer PE. Centrifuge twice to remove residual wash buffer. After, place the column in a clean 1.5 ml eppendorf tube and add 50 µl buffer EB or ddH_2O_2. Incubate 2-3 min and collect plasmid DNA with centrifugation. Further plasmid DNA was sequenced and used for directional TOPO cloning.

3.2.10.7. Directional TOPO cloning in pcDNA 3.1 vector.

In order to anneal with the -GTGG- overhang of the pcDNA 3.1 directional TOPO expression vector (Figure A2 (appendix)), the forward primer was modified at the 5' end to contain a corresponding 4-bp CACC sequence. The reverse primer was designed in such a way that the stop codon was ignored so as to ensure the presence of C terminal His-tag expression. PCR amplification was carried on 10-100 ng purified plasmid DNA samples, using *Pfu* DNA polymerase as described (section 3.2.10.1). The principle of directional TOPO cloning is given in Figure A3 (appendix).

3.2.10.8. TOPO cloning reaction.

For cloning in pcDNA3.1 directional TOPO expression vector the following reaction was prepared:

TOPO cloning reaction mix

Reagent	**Reaction volume (μl)**
JM 109 cells (>10^8 cfu/ μg)	50
Fresh PCR product	X
Salt solution	1.0
TOPO vector	1.0
ddH_2O_2	X
Final volume	**X**

The rection was mixed gently and incubated for 5-30 min at room temperature. After the TOPO cloning reaction mix was subjected to heat shock transformation (section 3.2.10.4)

3.2.10.9. pcDNA 3.1 clone analysis.

Individual recombinant clones were analyzed by restriction analysis and sequencing with primers listed in Table IV (appendix). pcDNA3.1/V5-His-TOPO vector does not contain β-galactosidase gene sequence for blue-white screening (Figure A2 (appendix)).

3.2.10.10. Large scale endotoxin free plasmid extraction.

Plasmid DNA was prepared in large scale using Qiagen endofree plasmid maxi kit. Large scale plasmid DNA isolation is based on the same strategy as miniprep isolation: alkaline lysis of bacteria cells followed by adsorption of DNA onto a silica column.

Briefly, innoculate a single colony with 2-5 ml selective LB medium (50 μg/ ml ampicillin). Incubate for 6-8 h in a 37°C incubator with shaking at 220-300 rpm. Then dilute the starter culture 1/500 to 1/1000 into selective LB medium (50 μg/ ml

ampicillin). Grow overnight (37°C, 220-300 rpm). Collect bacteria by centrifugation at 6000 x g for 15 min at 4°C. Resuspend the bacterial pellet in 10 ml pre-warmed buffer P1. Add 10 ml buffer P2, mix gently and incubate at room temperature for 5 min. Then add 10 ml of chilled buffer P3, mix immediately. Pour the lysate into the barrel of the QIAfilter cartridge. Incubate for 10 min and filter through the cartridge using plunger. Then add 2.5 ml of buffer ER to the filtered lysate, mix by inverting the tube and incubate on ice for 30 min. Then apply the filtered lysate to an equilibrated QIAGEN-tip (2x 10 ml buffer QBT) and allow it to enter the resin by gravity flow. Wash the QIAGEN-tip with 2 x 30 ml of buffer QC. Elute DNA with 15 ml buffer QN. Then precipitate DNA by adding 0.7 volumes of room temperature isopropanol. Mix and centrifuge immediately at ≥ 15 000 x g for 30 min at 4°C. Wash the resultant pellet twice with 70% endotoxin free ethanol and air dry at room temperature. The pellet is carefully resuspended in a suitable volume of endotoxin-free buffer TE and used for transfection of cultured mammalian cells. The endotoxins removal step with ER buffer is essential for optimal transfection efficiency and high reproducibility of results.

3.2.10.11. Glycerol stock.

For storage of recombinant clones, 500 µl of an overnight bacterial culture were mixed throughly with 500 µl of 100% glycerol in a 1.5 ml ependorff tube. This 50% glycerol stock solution was subsequently frozen at –80°C.

3.2.11. siRNA

Endogeneous PDE6D expression was knockdowned with PDE6D siRNA target sequence (Eurogentec, Seraing, Belgium, 100 nM). Negative control siRNA sequence (Eurogentec, Seraing, Belgium, 100 nM) was used as a specificity control.

3.2.12. Cell culture.

A549 human AEC line was obtained from American Type Culture Collection (Manassas, VA). The cells were propagated and maintained in complete DMEM F12 medium in a humidified atmosphere with 5% CO_2 and 95% air. The antibiotics were excluded from the growing medium to avoid possible side effects on cell metabolism, differentiation and viability. The utilized transfection protocol as well required antibiotic-

free medium. Cellular growth and viability were assessed by phase contrast microscopy. The culture medium was replaced every other day. After attaining confluence, medium was aspirated from the cells, the cells were washed with PBS (2x times) and trypsinized with 1x trypsin-EDTA solution,diluted in 1x PBS. The trypsin-EDTA solution was neutralized with complete DMEM F12 medium. For experiment purposes, A549 cells were seeded at density $2x10^5$/ml, which gave 80% confluence in 24 h. All the solutions added to cell cultures were pre-warmed in a 37°C water bath. All manipulations were performed aseptically in a cell culture hood using sterile equipment.

Primary human ATII cells: were isolated after the lungs had been preserved for 4–8 h at 4°C. The pulmonary artery was perfused with a 37°C PBS solution, and the distal air spaces were lavaged with pre-warmed Ca^{2+} - and Mg^{2+} -free PBS solution (0.5 mM EGTA and 0.5 mM EDTA) 10 times. Next, 13 U/ml elastase in Ca^{2+} - and Mg^{2+} -free HBSS were instilled into the distal air spaces through segmental bronchial intubation. After digestion for 45 min, the lung was minced finely in the presence of FBS and DNase (500 μg/ml). The cell-rich fraction was filtered by sequential filtration through one layer of sterile gauze, two layers of gauze, and 150 μm and 30 μm nylon mesh. The solution was then layered onto a discontinuous Percoll density gradient 1.04 –1.09 g/ml solution and centrifuged at 1,500 rpm for 20 min. The upper band containing a mixture of type II pneumocytes and alveolar macrophages was collected and centrifuged at 800 rpm for 10 min. The cell pellet was washed and resuspended in Ca^{2+} - and Mg^{2+} -free PBS containing 5% FBS. The cells were then incubated with magnetic beads coated with anti-CD-14 antibodies at 4°C for 40 min under constant mixing. Then the beads were depleted with a Dynal magnet (Dynal Biotech, Oslo, Norway). The remaining cell suspension was incubated in human IgG-coated tissue culture-treated Petri dishes in a humidified incubator (5% CO_2, 95% air) at 37°C for 90 min. Unattached cells were collected and counted. Cell viability was assessed by the trypanblue exclusion method. The purity of isolated human AT II cells was examined by Papanicolaou staining [232].

3.2.12.1. Cryopreservation and thawing of cell cultures.

Cultured cells were cryopreserved by resuspending the harvested pellet in freeze medium. The cells were transferred to a cryogenic vial and immediately placed in a -

80°C freezer overnight before transfer to -195°C liquid nitrogen for long term storage. Vials removed from liquid nitrogen were thawed rapidly in a 37°C water bath and cells were immediately rinsed twice in growth medium to remove the freeze medium.

3.2.13. Transient transfection.

Cells were transiently transfected using lipofectin 2000 reagent (Invitrogen), a 1:1 (w/w) liposome formulation of the cationic lipid N-[1-(2,3-dioleyloxy)propyl] n,n,ntrimethylammonium chloride (DOTMA) and dioleoyl phosphotidylethanolamine (DOPE) in membrane filtered water.

Cells were maintained as described (Section 3.2.12). 80% confluent cells were used for the transfection experiments. On the day of transfection, plasmid DNA or siRNA were diluted in Opti MEM-I +glutaMax-I medium (Gibco). Separately, Lipofectin 2000 reagent (Invitrogen) was diluted in Opti MEM-I +glutaMax-I medium. The diluted plasmid DNA/ siRNA and the diluted lipofectamine 2000 reagent were pre-incubated at room temperature for 5-10 min before being mixed to make complexes. Complexes were allowed to form for a further 15 min at room temperature. Complexes were finally diluted with 0.1% DMEM F12 medium which in turn was added onto cells that had been washed with 2 ml of OPTI-MEM I. After 5-6 h, this medium was replaced with complete DMEM F12 medium. Cells were analysed after a given time point. Transfection volumes were scaled up or down according to the surface area of the tissue culture vessel in use (Lipofectamine 2000 reagent, Invitrogen, data sheet).

3.2.13.1. Transient transfection efficiency assessment.

For overexpression studies, transfection efficiency was monitored with anti-PDE6D (FabGennix) and anti His-HRP conjugate (Clontech) antibodies. For siRNA-mediated inhibitory studies, transfection efficiency was assessed with anti-PDE6D (FabGennix) antibody.

3.2.14. Measurement of cell proliferation.

A549 cells were transfected under starvation conditions for 6 h, rendered quiescence for 24 h in 0.1% FBS DMEM F12 medium and then subjected to serum stimulation for 24 h. The effects on cell growth were measured by 3-(4,5-dimethylthiazol-2-yl)-2,5-

diphenyltetrazolium bromide (MTT) and [^3H]-Thymidine incorporation assay.

3.2.14.1. MTT cell proliferation assays.

MTT (3-4,5-dimethylthiazol-2,5 diphenyl tetrabromide) is reduced in viable cells by mitochondrial dehydrogenase to a purple coloured crystal, formazan, allowing cell viability to be determined by a colourimetric assay.

Cells ($2x10^5$/ ml) were seeded in 96-well plates. For the last 4 h of proliferation experiments, cells were stained with 0.05 mg/ ml of MTT solution per well at 37°C. Medium was aspirated and the wells were incubated with 100 µl of 0.04N HCL solution in isopropanol for 15-20 min at 37°C. This allowed complete solubilization of the converted dye (formazan). The absorbance of each well was then read in a ELISA reader (Tecan) at 570 nm wavelength.

3.2.14.2. [^3H]-Thymidine incorporation assay.

Tritiated [^3H]-Thymidine is incorporated into cellular DNA during S-phase of DNA synthesis, allowing radioactive monitoring of cell proliferation rate. Cells ($2x10^5$/ ml) were seeded in 48-well plates. For the last 4 h of proliferation experiments, cells were labeled with 0.1 µCi [^3H]-Thymidine per well at 37°C. Medium was aspirated and cells were washed with 500 µl ice cold HBSS (2x times). Next, cells were fixed in 250 µl ice cold methanol for 15 min at 4°C. Without aspiration step, 250 µl 10% TCA solution was added to the wells to precipitate nucleic acid polymers. TCA incubation was kept for 15 min at 4°C. Cells were washed extensively with sterile H_2O_2 (Aqua B Braun) and solubilized in 0.1 M NaOH. The [^3H]-Thymidine content of the cell lysates was determined by scintillation counting (Canberra -Packard).

3.2.15. Statistical analysis.

All data were expressed as the means ± S.E. Data were compared using a two-tailed Student's *t*-test, or a 1-way ANOVA with the Student-Newman- Keuls post hoc test for studies with more than 2 groups. Statistical significance was assumed when $P<0.05$.

CHAPTER 4: RESULTS

IV. Results.

4.1. mRNA expression profile of cGMP PDEs in IPF lungs.

We used semi-quantitative RT-PCR to analyse the mRNA expression profile of cGMP PDEs in lung tissue samples of donors and IPF patients. Initially, we assessed the mRNA expression levels of PDE1A, PDE1B, PDE1C, PDE2A, PDE5A, PDE9A, PDE10A and PDE11A. Despite of the intergroup individual differences significant upregulation was detected for PDE1A and upregulation tendency was observed for PDE10 and PDE11 in the IPF lungs as compared to donor lungs (Figure 11 a, b).

a)

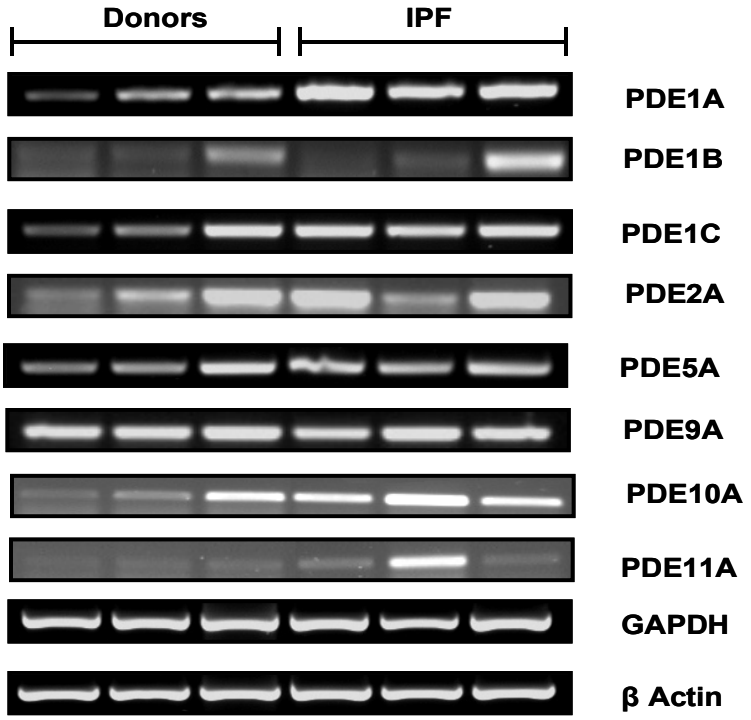

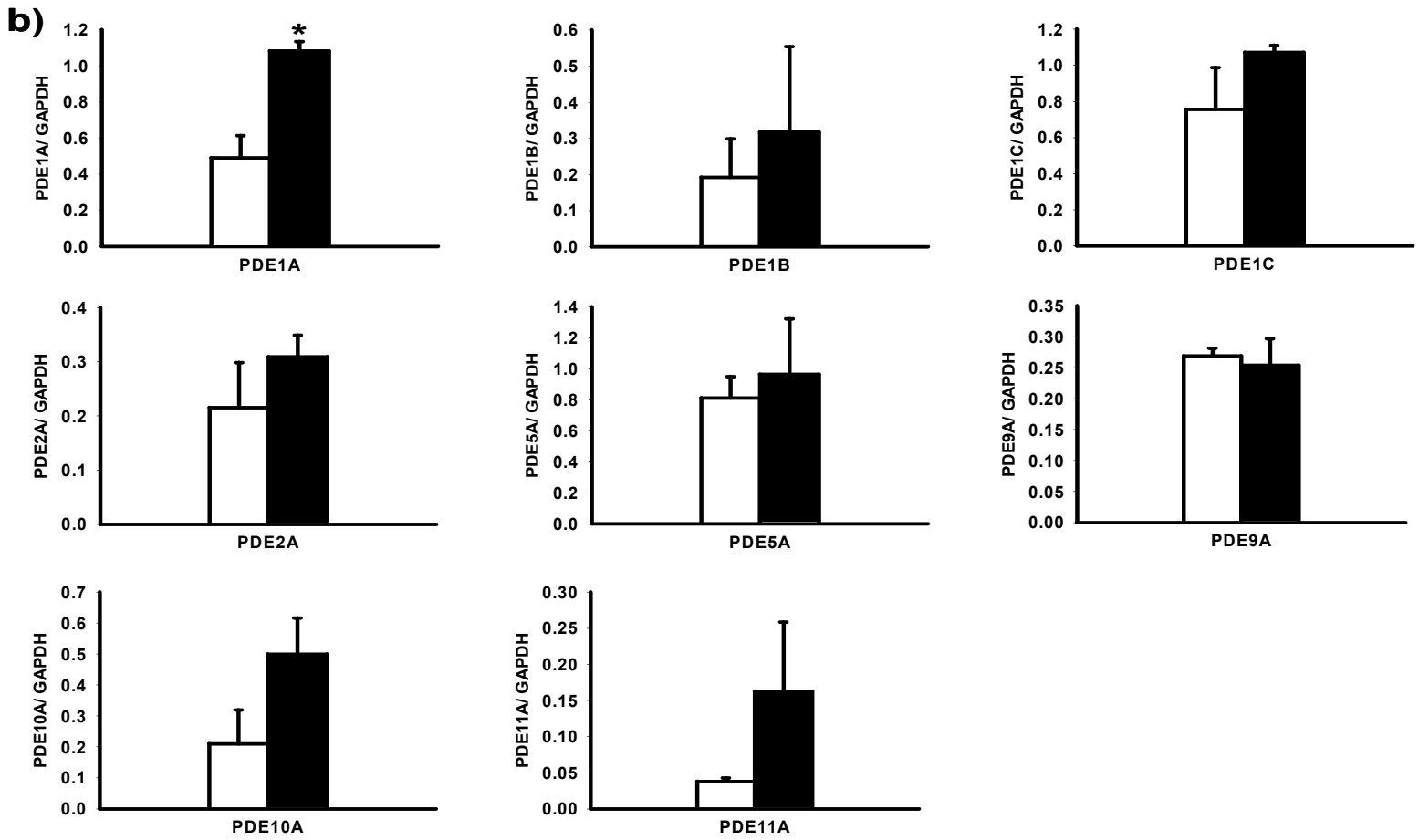

Figure 11. mRNA profile of cGMP PDEs in lung tissue samples of donors and IPF patients.

a) Semi-quantitative RT-PCR analysis was used to assess cGMP PDE expression in lung tissue samples of donors (n=3) and IPF patients (n=3). GAPDH served as an internal control for equal loading. b) Corresponding densitometric quantification, normalization was carried out with respect to GAPDH expression, □ donor and ■ IPF lungs.

4.2. mRNA detection of the PDE6 enzyme subunits in lung tissue samples of donors and IPF patients.

The mRNA expression of each PDE6 subunit in lung tissue samples of donors and IPF patients was analyzed by a semi-quantitative RT-PCR technique. As illustrated in Figure 12a, all PDE6 mRNAs were RT-PCR amplified. Parallel minus-RT control reactions were carried out to exclude the possibility of genomic DNA contamination. The densitometric analysis indicated moderate mRNA alterations of PDE6B, PDE6D and PDE6H genes in the IPF lungs compared to the donor lungs (Figure 12b). The resulting PCR products were validated by direct sequencing, followed by BLAST analysis that confirmed the similar sequence alignment for each subunit (Figure 12c).

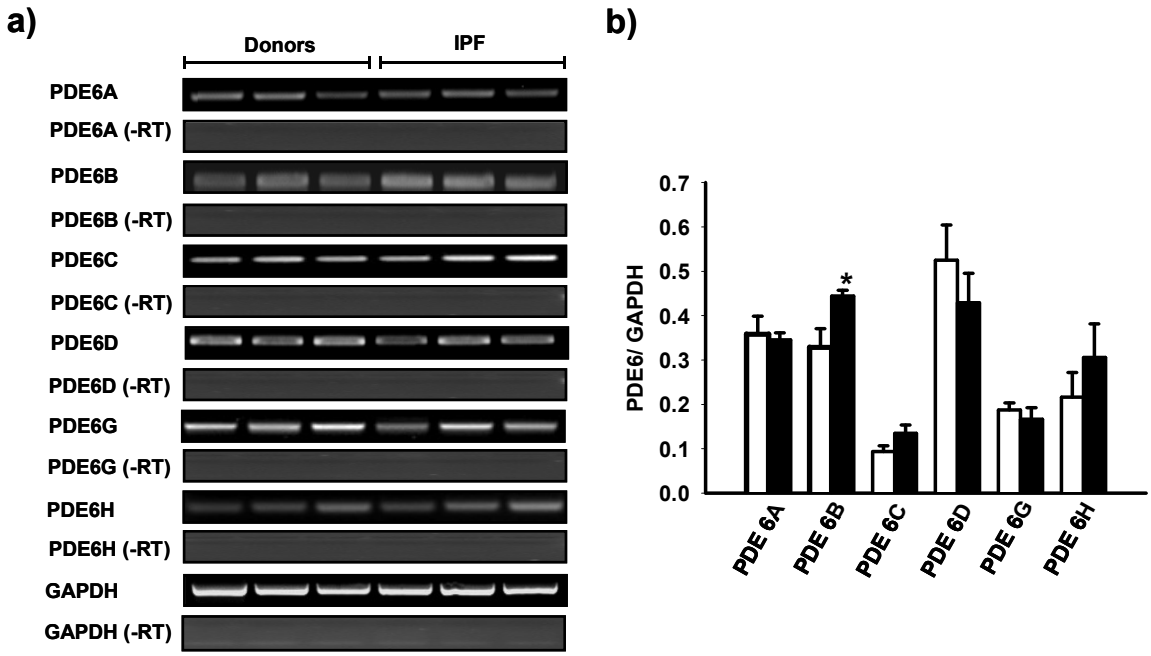

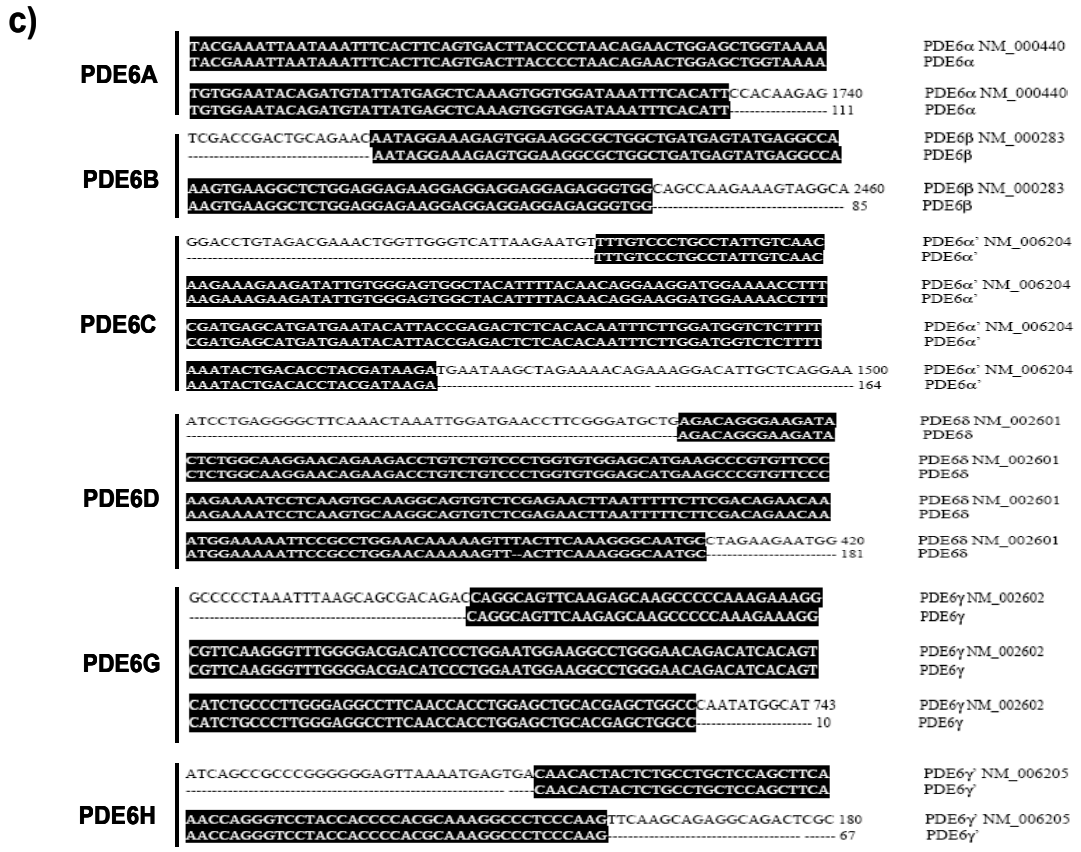

Figure 12. PDE6 mRNA detection in lung tissues from donors and IPF patients.

a) Semi-quantitative RT-PCR analysis was used to assess PDE6 expression in lung tissues from donors (n=3) and IPF patients (n=3), minus-RT control reactions excluded genomic DNA contamination. b) Corresponding densitometric analysis normalized to GAPDH expression, □ donor and ■ IPF lungs, *P<0.05. c) Sequence alignment of the PDE6 subunits.

4.3. Protein expression of the PDE6 enzyme subunits in lung tissue samples of donors and IPF patients.

The protein content of the PDE6 subunits in lung tissue samples of donors and IPF patients was quantified by immunoblotting. As illustrated in Figure 13 immunoreactivity was detected for all PDE6 proteins: PDE6A (105 kDa), PDE6B (105 kDa), PDE6G (11 kDa) and PDE6D (17 kDa) subunits. Pig retinal lysate served as a possitive control for immunoreactivity and proper protein size. Additionally, PDE6A and PDE6B blocking peptide studies reconfirmed the PDE6A and PDE6B lung immunoreactivity (Figure 13c, d). Notably, the protein content of PDE6 varied between donor and IPF-derived lung tissues. PDE6A and PDE6B exhibited a 2 fold up-regulation (Figure 13a, b), PDE6D a 2 fold down-regulation (Figure 13c, d) and PDE6G membrane localization (Figure 13e, f) in the IPF lungs as compared to donor lungs.

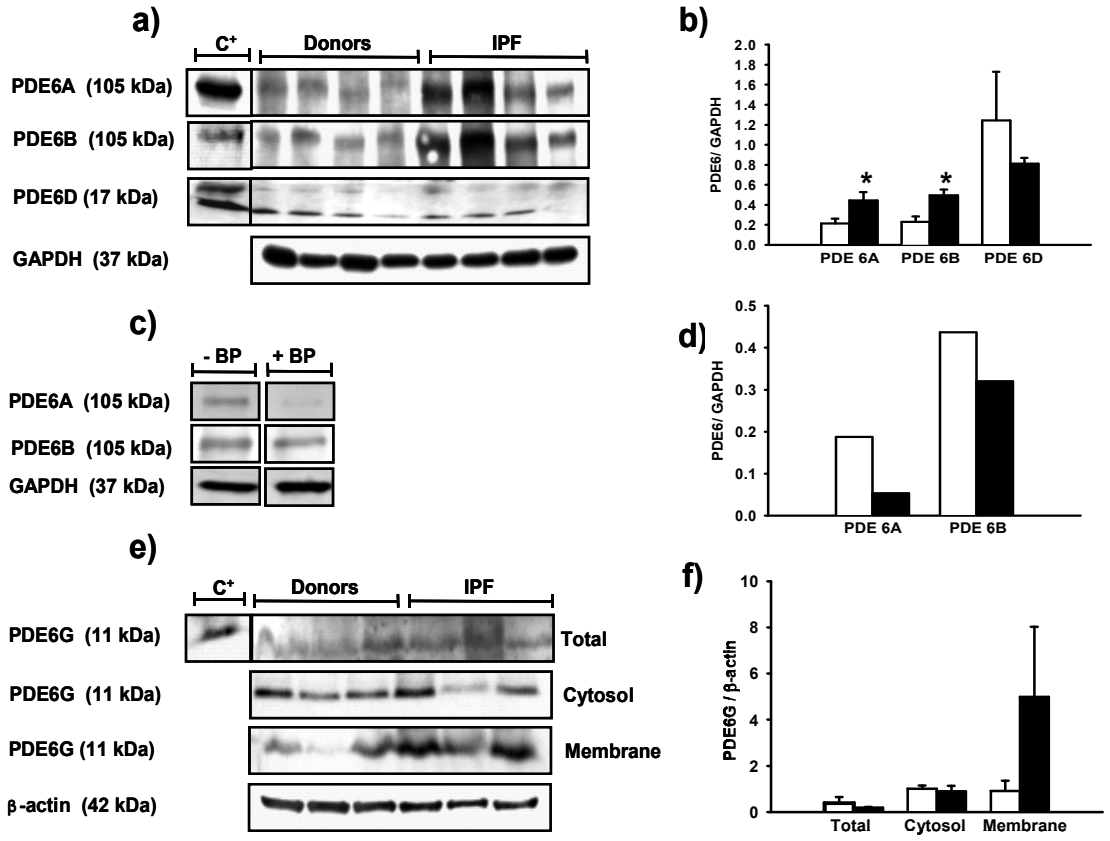

Figure 13. PDE6 immunoreactivity in lung tissues from donors and IPF patients.

a) Western blotting analysis was used to assess PDE6 expression in lung tissues from donors (n=4) and IPF patients (n=4), pig retinal lysate was used as a positive control (C+) for PDE6 immunoreactivity. b) Corresponding densitometric analysis, normalized to GAPDH expression, □ donor and ■ IPF lungs, $*P<0.05$. c) Demonstration of PDE6A and PDE6B antibodies' specificity by an antigen (peptide/protein) blocking technique. d) Corresponding densitometric analysis normalized to GAPDH expression, BP (blocking peptide, □ without BP and ■ with BP. e) Total and fractionated cytosolic and membrane proteins which were immunoblotted with PDE6G antibody. f) Corresponding densitometric analysis normalized to β-actin expression , □ donor and ■ IPF lungs.

4.4. Cellular localization of the PDE6 enzyme subunits in lung tissue samples of donors and IPF patients.

The cellular localization of the PDE6 subunits was assessed by serial immunohistochemical stainings on tissue sections from donor and IPF lungs. As shown in Figure 14, PDE6A, PDE6B, PDE6D and PDE6G were co-stained with pro-SPC, suggesting the presence of PDE6 subunits in the ATII AECs. PDE6A and PDE6D immunoreactivity was recognized in the cytoplasm, PDE6B immunoreactivity in the nuclei and PDE6G immunoreactivity in the membrane of ATII cells.

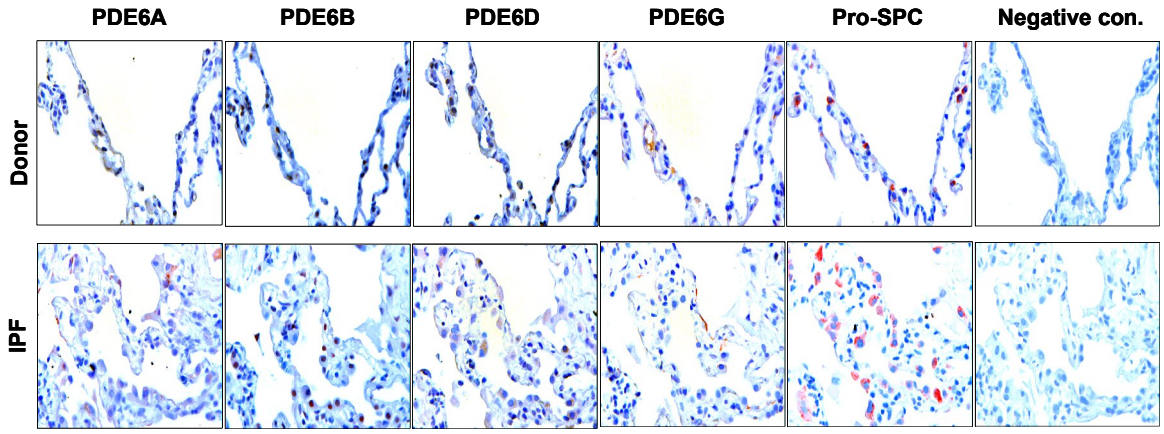

Figure 14. Immunohistochemical localization of PDE6 in lung sections from donors and IPF patients.

Immunohistochemical stainings were performed on serial tissue sections of donor (upper row) and IPF (bottom row) lungs. PDE6A, PDE6B, PDE6D and PDE6G were co-stained with pro-SPC, a marker specific for ATII cells. PDE6A and PDE6D immunoreactivity was recognized in the cytoplasm, PDE6B immunoreactivity in the nuclei and PDE6G immunoreactivity in the membrane of ATII cells. The red and dark brown color is indicative of immunoreactivity. Tissue slides were counterstained with hematoxylin (blue color). Negative control stands for no antibody reaction, magnification 400x.

4.5. The PDE6 enzyme subunits are expressed in human ATII cells.

To confirm this cellular localization pattern, the PDE6. subunits were RT-PCR amplified from human primary donor and IPF-derived ATII cells. All PDE6 subunits (except for PDE6C) were found expressed by these cells. Densitometric normalization to GAPDH expression revealed significantly decreased mRNA levels of the PDE6D subunit in IPF-derived ATII cells (Figure 15a). Importantly, independent densitometric normalization to pro-SPC (AECs specific marker) reconfirmed the downregulation pattern of PDE6D in ATII cells from IPF patients (Figure 15b). Supplementary, we showed that the mRNAs of all PDE6 subunits (except for PDE6C and PDE6H) and the complete set of PDE6 proteins (PDE6A, PDE6B, PDE6D and PDE6G) are expressed in A549 cells (Figure 15c, d). Considering the facts that (i) the A549 cells possess ATII cell phenotype and (ii) transient transfection of primary isolated ATII cells continues to be largely inefficient, we used this cell line for further functional experiments.

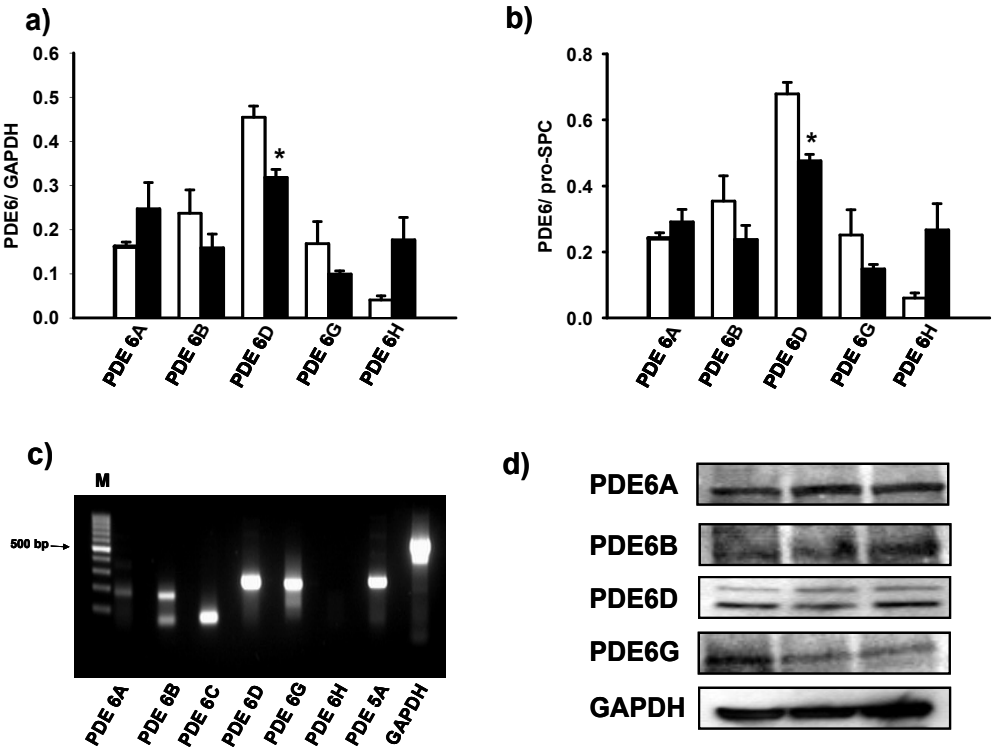

Figure 15. The PDE6 enzyme subunits are expressed in human ATII cells. Semi-quantitative RT-PCR was used to assess PDE6 expression in human primary donor and IPF-derived ATII cells. a) Densitrometric analysis of PDE6 subunits expression normalization was carried out with respect to GAPDH expression, □ donor ATII cells and ■ IPF-derived ATII cells, *P<0.05. b) Densitometric analysis of PDE6 subunits expression, normalization was carried out with respect to proSP-C expression, □ donor ATII cells and ■ IPF-derived ATII cells, *P<0.05. c) mRNA expression profile of PDE6 subunits in A549 AECs, M →DNA molecular marker. d) Protein expression profile of PDE6 subunits in A549 AECs.

4.6. Effects of PDE6D modulations on A549 cell proliferation.

Further, we studied the effects of PDE6D downregulation in A549 cells. siRNA silencing of PDE6D resulted in a significant loss of PDE6D protein expression 24 and 48h post transfection. The negative control siRNA caused no change in PDE6D protein expression (Figure 16a). The loss of PDE6D expression was coupled to a slightly decreased MTT conversion (Figure 16b) and a significantly decreased [^3H]-Thymidine uptake (Figure 16c) as compared to control siRNA and no siRNA transfected cells 24 h post serum stimulation. Complementary, transient overexpression of PDE6D in A549 cells resulted in a significantly enhanced PDE6D expression and detection of PDE6D His-tagged protein 24 and 48 h post transfection. Empty vector transfection caused no change in PDE6D protein expression (Figure 17a). The gain of PDE6D expression was coupled to a slightly increased MTT conversion (Figure 17b) and a significantly increased [^3H]-Thymidine uptake (Figure 17c) as compared to empty vector expressing cells and no DNA transfected cells 24 h post serum stimulation.

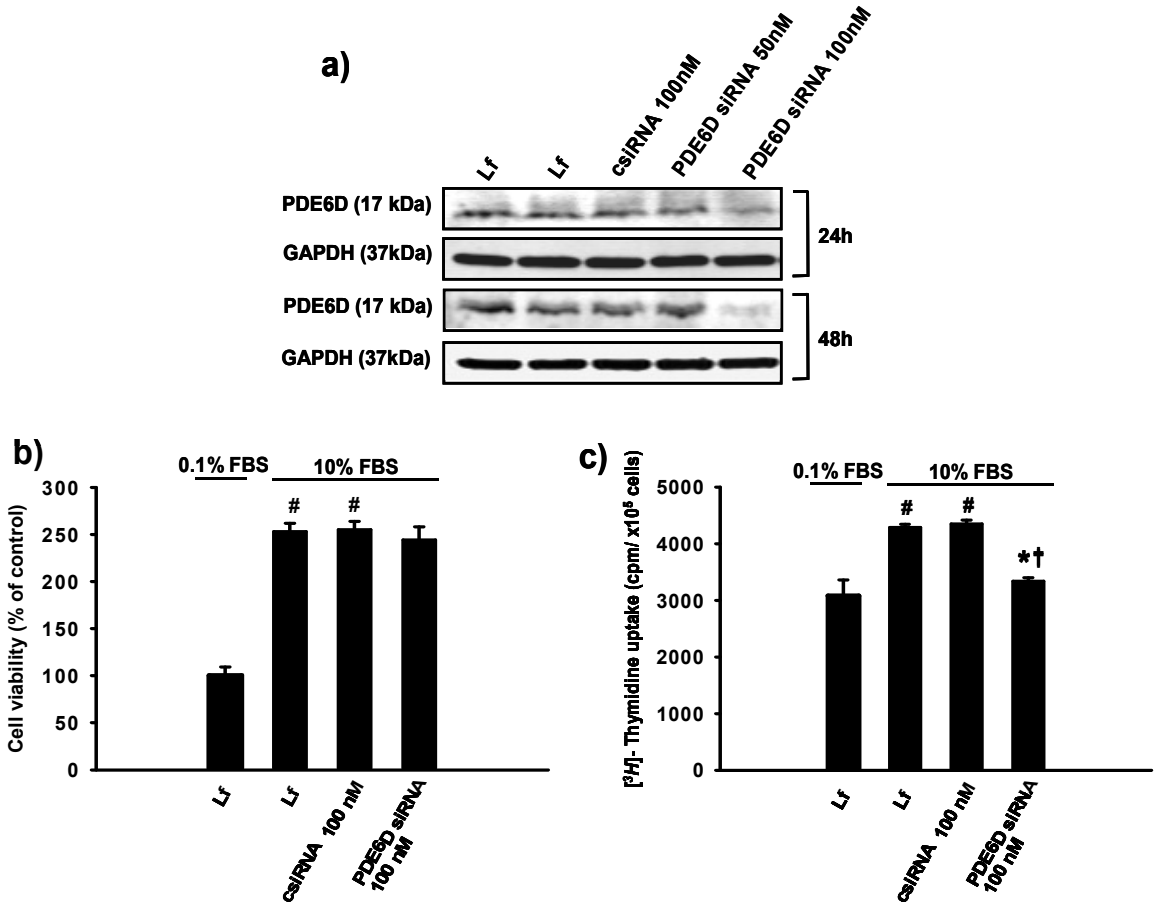

Figure 16. Knockdown of endogenous PDE6D expression decelerates the proliferation rate of human A549 AECs.

a) Demonstration of PDE6D knockdown in A549 cells: upper panel: decreased PDE6D immunoreactive protein 0-48 h post transfection with 100 nM PDE6D siRNA. The negative control siRNA (100 nM) caused no change in PDE6D protein expression. The bottom panel represents GAPDH used as a control for equal protein loading. b) Bar graph presentation of MTT conversion in PDE6D siRNA transfected cells 24 h post serum stimulation. Data were expressed as % of control. Serum stimulation was significant $^{\#}P<0.001$. c) Bar graph presentation of [^{3}H]-Thymidine uptake in PDE6D knockdown cells 24 h post serum stimulation. Data were expressed as cpm/ x10^5 cells. Serum stimulation was significant $^{\#}P<0.001$. [^{3}H]-Thymidine uptake of PDE6D knockdown cells was significantly decreased as compared to control siRNA transfected cells (*$P<0.001$) and no siRNA transfected cells (only lipofectamine (Lf)) ($^{\dagger}P<0.001$). Lipofectamine concentration was kept constant throughout the experimental settings and had no effect on cell viability (P= 0.2699).

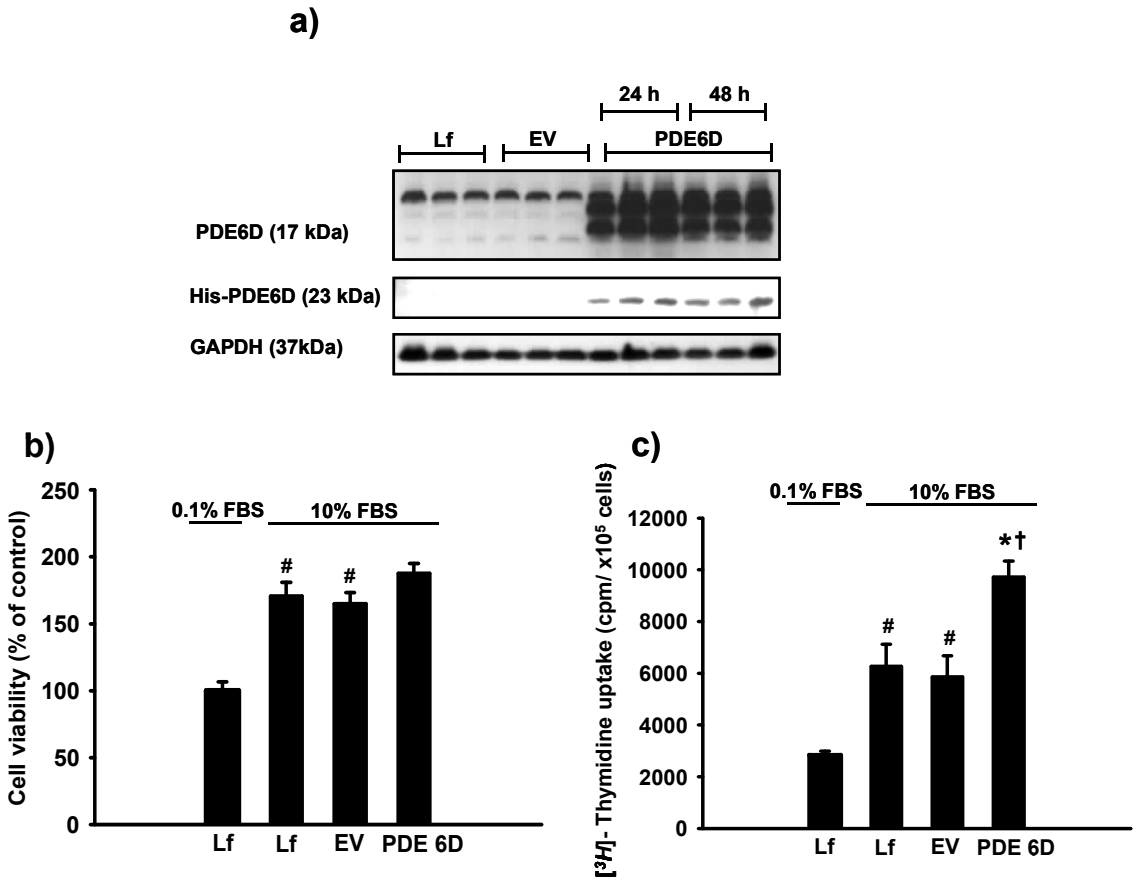

Figure 17. Overexpression of PDE6D accelerates the proliferation rate of human A549 AECs.

a) Demonstration of PDE6D overexpression in A549 cells: upper panel: increased PDE6D immunoreactive protein 0-48 h post transfection with pcDNA3.1/His-PDE6D vector. These expressional changes were not observed in pcDNA3.1/His-lacZ empty vector transfected or no DNA transfected cells (only lipofectamine (Lf)). Middle panel: The membrane was probed with anti –C-His antibody. A band of approximately 23 kDa was detected in the pcDNA3.1/His-PDE6D transfected cells but not in the pcDNA3.1/His-lacZ empty vector transfected or no DNA transfected cells (only lipofectamine (Lf)). The bottom panel represents GAPDH used as a control for equal protein loading. b) Bar graph presentation of MTT conversion in PDE6D overexpressing cells 24 h post serum stimulation. Data were expressed as % of control. Serum stimulation was significant $^{\#}P<0.001$. c) Bar graph presentation of [^{3}H]-Thymidine uptake in PDE6D overexpressing cells 24 h post serum stimulation. Data were expressed as cpm/x10^{5} cells. Serum stimulation was significant $^{\#}P<0.001$. [^{3}H]-Thymidine uptake of PDE6D overexpressing cells was significantly increased as compared to pcDNA3.1/His-lacZ empty vector transfected ($^{*}P<0.01$) and no DNA transfected cells (only lipofectamine (Lf)) ($^{\dagger}P<0.01$). Lipofectamine concentration was kept constant throughout the experimental settings and had no effect on cell viability (P= 0.3552), EV→ empty vector.

4.7. PDE6D knockdown inhibits ERK phosphorylation.

We then, opted to explore signaling pathways related to PDE6D-mediated proliferative responses. In particular, we studied the effects of PDE6D downregulation on serum induced phosphorylation of ERK and AKT proteins in A549 cells. Downregulation of PDE6D by siRNA was found to suppress serum-induced phosphorylation of ERK 24 h post stimulation compared to control siRNA. Whereas, PDE6D had no effect on the phosphorylation status of AKT (Figure 18 a-c).

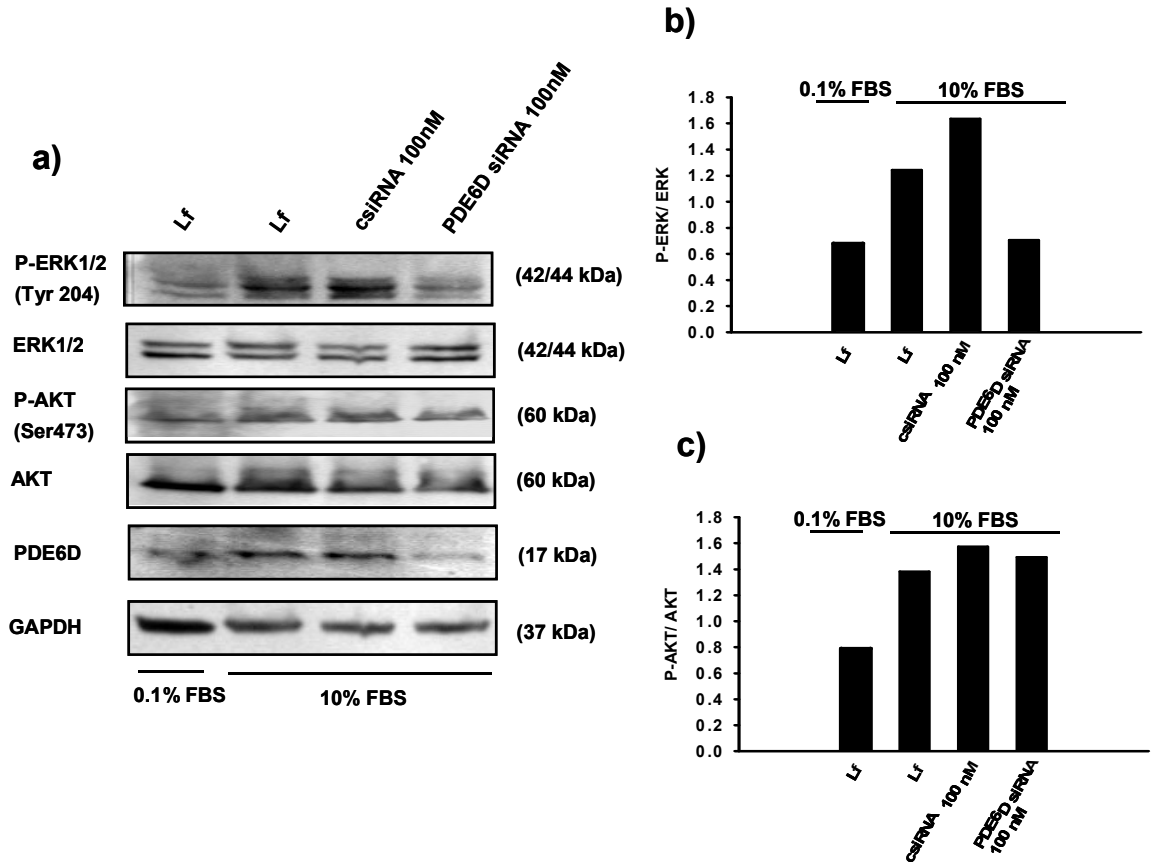

Figure 18. PDE6D siRNA knockdown inhibits serum stimulated ERK phosphoprylation.

a) Western blot analysis of kinase proteins associated with PDE6D knockdown effects in serum stimulated A549 cells (24 h time point), GAPDH is a loading control. b) densitometric analysis of ERK phosphorylation normalized to total ERK. c) Densitometric analysis of AKT phosphorylation normalized to total AKT. Data are representative for two independent experiments.

CHAPTER 5: DISCUSSION

V. Discussion

5.1. mRNA profile of cGMP PDEs in lung tissue samples of donors and IPF patients.

IPF is an unresolved clinical issue. This situation demands a better understanding of the molecular and cellular mechanisms involved in the pathogenesis of IPF. The members of the PDE superfamily, PDE1, PDE2, PDE3, PDE4 and PDE5 are highly expressed in the lung and have been shown to potentially contribute to the pathogenesis of various lung diseases [153-156, 233-235]. Nevertheless, information regarding plausible PDEs contribution into IPF pathogenesis is lagging behind. Several reports have shown the positive effects of the PDE5 inhibitor, sildenafil on the pulmonary hemodynamics and walk distance capacities in patients with pulmonary fibrosis [160, 231]. This brings up an important question whether other cGMP PDEs have a potential relevance to pulmonary fibrosis. Thus the first aim of the present study was to characterize the mRNA expression profile of cGMP PDEs in lung tissue samples of donors and IPF patients. mRNA levels of PDE1A, PDE10A and PDE11A were found increased in the IPF lungs as compared to donor lungs (Figure 11a, b). These mRNA alterations need to be further explored and confirmed on protein level. Characterization of the cellular and subcellular localization patterns of cGMP PDEs in donor and IPF-derived lungs is of interest for future studies, aiming to delineate the functional contribution of these enzymes into IPF pathogenesis.

5.2. Detection of PDE6 enzyme subunits in lung tissue samples of donors and IPF patients.

PDE6 expression and function are thought to be confined to the the retina. PDE6 is extensively studied in the context of retinal degenerative diseases. Nevertheless, reports show that PDE6 might have roles in circadian rhythms in avian pineal gland [236] and that PDE6 activity may be involved with wnt signalling and zebrafish development [237]. Studies regarding lung PDE6 expression and function, however, are lagging behind. Herein, we report previously unrecognized PDE6 expression in the human lung, as evidenced by mRNA and protein detection of all rod and cone subunits, encoding the PDE6 multi-component enzymes (Figure 12, 13). Interestingly, the PDE6 subunits were found differentially altered in the IPF

lungs, with PDE6A and PDE6B 2-fold up-regulated, PDE6D 2-fold down-regulated and PDE6G membrane localized, suggesting a plausible contribution of PDE6 to the pathogenesis of IPF (Figure 13).

To our knowledge this is the first report that has described the expression and characterization of PDE6 isoforms in both the physiology and pathophysiology of the lung. This finding is further supported by the reports that have demonstrated solitary PDE6 subunit expression in a variety of non-retinal tissues. The rod catalytic PDE6A and PDE6B subunits were found to be weakly expressed in brain [238, 239]. Piriev *et al*. demonstrated that the catalytic core of the rod PDE6 enzyme (PDE6A and PDE6B subunits) can be synthesized in human kidney cells with consequent expression of enzymatic activity [240]. The inhibitory and the regulatory PDE6G and PDE6D subunits, respectively, have been reported to be expressed in a variety of heterogeneous tissues, including the lung [225, 241].

5.3. PDE6 enzyme subunits expression in human AECs.

Based on immunohystochemical data all PDE6 subunits were co-stained with pro-SPC, suggesting the presence of PDE6 subunits in the ATII AECs (Figure 14). Furthermore this cellular localization pattern was confirmed by RT-PCR amplification of the PDE6 subunits from human primary donor and IPF-derived ATII cells (Figure 15). Thus, we believe that PDE6 alterations (subsequent cGMP alterations) may play a crucial role in epithelial apoptosis, proliferation, surfactant synthesis and ROS generation. cGMP modulation is further supported by recent reports in the literature that suggest the beneficial effects of sildenafil, a PDE5 inhibitor, in experimental models of pulmonary fibrosis and IPF secondary to PAH [160, 161]. Considering the fact that sildenafil not only inhibits PDE5, but also PDE6 (9 fold less) [242], we believe that the attenuation of pulmonary fibrosis in sildenafil treated mice may be also due to its inhibition of PDE6.

Interestingly the PDE6 subunits displayed different sub-cellular localization pattern. PDE6A and PDE6D immunoreactivity was recognized in the cytoplasm, PDE6B immunoreactivity in the nuclei and PDE6G immunoreactivity in the membrane of ATII cells (Figure 14). The nuclear staining of PDE6B is suggestive for PDE6B playing a role as a transcriptional factor in the alveolar epithelium. The

membraneous staining of PDE6G corroborates with the membrane localization pattern of this subunit in IPF-derived lungs. PDE6G has been reported to function as an important intermediate to regulate mitogen-activated ptotein kinase (MAPK) pathway in animal and cellular models of hypoxia-mediated pulmonary hypertension [243]. PDE6G has been shown to affect receptor internalization-dependent MAPK activity and EGF stimulated/ G-protein coupled receptor kinase 2 (GRK2) mediated MAPK activity in human embryonic kidney 293 cells [244, 245]. Additionally, the PDE6G subunit has been shown to modulate the proteolysis of PDE5 by caspase-3 in mouse lung and testis [246]. Thus, we could predict that PDE6G detected in the lung alveolar epithelium and membrane-localized in IPF-derived lungs might affect AEC proliferation, apoptosis and/or transdifferentiation.

5.4. Functionality of PDE6.

Although at present the physiological roles of the rod and cone PDE6 enzymes in the lung are unknown and the functionality of PDE6 enzyme in IPF needs to be confirmed, the study of Wang *et al*. [220] does provide evidence for the presence of functional PDE6 enzyme in non-retinal tissues. The authors claimed PDE6 to be an effector for the Wnt/Ca^{2+}/cGMP signalling pathway in development, which is mediated by Frizzled-2 receptors. Supplementary, the study of Ma L *et al.* describes a central role of PDE6 in Wnt5a mediated cGMP responses [247].

To carry out studies on the structure and function of PDE6 in normal and diseased conditions of the lung, each of the biologically active subunits of the enzyme is necessary. Our immunohystochemical data (Figure 14) are suggestive for possible PDE6 complex assembly in ATII cells. Nevertheless, analysis of a functional PDE6 assembly is tricky, considering the unique characteristics of these enzymes. Moreover, research carried out in bacteria and in yeast systems have failed to yield expression of functional PDE6 complexes that have all of the properties of the native enzymes [248-252].

Interestingly, there is evidence of independent catalytic activity of PDE6 subunits from bovine heart and adrenal cortex [253]. In line, Piriev *et al.* have demonstrated that the PDE6A and PDE6B subunits can be synthesized in human kidney cells with consequent expression of enzymatic activity. In deed, the domain organization of PDE6A and PDE6B subunits is suggestive for their independent cGMP-

hydrolytic activity. This is of particular importance since this may mean that rod PDE6 subunits in the lung may be present and functional not only as αβγγ heterotetramer, but also as ααγγ and ββγγ complexes. PDE6 of other tissues have this type of composition. For example, the catalytic subunit of cone cGMP-PDE exists as a homodimer, α'α' [254], and the catalytic and allosteric domains of PDE6 from bovine heart and adrenal cortex are also homodimeric [253].

Intriguingly, a significant body of research shows that recessive retinitis pigmentosa is associated with mutations in the PDE6A and PDE6B genes [255, 256]. In line, an absence of PDE6 activity accompanied by elevation of cGMP levels had been described in animal models of retina degeneration. Rapid photoreceptor degeneration is ensued in mice by a recessive nonsense mutation in the PDE6B subunit (rd1 mice). A defect in the corresponding canine PDE6B subunit gene causes another retinal degenerative disorder (rcd1) in Irish setters, and a defect in the PDE6A subunit gene in Cardigan Welsh corgi dogs (rcd3) generates a similar phenotype [222]. We could speculate that mutations in the PDE6A and PDE6B genes might be associated with inherited form of IPF and that these mutations might increase the susceptibility to IPF development.

5.5. Individual functional capacity of PDE6D.

The individual functional capacity of the specific PDE6D subunit has been widely speculated in the literature. PDE6D functionality is mainly linked to its prenyl protein binding properties. It is assumed that PDED interacts with proteins that carry COOH-terminal CAAX sequence in two distinct ways: 1) through a lipid binding pocket and 2) β-sheet/β-sheet interactions [227]. The list of PDE6D interacting partners comprises of: PDE6A and PDE6B catalytic subunits of the rod PDE6 enzyme, rhodopsin kinase, the γ subunit of transducin, lamins A and B, the γ subunits of heterotrimeric G proteins, [257], small GTPases of the Ras superfamily, including Ras and Rap [221], Rho6 and Rheb [227], and Rab8 [214].

The Ras/ERK and Ras/AKT signaling pathways mediate the proliferation and differentiation of many cell types [258-261]. ERK activation has been shown to be of critical importance for ATII cell proliferation [261]. ERK signaling has also been

documented to regulate differentiation of fetal ATII cells [262]. Akt signaling has been implicated in lipogenesis pathways required for surfactant protein synthesis [263, 264]. Additionally, AKT activation has been shown to have a protective function in the context of lung injury [265]. These observations led us to hypothesize that PDE6D might regulate the proliferation rate of ATII cells.

We were able to show that PDE6D exerts pro-proliferative effects in AECs, as deduced from PDE6D siRNA-mediated knockdown and overexpression studies in an A549 human AEC line (Figure 16, 17). Further, our study indicates that PDE6D mediated proliferative responses are related to ERK phosphorylation status. siRNA mediated inhibition of PDE6D decreased the serum induced phosphorylation of ERK (Figure 18). Thus, we propose PDE6D as a critical regulator of ERK mediated ATII cells proliferation. This functional property of PDE6D is significant, considering its c-Myc/E2F4 controlled expression. In line with our hypothesis, PDE6D (-/-) mice are consistently smaller in size, indicating a plausible involvement of PDE6D in growth arrest [266]. Thus, it can be imagined that the proliferative phenotype of IPF-derived ATII cells is associated with the observed PDE6D depletion in IPF lungs.

Based on the unique functional properties of the PDE6D subunit, it is tempting to further speculate that the PDE6D subunit itself might directly affect the rate of cGMP hydrolysis. The study of Cook TA *et al.*,in deed, does demonstrate that PDE6D can modify cGMP hydrolytic activity in preparations of broken rod outer segments and that these effects might be due to PDE6D ruled solubilization of PDE6, involving functional uncoupling of transducin [267].

5.6. Summary points.

cGMP PDEs are key enzymes in cellular signaling pathways. Several lines of evidence have underlined the broad therapeutic potential of cGMP PDE inhibitors. PDE5 inhibitors such as sildenafil, tadalafil and vardenafil have had distinctive clinical benefit and notable commercial success. Thus, the topic questioned in the present PhD thesis “Role of cGMP PDEs in IPF is of significant importance. The data shown demonstrate that:

1. Multiple cGMP PDE isoenzymes are expressed in human lung.

2. PDE1A and PDE10A and PDE11A mRNA expression is alterated in IPF lungs as compared to donor lungs.

3. PDE6 mRNAs and proteins are expressed in human lung.

4. Protein levels of the individual PDE6 subunits are differentially altered in IPF lungs as compared to donor lungs:

5. The individual PDE6D subunit has a specific functional role in AEC proliferation (siRNA – mediated knockdown and ectopic expression studies)

6. PDE6D effects on AEC proliferation are related to ERK phosphorylation (siRNA-mediated knockdown studies).

5.7. Future issues.

The present report opens up numerous questions in specific need to be addressed in future studies:

(1) The physiology of rod and cone PDE6 enzymes in the retina is remarkably distinct. Rod PDE6 provides for the scotopic vision and cone PDE6 provides for the photopic vision. More specific research is required to characterize the physiological roles of rod and cone PDE6 subunits in the lung. Can rod and cone PDE6 subunits govern different physiological process in the lung? Do they have same, different or opposing functions in the lung? Cone PDE6 subunits are 10-fold less abundant than rod PDE6 subunits in the photoreceptors. However, vison alterations in color perception, reported following sildenafil usage are suggestive for preferential targeting of cone PDE6 [268]. Logistically, what is the susceptibility of rod and cone PDE6 subunits, expressed from lung, to PDE5-targeted drugs? Are cone PDE6 subunits more sensitive? Attempts to address these questions might utilize the already available methods for rod and cone PDE6 enzymes purification from retina (Figure 19). Specific antibodies that detect cone PDE6 subunits are of specific need.

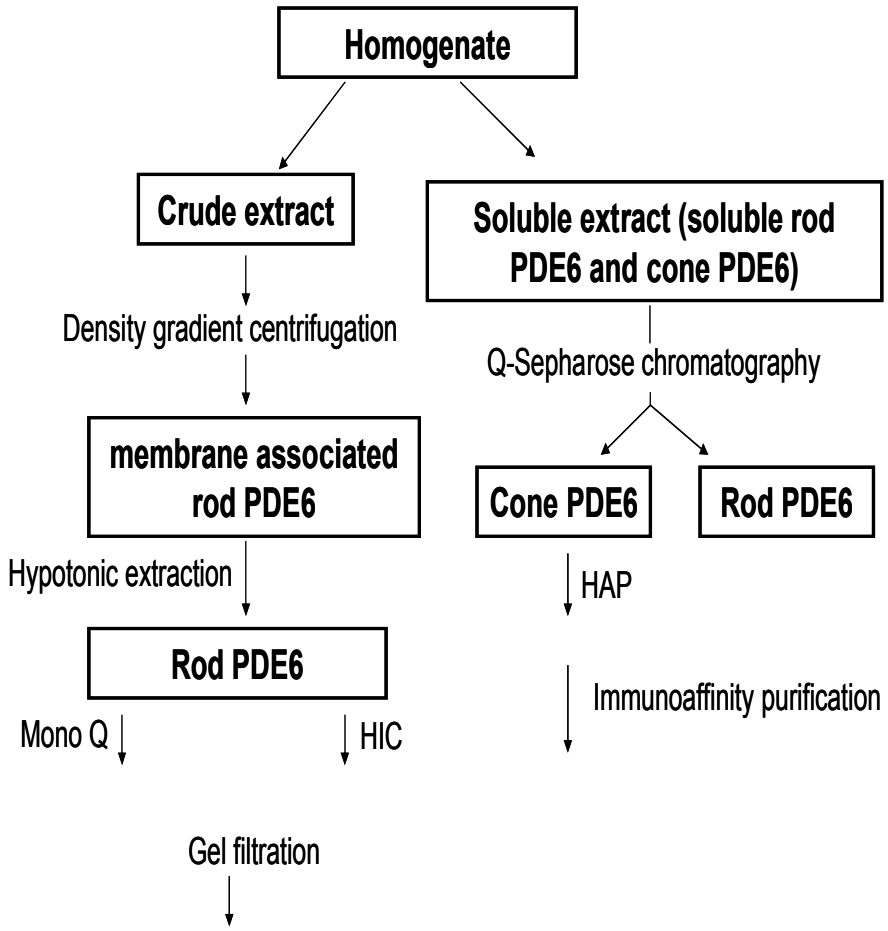

Figure 19. Schematic presentation of the major strategies used to purify rod PDE6 and cone PDE6 enzymes from retina.

Mono Q- anion-exchange chromatography using Mono G resin, HIC-hydrophobic interaction chromatography on butyl-Sepharose resin, HAP- hydroxyapatite chromatography, adapted from [269].

(2) PDE6 is dedicated to high affinity specific hydrolysis of cGMP. Indeed, the retinal PDE6 enzyme operates with a very high catalytic efficiency for cGMP [$k_{cat}/K_M = 4 \times 108\ M^{-1}s^{-1}$[211]. Are the low substrate affinity (K_M = 20 µM for cGMP) and the high catalytic constant (K_{cat} up to 8000 cGMP hydrolyzed per sec) unique characteristics of retinal PDE6? Or lung PDE6 is subjected to a millisecond timescale activation as well? For getting an initial answer to that question rod and cone PDE6 enzymes isolated from human lung could be subjected to *in vitro* kinetic assay.

(3) Regarding PDE6 cGMP specificity, another interesting point would be to figure out which pool of cGMP synthesis PDE6 controls in the lung. It could be hypothesized that PDE6 is a part of the sGC pathway, particulate GC pathway, or both pathways. Such possibilities could be tested by using natriuretic peptides, which elevate cGMP via the particulate GCs and NO-donor like DEA-NO, which stimulates the sGC in cell culture models, where the catalytic subunits of PDE6 (PDE6A, PDE6B and PDE6C) are genetically modified (siRNA silenced and/or overexpressed).

(4) Another remaining issue is to characterize PDE6 expression pattern in mouse and rat lungs. It remains to be seen whether rodent lung expresses PDE6 enzyme subunits. A paucity of data exists on the degree of similarity/identity between rodent and human PDE6 enzymes, expressed from lung. The cellular and sub-cellular localization of the PDE6 subunits in rodent lung is of further interest. Such information will aid future studies aiming to characterize PDE6 subunits expression, regulation and function in animal models of pulmonary fibrosis.

(5) A number of approaches exist for inducing pulmonary fibrosis in animal models (Table VI). The most commonly used is the bleomycin model. This model is extensively studied in our group. Thus, further analysis of PDE6 subunits expression in bleomycin-challenged rodent lungs is of significant importance, so as to validate the noted regulation pattern of the PDE6 subunits in IPF-derived human lungs (Figure 13). It is worth mentioning, that the rat bleomycin model is of better value to study alterations in the alveolar epithelium, considering the significant similarities of alveolar structural remodeling (*i.e.* intra-alveolar buds formation,

mural incorporation of collagen and obliteration of the alveolar space), observed in IPF lungs and bleomycin-challeged rat lungs [270].

Table VI. Approaches for inducing pulmonary fibrosis in animal models.

Exogenous Agent/Approach	Nature of Tissue Damage	Animal Species Used
Bleomycin	Oxidant-mediated DNA scission leading to fibrogenic cytokine release	Mice, rats, hamsters, rabbits
Inorganic particles (silica, asbestos)	Type IV hypersensitivity reactions with or without granuloma formation	Mice, rats, hamsters, sheep, rabbits
Irradiation	Free radical-mediated DNA damage	Mice, rats, rabbits, dogs, hamsters, sheep, primates
Gene transfer (TGF-β, IL-1β, GM-CSF)	Downstream activation of specific cytokine pathway/s	Mice, rats
Fluorescein isothiocyanate	Incompletely understood. Presumed T-cell-independent.	Mice
Vanadium pentoxide	Incompletely understood. An inorganic metal oxide.	Mice, rats
Haptenic antigens (e.g. trinitrobenzene sulphonic acid compounds)	Recall cell-mediated immune response	Mice, hamsters

Adapted from [271].

(6) As a next step, one could consider the possibility of PDE6 targeted therapy for bleomycin-induced pulmonary fibrosis and perspectively for IPF. As a matter of a fact several classes of PDE inhibitors equally well inhibit PDE6 as the PDE family to which they are targeted. These effects are most prominent for the PDE5 family. Indeed, most of the PDE5-targeted drugs could be considered PDE5/6 inhibitors (Table VII). Nevertheless, PDE5/6 inhibitors such as sildenafil, vardenafil, tadalafil, and zaprinast display different selectivity threshold for PDE5 and PDE6 [242, 272, 273]. Sildenafil shows 9 folds selectivity for PDE5 over PDE6. Vardenafil is 15 fold more potent for PDE5 than for PDE6. Only, tadalafil [selectivity ratio of 210 (cone PDE6) or 640 (rod PDE6)] represents an authentic PDE5-selective inhibitor. Interestingly, zaprinast, a first generation PDE5-targeted inhibitor (which also weakly inhibits PDE1 with a 10-fold higher K_I value), has 10-fold higher potency for PDE6 than for PDE5 (Table VII), and could be considered a “PDE6-selective” inhibitor [274, 275]. Thus, a goal of a future study could be to compare the effects of vardenafil and zaprinast on the development and progression of bleomycin-induced lung fibrosis. The inhibitors’ effects could be estimated with respect to

survival rate, inflammation, collagen deposition and emphysema formation. It remains to be seen which inhibitor will have better effect. It could be evaluated as well whether the combination of vardenafil and zaprinast confers an additional beneficial effect. When assessing the effectiveness of PDE6 inhibition (cGMP hydrolysis) one should consider the calcium feedback mechanism this enzyme is subjected to (at least in the retina, Figure 10). PDE6 inhibitor ineffectiveness could be due to elevated intracellular calcium levels, resulting in GC inhibition.

PDE5/6 inhibitors have been claimed to have side effects on photoreceptor viability and visual function [268]. These side effects, however, have been considered related to the systemical administration of the inhibitors. Moreover, Behn D *et al.* have shown that sildenafil has a substantial side effects on retinal function in PDE6G knockout mice, but not in their wild type littermates [276]. Based on our findings mRNA transcripts of all PDE6 subunits are expressed from lung, including the inhibitory PDE6G and PDE6H subunits. Thus, it is reasonable to asume that inhibitor targeting therapy of lung PDE6 would not prove major adverse or irreversible side effects on retinal function, if any.

Table VII. Efficacy and selectivity of PDE inhibitors to inhibit purified, activated bovine rod and cone PDE6.

Class	Inhibitor	PDE(X) K_I (nM)[a]	PDE6 K_I (nM)[b] Rod	PDE6 K_I (nM)[b] Cone	6R/6C	Selectivity[c] 6R/X	Selectivity[c] 6C/X
1	vinpocetine	11500	21000 ± 6100	13000 ± 1200	1.6	1.8	1.1
	8-Me-IBMX	3300	1600 ± 100	430 ± 30	3.7	0.5	0.1
2	EHNA	2500	28000 ± 2400	13000 ± 1600	2.2	11	5
3	cilostamide	10	2800 ± 170	3400 ± 660	0.8	280	340
4	rolipram	490	28000 ± 620	22000 ± 4000	1.3	57	45
	YM 976	3.3	19000 ± 1500	5200 ± 630	3.7	5760	1580
5	tadalafil	3.3	2100 ± 150	700 ± 60	3.0	640	210
	dipyridamole	580	480 ± 30	190 ± 14	2.5	0.8	0.3
	T-1032	1.2	75 ± 12	26 ± 7	2.9	63	22
	T-0156	23[d]	51 ± 4.0	61 ± 5	0.8	2.2	2.6
	zaprinast	325	30 ± 3.0	32 ± 6	0.9	0.1	0.1
	sildenafil	4.4	11 ± 1.0	4.7 ± 0.5	2.3	2.5	1.1
	E4021	2.9	2.9 ± 0.5	2.9 ± 0.5	1.0	1.0	1.0
	vardenafil	0.25	0.71 ± 0.06	0.3 ± 0.03	2.4	2.8	1.2
NS	IBMX	--	4490 ± 804	1410 ± 453	3.2	--	--

[a]Average of K_I values for each family of PDE obtained from the literature. IBMX is non-selective (NS); [b] The K_I was determined from the equation: $K_I = IC_{50}$ (1+ [cGMP]/K_M), where the IC_{50} was obtained from the dose-response curve for each inhibitor for rod and cone PDE6 and the KM values for bovine rod and cone PDE6 are 14 μM or 7.0 μM, respectively; [c] Selectivity is defined as the ratio of the $_{KI}$ values for the two indicated PDEs: 6R = rod PDE6; 6C = cone PDE6, and; X = PDE family 1 through 5; [d] Reported value is the IC_{50}, because the K_I value could not be calculated, adapted from [275].

(7) Identifying the expression of PDE isoforms in organs and cells that had not been reported previously is a subject gaining interest. Recently, PDE5 expression was reported in vascular, ganglion and bipolar cell layers of retinal tissue apart from the lung vasculature, and it was claimed to play a physiologic role in the retina and that there are PDE5 inhibitor-associated ocular side effects [277]. Importantly, the study of Foresta C *et al.* questions the differential expression pattern [211, 278, 279] of PDE5 and PDE6 enzymes. Our report on lung PDE6 expression is of further support to this notion. As a matter of a fact PDE5 and PDE6 enzymes resemble not only in their (i) pharmacological properties [272], but show as well high similarity in their: (ii) amino acid sequence composition [280], (iii) strong preference for cGMP over cAMP as a substrate at the catalytic site [281], (iv) catalytic requirement for divalent cations, including high-affinity binding sites for zinc ions that likely serve a structural role as well [282, 283], (v) the presence of a γ-like protein that may associate with both enzymes [284, 285]. Thus, pending questions are: How the catalytic activities of these two closely related enzymes can be discriminated? What are the differences in the drug interaction sites within the catalytic domains of PDE5 and of the various PDE6 isoforms, expressed from lung?

Catalytic site inhibitors: Rational drug design of compounds, which better discriminate PDE5 from PDE6, would require a deeper understanding of the molecular architecture of the active sites of PDE5 and rod/cone PDE6 enzymes, expressed from lung.

GAF domains manipulations: A particulary attractive option for discriminating between PDE5 and PDE6 may represent manipulation of cGMP binding to the regulatory domains in these two enzymes. Two types of functional ligands could be

designed to bind GAF domains: agonists and antagonists. Considering the differential regulation of PDE5 and PDE6 by cGMP. It can be imagined that agonist binding to the GAFa domain in PDE5 would result in permanent activation of the enzyme. Whereas agonist binding to the regulatory GAFa domain of PDE6 would result in an inactivation of the enzyme. And vice versa antagonizing cGMP binding to the GAFa domain in PDE5 should result in an enzyme inactivation. Whereas antagonizing cGMP binding to the GAFa domain in PDE6 should stimulate enzyme activity. Drug design at the GAFa domains might be a good strategy for attaining a higher selectivity pattern for PDE5 over PDE6 and vice versa than achieved with catalytic site inhibitors [286].

Rd mice: A plausibility to differentiate the roles of PDE5 and PDE6 enzymes in the lung is suggested by the study of Kuenzi F *et al.* [238]. The authors intelligently explored the options of a naturally occurring mutation in mice (rd mice) to study PDE6B function in the hippocampus. In rd mice, alterations in the PDE6B gene due to a single nonsense mutation (C to A transversion in codon 347) [287] and/or an integration of provirus Xmv-28 [288], causes a PDE6 loss of activity. Interestingly, a hippocampal phenotype for the rd mutation has been identified. Rd mutation has been shown to decrease the number of interneurons and granule cells in the adult dentate gyrus [289]. Thus, it is tempting to postulate that rd mice would prove to have a lung phenotype as well. To further study the fuction of PDE6 in the lung one could compare the responses of rd/rd and wild-type mice to relatively selective PDE5 and PDE6 inhibitors, *i.e*. vardenafil and zaprinast. Similar experimental settings could be utilized to study PDE6 contributions to pulmonary fibrosis, *i.e.* one could compare the pulmonary characteristics of rd/rd and wild type bleomycin-treated mice. PDE5/6 inhibitory studies could be undertaken in such scenario as well.

Knockout animal models: In addition to the naturally occurring rd mutation, investigations using mice with tissue-specific conditional gene disruption and RNA interference might be the best feasible option to probe lung PDE5 and PDE6 activities and validate inhibitors' targets. For example, by using the Cre-loxP site-specific recombination system, tissue-specific mouse mutants could be generated in which PDE5 protein is ablated in ATII cells (Cre recombinase under Pro-SPC/ CC10 promoters). It could be imagined that evaluating PDE5/6 inhibitors in such conditional inactivation of PDE5 would give unbiased information about PDE6

functionality in the alveolar epithelium. What would be the responses of such knockout mice to bleomycin treatment is another interesting point.

(8) In the retina, both Nrl and Crx are required for full transcriptional activity of the PDE6A gene [290], whereas Sp proteins have been implicated in the transcriptional regulation of the PDE6B gene [291, 292]. Characterization the promoter regions of PDE6 catalytic subunits, expressed from lung is an important issue. Do Nrl and Crx transactivate lung PDE6A promoter? Are Sp proteins involved in transactivation of lung PDE6B promoter? Or does the lung itself possess unique factors that control the transcription of the PDE6 catalytic subunits? To address such questions one should consider that promoter regions of genes that are transcriptionally active are often demarcated by a DNase I-accessible open chromatin region. Thus, to assess the chromatin status of the region around the PDE6A and PDE6B promoter region *in vivo*, a DNase I hypersensitivity assay could be performed with A549 cells, which transcribe PDE6A and PDE6B mRNAs (Figure 15c). To further delimit the core promoter regions of PDE6A and PDE6B, luciferase reporter gene constructs containing varying lengths of PDE6A/B promoter regions could be assayed by transient its are expressed in human ATII cells. □ PAGEREF _Toc213403314 \h □□59□ Fassay (EMSA) can be used to determine the relative binding strength of each potential promoter binding site.

Gaining such information will aid future studies aiming to delinate cone and rod PDE6-specific functions in the lung. For example, the Nrl (-/-) mouse is a promising mouse model for the investigation of cone function. This is so because, the developing Nrl (-/-) retina produces no rods [293]; rather, it is populated with photoreceptors exhibiting ultrastructural, histochemical, molecular, and kinetic features that support the hypothesis that they are indeed cones [294]. It remains an open possibility to see whether such scenario could be applied in the context of the lung.

(9) PDE6 is known for the fact that it undergoes numerous post-translational modifications resulting in carboxymethylation and isoprenylation of the C-terminus of the catalytic subunits. The incorporation of a farnesyl group (PDE6A subunit) or

a geranylgeranyl group (PDE6B) accounts for the high-affinity interaction of rod PDE6 with photoreceptor membranes [252, 295]. The PDE6G also acts as a substrate for phosphorylation at several distinct sites, *i.e.* PDE6G phosphorylation at Thr (22) or Thr (35) has little effect on the PDE6 holoenzyme itself, but greatly diminishes the ability of activated transducin to bind the PDE6G subunit and relieve inhibition of catalysis [296]. PDE6G phosphorylation at Thr (62) in human embryonic kidney 293 cells has been reported to regulate mitogenic signaling [244]. Scarcity of data exists on potential regulation of PDE6 catalytic subunits by phosphorylation. Further research should opt to characterize the posttranslational modifications the lung PDE6 enzymes might be subjected to (phosphorylation, farnesylation, geranyl-geranylation, methylation etc.).

(10) Characterization of PDE6 subunits expression and function in other pulmonary disease models could be of particular interest as well. We currently lack knowledge of the prevalence and functions of PDE6 in pulmonary vasculature, endothelium and in other tissues of the lung. For example, a goal of a future study could be to characterize PDE6 subunits expression profile in monocrotaline and hypoxia–induced pulmonary hypertension models. These models are well characterized in our group [297, 298]. Plausible beneficial effects of PDE6 inhibition (zaprinast) on pulmonary hemodynamics, pulmonary vascular remodeling, and survival could be anticipated. PDE5 and PDE6 roles in such models could be compared as well (inhibitory studies with vardenafil, sildenafil, zaprinast).

(11) One of the salient findings of this study was that PDE6D have a role in ATII cells proliferation. The challenge remains, however, to confirm PDE6D functionality *in vivo*. It could be interesting to see the responses of PDE6D (-/-) mice [266] to bleomycin treatment. However, the best feasible option to study PDE6D function *in vivo* would be to generate tissue-specific mouse mutants in which the PDE6D protein is ablated in ATII cells (Cre recombinase under Pro-SPC/ CC10 promoters) and study the responses of such mice to bleomycin treatment. It remains to be seen whether such mice would develop more severe pulmonary fibrosis. In that line, it is tempting to further speculate that PDE6D overexpression in animal models of pulmonary fibrosis (bleomycin etc.) may be beneficial to boost up alveolar re-epithealization and reduce or reverse the development of pulmonary fibrosis.

APPENDIX

VI. Appendix

Table I. Classification and contrasting histological features of IIPs.

Clinical presentation	**IPF/CFA**	NSIP	RB-ILD	DIP	AIP	LIP	COP
Histopathological pattern	**UIP**	NSIP	RB	DIP	AIP	LIP	COP
Distribution	**patchy (periphery of the acinus or lobule)**	diffuse	patchy (bronchiolocentric)	diffuse	diffuse	diffuse	patchy (centrilobular)
Spatio-temporal appearance	**heterogeneous**	homogeneous	homogeneous	homogeneous	homogeneous	homogeneous	homogeneous
Interstitial inflammation	**scanty**	prominent in cellular pattern	scanty (peribronchiolar)	scanty	scanty	prominent	scanty
Collagen fibrosis	**patchy**	prominent in fibrotic pattern	variable, if any, mild and peribronchiolar	variable, if any, diffuse	_	rare	rare
Fibroblast proliferation	**prominent, but focal (FF)**	prominent and diffuse in fibrotic pattern, rare FF	_	_	prominent and diffuse (no FF)	_	intra-alveolar prominent and patchy (Masson's bodies)
OP foci	**Rare**	occasional	_	_	_	rare	+
Intra-alveolar macrophage accumulation	**Focal**	occasional	peribronchiolar	diffuse	_	occasional, mild	_

IPF idiopathic pulmonary fibrosis, CAF cryptogenic fibrosing alveolitis, UIP usual interstitial pneumonia, NSIP non-specific interstitial pneumonia, RB-ILD respiratory bronchiolitis-associated interstitial lung disease, DIP desquamative interstitial pneumonia, AIP acute interstitial pneumonia, LIP lymphoid interstitial pneumonia, COP cryptogenic organizing pneumonia, FF fibroblastic foci, OP organizing pneumonia, summerized from [299, 300]

Table II. Properties of cyclic nucleotide PDE families.

Gene Family	Descriptive name	Substrate specificity	Regulation	Tissue expression	Intracellular localization	Inhibitors
PDE1A (1-4) PDE1B (1) PDE1C (1-6)	Ca2+/CAM stimulated PDE	cAMP < cGMP cAMP < cGMP cAMP & cGMP	(+) Ca2+/CAM (-) PKA, CamKII	Brain, heart, smooth muscle, olfactory cilia, testis	cytosolic	8-Methoxymethyl IBMX, Vinpocetine, SCH-51866
PDE2A (1-3)	cGMP-stimulated PDE	cAMP & cGMP	(+) cGMP, PKC (+/-) N terminal targeted domain	Adrenal cortex, brain, heart	PDE2A2, PDE2A3 membrane-bound, PDE2A1 cytosolic	EHNA, Trequinsin
PDE3A (1) PDE3B (1)	cGMP-inhibited PDE	cAMP > cGMP	(+) PKA, PKB (-) cGMP (+/-) N-terminal targeting domain	Heart, adipose tissue, pancreas, platelets	Membrane-bound or cytosolic depending on the splice variant and the cell type it is expressed in	Cilostamide, Cilostazol, Enoximone, Imazodan, Milrinone, Trequinsin
PDE4A (1-7) PDE4B (1-2) PDE4C (1-4) PDE4D (1-6)	cAMP-specific PDE	cAMP	(+) PKA, ERK, Phosphatidic Acid (-) ERK, Caspases (+/-) N-terminal targeting domains	Inflammatory cells, Lung, testis (human)	Membrane-bound Cytosolic or particulate fractions	Rolipram, YM976
PDE5A (1-3)	cGMP-specific PDE	cGMP	(+) cGMP, PKG, PKA (-) Caspases	Lung, platelets, smooth muscle, Corpus cavernosum	cytosolic	Dipyridamole, DMPPO, Sildenafil, T-0156, T-1032, Tadalafil, Vardenafil, Zaprinast
PDE6A (1) PDE6B (1) PDE6C (1) PDE6D (1) PDE6G (1) PDE6H (1)	**Photoreceptor cGMP-specific PDE**	**cGMP**	**(+) Transducin (-) cGMP, PDE6D and PDE6G/H**	**Rod and cone photoreceptor outer segments**	**Targeted to the membrane by isoprenylation Cytosolic by virtue of its association with the PDE6D subunit**	**Dipyridamole, Sildenafil, Tadalafil, Vardenafil, Zaprinast**

PDE7A (1-3) PDE7B	cAMP-specific PDE	cAMP	(+/-) PKA	Skeletal muscle, T-cells, B-cells	cytosolic	Dipyridamole
PDE8A PDE8B	cAMP-specific PDE	cAMP	PAS domain	Testis, liver, kidney Eye (human)	Cytosolic or particulate fractions	Dipyridamole
PDE9A (1-4)	cGMP-specific PDE	cGMP		Kidney, liver (human)	PDE9A5 cytosolic, PDE9A1 nucleous	Sildenafil, Zaprinast
PDE10A (1-2)	cAMP-inhibited cGMP PDE	cAMP < cGMP	(-) cAMP	Brain, testis (rat) Multiple (human)		Dipyridamole
PDE11A (1-4)	Dual specific cGMP binding PDE	cAMP and cGMP		Skeletal muscle, testis, prostate (human)	cytosolic	Zaprinast, dipyridamole, tadalafil

EHNA *erythro*-9-(2-hydroxy-3-nonyl)adenine, IBMX 3-isobutyl-1-methylxanthine, Ca2+/CAM calcium/calmodulin, Summerized from [301, 302].

Table III. Gene specific primer sequences and RT-PCR conditions.

gene (bp)	Primers (5'→3')	Gene accession number	Annealing T (°C°)	# of cycles	Extension time (min)
PDE1A (240)	F-ctggttggcttctacctttacac R-ctatgctctccacttgcttcatt	NM_001003683	58	35	1
PDE1B (199)	F-acattctctgtgctgactgacg R-ccttccatttctgcttattctcc	NM_000924	58	35	1
PDE1C (222)	F-gtcacttccaacaaatcaaagc R-ggtcacacagaggagaaaaagg	NM_005020	58	35	1
PDE5A (245)	F-ctattccctgttccttgtctgtg R-tgctttgtgtcttgtagcctgta	AY264918	58	35	1
PDE9A (193)	F-acctgatgggttcaagcagat R-tggacggacctcgttagagata	AF067226	58	35	1
PDE10A (207)	F-gagatgaacgatttccaagagg R-gaccctgatgtattgctactgaa	NM_006661	58	35	1
PDE11A (203)	F-actgtgtaggtggcttttgaca R-cattgttggttcccctgtg	NM_016953	58	35	1
PDE6A (176)	F-tggcaaagaggacatcaaagt R- taatcatccatccagactcatcc	NM_000440	58	35	1
PDE6B (163)	F-gcagaacaataggaaagagtgga R-caggatacagcaggttgaagact	NM_000283	58	35	1
PDE6C (240)	F-aagaatgttttgtccctgccta R-aagagtggctttggtttggtt	NM_006204	58	35	1
PDE6D (248)	F-ggatgctgagacagggaagata R-gccaggtatttgtggagttagg	NM_002601	58	35	1
PDE6G (230)	F-gacagaccaggcagttcaagag R-tgagcagggtttagagcacagt	NM_002602	58	35	1
PDE6H (141)	F-gacaacactactctgcctgctc R-gtcatctccaaatcctttcacac	NM_006205	58	35	1
GAPDH (461)	F-caccgtcaaggctgagaac R-cagtagaggcagggatgatgtt	M33197	56	35	1
β Actin (424)	F-actcttccagccttccttcct R-gccaatctcatcttgttttctg	M33197	56	35	1
PDE6D (452)	F-accagagtgagaaagccg R- cagtttcctcctccctccaa	NM_002601	60	35	3
Pro-SPC (191)	F-gaggctctcaatagaaaagtccac R-ctagatgtagtagagcggcacct	NM_003018	59	30	1

Table IV. Primers used for cloning.

Gene	Primers (5'→3')	Plasmid	Aplication
PDE6D (452)	F- accagagtgagaaagccg R- cagtttcctcctccctccaa	pGEMT-easy	cloning
PDE6D (452)	F- ***cacc***atgtcagccaaggac R- aacatagaaaagtctcactctgga	pcDNA 3.1	cloning
T7	F- taatacgactcacattaggg	pGEMT-easy pcDNA 3.1	sequencing
SP6	R- tatttaggtgacactatag	pGEMT-easy	sequencing
BGH	R- tagaaggcacagtcgagg	pcDNA 3.1	sequencing

Table V. Characteristics of IPF patients with UIP pattern.

No	Diagnosis	Gender	Age (yr)	Ex-smoker	Current smoker	FEV1 (%)	FVC (%)	$TLCO_{SB}$ (%)	TLCO/VA (%)
1	IPF (UIP)	male	58	yes	no	63	55	na	na
2	IPF (UIP)	male	23	yes	no	61	56	29	39
3	IPF (UIP)	male	65	no	no	40	32	27	58
4	IPF (UIP)	female	42	no	no	53	50	na	na
5	IPF (UIP)	male	68	no	no	37	41	17	35
6	IPF (UIP)	female	62	no	no	37	34	32	74
7	IPF (UIP)	female	66	yes	no	75	48	na	na
8	IPF (UIP)	male	56	yes	no	32	35	29	na
9	IPF (UIP)	male	63	yes	no	47	44	na	na
10	IPF (UIP)	female	54	yes	no	40	33	na	na

FEV= forced expiratory volume, FVC= forced vital capacity, TLCO= carbon monoxide lung transfer factor, SB= single breath, VA= alveolar volume,

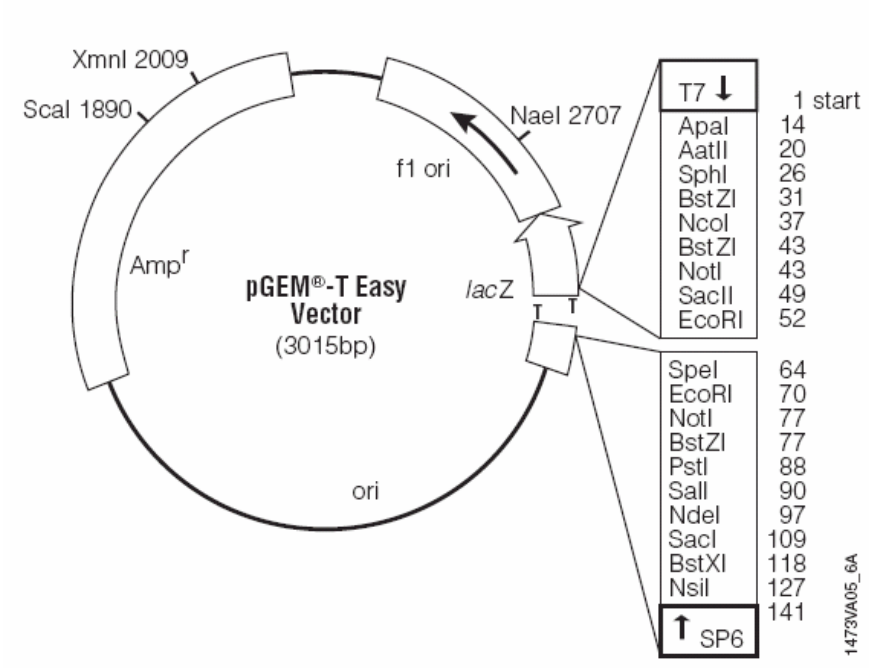

Figure A1. pGEM-T vector circle map and sequence reference points.

Inserts can be sequenced using the SP6 promoter primer, T7 promoter primer, pUC/M13 forward primer, or pUC/M13 reverse primer. A single digest with BstZI (will release inserts cloned into the pGEM-T Vector.

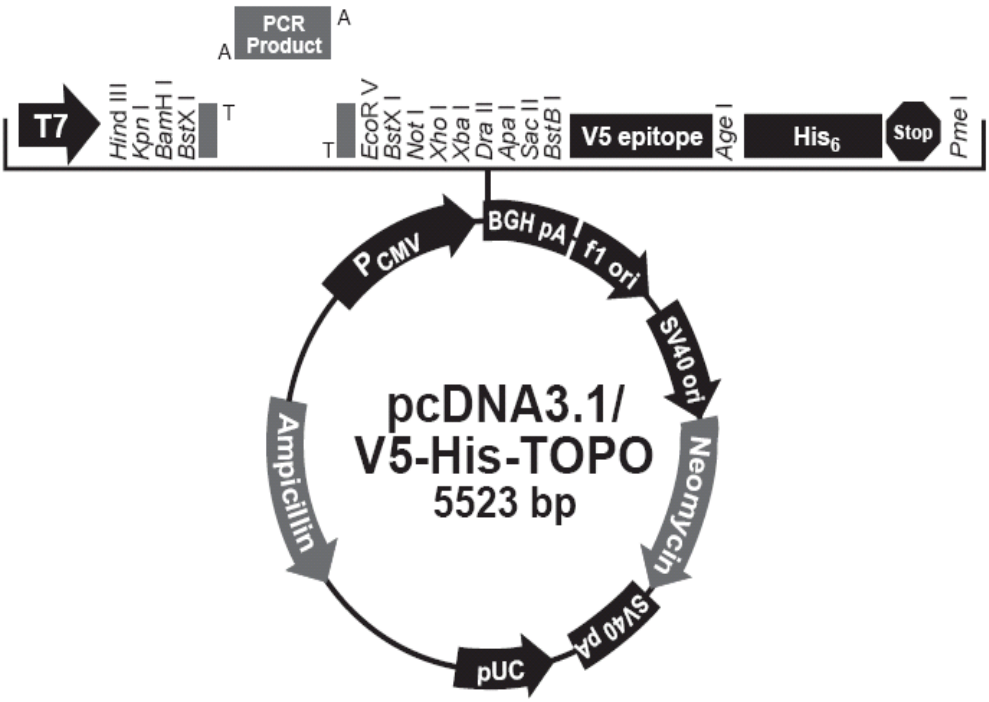

Figure A2. Structure of pcDNA3.1/V5-His-TOPO expression vector and sequence reference points.

The figure summarizes the features of the pcDNA3.1/V5-His-TOPO vector. The vector is supplied linearized between base pairs 953 and 954. This is the TOPO cloning site.

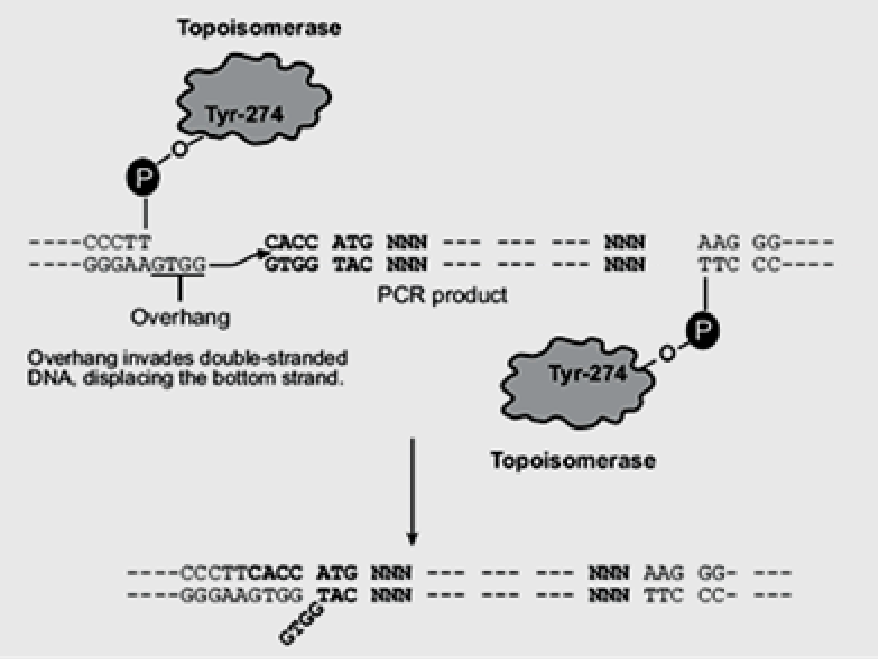

Figure A3. Principle of directional TOPO cloning protocol.

Taq polymerase has a nontemplate-dependent terminal transferase activity that adds a single deoxyadenosine (A) to the 3´ ends of PCR products. The linearized vector has single, overhanging 3´ deoxythymidine (T) residues. This allows PCR inserts to ligate efficiently with the vector. Topoisomerase I from *Vaccinia virus* binds to duplex DNA at specific sites and cleaves the phosphodiester backbone after 5′-CCCTT in one strand [303]. The energy from the broken phosphodiester backbone is conserved by formation of a covalent bond between the 3′ phosphate of the cleaved strand and a tyrosyl residue (Tyr-274) of topoisomerase I. The phospho-tyrosyl bond between the DNA and enzyme can subsequently be attacked by the 5′ hydroxyl of the original cleaved strand, reversing the reaction and releasing topoisomerase [304]. TOPO cloning exploits this reaction to efficiently clone PCR products.

DECLARATION

VII. Declaration

I declare that I have completed this dissertation single-handedly without the unauthorized help of a second party and only with the assistance acknowledged therein. I have appropriately acknowledged and referenced all text passages that are derived literally from or are based on the content of published or unpublished work of others, and all information that relates to verbal communications. I have abided by the principles of good scientific conduct laid down in the charter of the Justus Liebig University of Giessen in carrying out the investigations described in the dissertation.

CURRICULUM VITAE

VIII. Curriculum vitae

Sevdalina Vaskova Nikolova

University of Giessen School of Medicine,
Department of Medicine II, 35392 Giessen, Germany
+(49) 641 99 467 53
Sevdalina.Nikolova@uglc.de
sevv78@yahoo.com

PERSONAL DATA:	
Date of birth:	2nd October 1978
Place of birth:	Varna, Bulgaria
Nationality:	Bulgarian
Sex:	Female
Status:	Single
Address:	42 Kapitan Parvi Rang Georgi Kupov, Galata, Varna (9000), Bulgaria
Telephone:	

EDUCATION:	
	PhD student: PhD programme of the Faculties of Veterinary Medicine and Medicine, Justus Liebig University Giessen
2005 – to date	**PhD thesis topic:** "Role of cGMP Phosphodiesterases in Idiopathic Pulmonary Fibrosis" **Supervisor: Prof. R.T. Schermuly**
2005 - 2007	International Graduate Program: "Molecular Biology and Medicine of the Lung (MBML)", University of Giessen School of Medicine, Germany

2002-2004	**M.S. in Biotechnology:** Physiology laboratory, College of Pharmacy, and College of Biotechnology, Yeungnam University, Kyongsan, Kyungbuk, Korea South **Concentrations:** Advanced Molecular Biology, Advanced Animal Molecular Biology, Advanced Physiology, Signal Transduction, Gene Analysis Techniques, Advanced Biochemistry, Advanced Protein Engineering, GPA 4.26 of maximum 4.50. Research GPA 4.50 of maximum 4.50 **M.S. thesis topic:** "Role of Plasma Membrane-bound NADPH Oxidase Complex in Glutamate-induced Apoptosis of SH-SY5Y Human Neuroblastoma Cells", Grade 4.50 of maximum 4.50. **Supervisor: Prof. Dr. Jung-Ae Kim**
1998-2002.	**B.S. in Biotechnology:** Department of Biotechnology, Faculty of Chemical and System Engineering, University of Chemical Technologies and Metallurgy (UCTM), Sofia, Bulgaria **Concentrations:** Biochemistry, Microbiology, Enzymology, Gene-Engeneering Technologies, Organic Chemistry, Inorganic Chemistry, Analytic Chemistry, GPA during the course of study 5.57 of maximum 6.00. **B.S. thesis topic:** "Non-enzymatic glycosylation in *Escherichia coli*", Grade 6.00 of maximum 6.00. **Supervisors: Ass. Prof. Roumyana Mironova and Prof. Ivan Ivanov**

PROFESSIONAL EXPERIENCE:

August 2001	**Internship:** Chemistry laboratory, Marine Chemistry Sector, Institute of Oceanology, Bulgarian Academy of Sciences, Varna, Bulgaria
August 2000	**Internship:** Clinical laboratory, Asparuhovo Local Hospital, Varna, Bulgaria

PUBLICATIONS:

Lee, Y. S., Kang, Y. S., Lee, J.S., **Nikolova, S.** and Kim, J. A., " Involvement of NADPH oxidase-mediated generation of reactive oxygen species in the apoptotic cell death by capsaicin in HepG2 human hepatoma cells", Free Radical Res 38: 405-412, 2004,

Nikolova, S., Lee, Y.S., Lee, Y.S. and Kim, J. A., "Rac1-NADPH oxidase-regulated generation of reactive oxygen species mediates glutamate-induced apoptosis in SH-SY5Y human neuroblastoma cells", Free Radical Res 39:1295-12304, 2005,

Klein, M.; Schermuly, R.T., Ellinghaus, P., Milting, H., Riedl, B., **Nikolova, S.**, Pullamsetti, S.S, Weissmann, N., Dony, E., Savai, R.; Ghofrani, H.A., Grimminger, F., Busch, A.E., Schäfer, S., "Combined tyrosine and serine-/threonine kinase inhibition by sorafenib prevents experimental pulmonary hypertension and myocardial remodeling", Circulation 118: 2081-2090, 2008

Nikolova, S., Guenther, A., Weissmann, N., Ghofrani, H.A., Konigshoff, M., Eickelberg, O., Klepetko, W., Voswinckel, R., Seeger, W., Grimminger, F., Schermuly, R.T., Pullamsetti, S.S., "Phosphodiesterase 6 subunits are expressed and altered in idiopathic pulmonary fibrosis", Am J Respir Cell Mol Biol (in revision)

POSTER PRESENTATIONS:

Nikolova, S., Jin, D. Q. and Kim, J. A., "Hypothetical mechanisms of G protein-coupled neurodegeneration in glutamate excitotoxicity in human SH-SY5Y

neuroblastoma cells", Proceedings of the Convention of the Pharmaceutical Society of Korea, COEX Convention Center, Seoul, South Korea, 2003,

Nikolova, S. and Kim, J. A., "Glutamate-induced apoptosis in SH-SY5Y human neuroblastoma cells. Role played by plasma membrane NADPH oxidase complex and intracellular calcium ions", Signal Transduction Pathways as Therapeutic Targets, European Conference Center, Kirchberg- Luxembourg, Luxembourg, 2004 http://www.transduction-meeting.lu/,

Son Byeng, W., **Nikolova, S.**, Kim, S. J. and Kim, J. A., ”Cytotoxic effect of compounds isolated from marine-derived fungal metabolities on HT 29 human colorectal cancer cells”, Proceedings of the Convention of the Pharmaceutical Society of Korea, Chungnam National University, Taejon, South Korea, 2004,

Nikolova, S., Pullamsetti, S., Ghofrani, A., Weissmann, N., Seeger, W., Grimminger , F. and Schermuly, R., “Role of phosphodiesterases in idiopathic pulmonary fibrosis”, Kongress der Deutschen Gesellschaft für Pneumologie und Beatmungsmedizin, Nürnberg, Germany, 2006,

Nikolova, S., Pullamsetti, S., Ghofrani, H., Weissmann, N., Seeger, W., Grimminger, F., Scgermuly, R:, “Expression profile of phosphodiesterases in idiopathic pulmonary fibrosis“, Kongress der Deutschen Gesellschaft für Innere Medizin, Wiesbaden 2007,

Nikolova, S., Pullamsetti, S.S., PhD., Ghofrani, H.A., Weissmann, N., Seeger, W., Grimminger, F., Schermuly, R.T., ”The retinal PDE 6 enzyme complex Is expressed and altered in idiopathic pulmonary fibrosis”, American Thoracic Society, San Francisco, California, USA, 2007

SCHOLARSHIPS:

2002-2004 “Scholarship for Foreigners” granted by Yeungnam University, South Korea as an intergovernmental agreement between the Republic of Bulgaria and South Korea in support of higher

education of foreign citizens,

2005- “PhD Scholarship”, granted by UGLC, Germany

ACKNOWLEDGEMENTS

IX. Acknowledgements

A thesis is never solely the work of the author. Support and encouragement comes from different sources in different ways. It is a pleasant aspect that I have now the opportunity to express my gratitude to all of them.

Foremost, I would like to thank my supervisor Professor Ralph Schermuly for providing me with the excellent opportunity to be a part of his research group. His encouragement, guidance and assistance throughout my doctoral course have made the completion of my PhD degree possible.

I especially want to thank my advisor on the spot, Dr. Soni Savai Pullamsetti. Her guidance and superb analytical skills have been instrumental in the success of this project.

I also express special gratitude to Professor Werner Seeger as the Head of University Hospital Giessen.

Special thanks go out to Dr. Oliver Eickelberg, Dr. Rory Morty, Malanie Königshoff and Grazyna Kwapiszewska for ‘shaping’ us into excellent lung scientists during the MBML graduate course.

I owe a deep of gratitude to Rajkumar Savai, Eva Dony, Michael Seimetz, Ewa Bieniek and Djuro Kosanovic for their valuable assistance.

I would like to thank especially to Svetlin Tchatalbachev for translating the summary into german. It was a great help.

I would also like to thank the members of the Volhard lab: Kathrin Woyda, Ying-Ju Lai, Ewa Kolosionek, Piotr Sklepkiewicz, Xia Tian, Sergey Udalov, Marcin Szymanski, Alexandra Tretyn, Lal Kurian, Mathias Eschenhagen, Swetlana Spielmann for the precious moments.

I would like to thank particularly Ruth Pinto, Fotini Kouri and Markus Queisser for

being good friends. I consider myself fortunate that I had the opportunity of meeting them.

Last but not least, I dedicate this thesis to the ones who are always there for me. You kept the light for me when it was really dark. I love you from the bottom of my hearth, my dear family: my father Vasko, my mother Galina and my brother Ivailo!

Sevdalina Vaskova Nikolova

October 2008

REFERENCES

X. References

1. *American Thoracic Society. Idiopathic pulmonary fibrosis: diagnosis and treatment. International consensus statement. American Thoracic Society (ATS), and the European Respiratory Society (ERS).* Am J Respir Crit Care Med, 2000. **161**(2 Pt 1): p. 646-64.
2. *American Thoracic Society/European Respiratory Society International Multidisciplinary Consensus Classification of the Idiopathic Interstitial Pneumonias. This joint statement of the American Thoracic Society (ATS), and the European Respiratory Society (ERS) was adopted by the ATS board of directors, June 2001 and by the ERS Executive Committee, June 2001.* Am J Respir Crit Care Med, 2002. **165**(2): p. 277-304.
3. Selman, M., T.E. King, and A. Pardo, *Idiopathic pulmonary fibrosis: prevailing and evolving hypotheses about its pathogenesis and implications for therapy.* Ann Intern Med, 2001. **134**(2): p. 136-51.
4. Hubbard, R., et al., *Occupational exposure to metal or wood dust and aetiology of cryptogenic fibrosing alveolitis.* Lancet, 1996. **347**(8997): p. 284-9.
5. Iwai, K., et al., *Idiopathic pulmonary fibrosis. Epidemiologic approaches to occupational exposure.* Am J Respir Crit Care Med, 1994. **150**(3): p. 670-5.
6. Monso, E., et al., *Mineralogical microanalysis of idiopathic pulmonary fibrosis.* Arch Environ Health, 1990. **45**(3): p. 185-8.
7. Scott, J., I. Johnston, and J. Britton, *What causes cryptogenic fibrosing alveolitis? A case-control study of environmental exposure to dust.* BMJ, 1990. **301**(6759): p. 1015-7.
8. Baumgartner, K.B., et al., *Cigarette smoking: a risk factor for idiopathic pulmonary fibrosis.* Am J Respir Crit Care Med, 1997. **155**(1): p. 242-8.
9. Ryu, J.H., et al., *Smoking-related interstitial lung diseases: a concise review.* Eur Respir J, 2001. **17**(1): p. 122-32.
10. Tobin, R.W., et al., *Increased prevalence of gastroesophageal reflux in patients with idiopathic pulmonary fibrosis.* Am J Respir Crit Care Med, 1998. **158**(6): p. 1804-8.
11. Cooper, J.A., Jr., D.A. White, and R.A. Matthay, *Drug-induced pulmonary disease. Part 1: Cytotoxic drugs.* Am Rev Respir Dis, 1986. **133**(2): p. 321-40.
12. Batist, G. and J.L. Andrews, Jr., *Pulmonary toxicity of antineoplastic drugs.* JAMA, 1981. **246**(13): p. 1449-53.
13. Weiss, R.B. and F.M. Muggia, *Cytotoxic drug-induced pulmonary disease: update 1980.* Am J Med, 1980. **68**(2): p. 259-66.
14. O'Sullivan, B. and W. Levin, *Late radiation-related fibrosis: pathogenesis, manifestations, and current management.* Semin Radiat Oncol, 2003. **13**(3): p. 274-89.
15. Egan, J.J., et al., *Epstein-Barr virus replication within pulmonary epithelial cells in cryptogenic fibrosing alveolitis.* Thorax, 1995. **50**(12): p. 1234-9.
16. Vergnon, J.M., et al., *Cryptogenic fibrosing alveolitis and Epstein-Barr virus: an association?* Lancet, 1984. **2**(8406): p. 768-71.
17. Jakab, G.J. and D.J. Bassett, *Influenza virus infection, ozone exposure, and fibrogenesis.* Am Rev Respir Dis, 1990. **141**(5 Pt 1): p. 1307-15.
18. Pinsker, K.L., et al., *Usual interstitial pneumonia following Texas A2 influenza infection.* Chest, 1981. **80**(2): p. 123-6.
19. Sinclair, D.J., F.G. Stuart, and G.W. Ritchie, *Pulmonary complications of influenza: a radiological review of 30 cases.* Can Med Assoc J, 1969. **101**(13): p. 46-50.

20. Winterbauer, R.H., W.R. Ludwig, and S.P. Hammar, *Clinical course, management, and long-term sequelae of respiratory failure due to influenza viral pneumonia.* Johns Hopkins Med J, 1977. **141**(3): p. 148-55.
21. Jiwa, M., et al., *Three sensitive methods for the detection of cytomegalovirus in lung tissue of patients with interstitial pneumonitis.* Am J Clin Pathol, 1990. **93**(4): p. 491-4.
22. Meliconi, R., et al., *Incidence of hepatitis C virus infection in Italian patients with idiopathic pulmonary fibrosis.* Thorax, 1996. **51**(3): p. 315-7.
23. Ueda, T., et al., *Idiopathic pulmonary fibrosis and high prevalence of serum antibodies to hepatitis C virus.* Am Rev Respir Dis, 1992. **146**(1): p. 266-8.
24. Egan, J.J., A.A. Woodcock, and J.P. Stewart, *Viruses and idiopathic pulmonary fibrosis.* Eur Respir J, 1997. **10**(7): p. 1433-7.
25. Jakab, G.J., *Sequential virus infections, bacterial superinfections, and fibrogenesis.* Am Rev Respir Dis, 1990. **142**(2): p. 374-9.
26. Bitterman, P.B., et al., *Familial idiopathic pulmonary fibrosis. Evidence of lung inflammation in unaffected family members.* N Engl J Med, 1986. **314**(21): p. 1343-7.
27. Ellis, R.H., *Familial Incidence of Diffuse Interstitial Pulmonary Fibrosis.* Postgrad Med J, 1965. **41**: p. 150-2.
28. Murphy, A. and B.J. O'Sullivan, *Familial fibrosing alveolitis.* Ir J Med Sci, 1981. **150**(7): p. 204-9.
29. Solliday, N.H., et al., *Familial chronic interstitial pneumonia.* Am Rev Respir Dis, 1973. **108**(2): p. 193-204.
30. Geddes, D.M., et al., *alpha 1-antitrypsin phenotypes in fibrosing alveolitis and rheumatoid arthritis.* Lancet, 1977. **2**(8047): p. 1049-51.
31. Hubbard, R., et al., *Alpha1-antitrypsin phenotypes in patients with cryptogenic fibrosing alveolitis: a case-control study.* Eur Respir J, 1997. **10**(12): p. 2881-3.
32. Musk, A.W., et al., *Genetic studies in familial fibrosing alveolitis. Possible linkage with immunoglobulin allotypes (Gm).* Chest, 1986. **89**(2): p. 206-10.
33. Thomas, A.Q., et al., *Heterozygosity for a surfactant protein C gene mutation associated with usual interstitial pneumonitis and cellular nonspecific interstitial pneumonitis in one kindred.* Am J Respir Crit Care Med, 2002. **165**(9): p. 1322-8.
34. Armanios, M.Y., et al., *Telomerase mutations in families with idiopathic pulmonary fibrosis.* N Engl J Med, 2007. **356**(13): p. 1317-26.
35. Mannino, D.M., R.A. Etzel, and R.G. Parrish, *Pulmonary fibrosis deaths in the United States, 1979-1991. An analysis of multiple-cause mortality data.* Am J Respir Crit Care Med, 1996. **153**(5): p. 1548-52.
36. Chetty, A., et al., *Cryptogenic fibrosing alveolitis in children.* Ann Allergy, 1987. **58**(5): p. 336-40.
37. Hewitt, C.J., D. Hull, and J.W. Keeling, *Fibrosing alveolitis in infancy and childhood.* Arch Dis Child, 1977. **52**(1): p. 22-37.
38. Riedler, J., A. Golser, and I. Huttegger, *Fibrosing alveolitis in an infant.* Eur Respir J, 1992. **5**(3): p. 359-61.
39. Gribbin, J., et al., *Incidence and mortality of idiopathic pulmonary fibrosis and sarcoidosis in the UK.* Thorax, 2006. **61**(11): p. 980-5.
40. Olson, A.L., et al., *Mortality from pulmonary fibrosis increased in the United States from 1992 to 2003.* Am J Respir Crit Care Med, 2007. **176**(3): p. 277-84.
41. Raghu, G., et al., *Incidence and prevalence of idiopathic pulmonary fibrosis.* Am J Respir Crit Care Med, 2006. **174**(7): p. 810-6.

42. Hamman L, 1994, Acute diffuse interstitial fibrosis of the lungs, Bull John Hopkins Hospital 74, 177-204
43. Scadding, J.G. and K.F. Hinson, *Diffuse fibrosing alveolitis (diffuse interstitial fibrosis of the lungs). Correlation of histology at biopsy with prognosis.* Thorax, 1967. **22**(4): p. 291-304.
44. Liebow AA, Carrington CB (1969) The interstitial pneumonias, frontiers of pulmonary radiology, New York: Grune and Stratton, 1969
45. Cherniack, R.M., et al., *Correlation of structure and function in idiopathic pulmonary fibrosis.* Am J Respir Crit Care Med, 1995. **151**(4): p. 1180-8.
46. Crystal, R.G., et al., *Idiopathic pulmonary fibrosis. Clinical, histologic, radiographic, physiologic, scintigraphic, cytologic, and biochemical aspects.* Ann Intern Med, 1976. **85**(6): p. 769-88.
47. Katzenstein, A.L. and J.L. Myers, *Idiopathic pulmonary fibrosis: clinical relevance of pathologic classification.* Am J Respir Crit Care Med, 1998. **157**(4 Pt 1): p. 1301-15.
48. Stack, B.H., Y.F. Choo-Kang, and B.E. Heard, *The prognosis of cryptogenic fibrosing alveolitis.* Thorax, 1972. **27**(5): p. 535-42.
49. Turner-Warwick, M., B. Burrows, and A. Johnson, *Cryptogenic fibrosing alveolitis: clinical features and their influence on survival.* Thorax, 1980. **35**(3): p. 171-80.
50. Winterbauer, R.H., et al., *Diffuse interstitial pneumonitis. Clinicopathologic correlations in 20 patients treated with prednisone/azathioprine.* Am J Med, 1978. **65**(4): p. 661-72.
51. Costabel, U. and T.E. King, *International consensus statement on idiopathic pulmonary fibrosis.* Eur Respir J, 2001. **17**(2): p. 163-7.
52. Visscher, D.W. and J.L. Myers, *Histologic spectrum of idiopathic interstitial pneumonias.* Proc Am Thorac Soc, 2006. **3**(4): p. 322-9.
53. Kuhn, C. and J.A. McDonald, *The roles of the myofibroblast in idiopathic pulmonary fibrosis. Ultrastructural and immunohistochemical features of sites of active extracellular matrix synthesis.* Am J Pathol, 1991. **138**(5): p. 1257-65.
54. Travis WD, Colby TV, Koss MN, Rosado-de Christenson ML, Muller NL & King TE (2002) Nonplastic disorders of the lower respiratory tract. 2nd editon, American Registery of Pathology and Armed Forces Institute of Pathology, Washington DC
55. Burdick, M.D., et al., *CXCL11 attenuates bleomycin-induced pulmonary fibrosis via inhibition of vascular remodeling.* Am J Respir Crit Care Med, 2005. **171**(3): p. 261-8.
56. Cosgrove, G.P., et al., *Pigment epithelium-derived factor in idiopathic pulmonary fibrosis: a role in aberrant angiogenesis.* Am J Respir Crit Care Med, 2004. **170**(3): p. 242-51.
57. Ebina, M., et al., *Heterogeneous increase in CD34-positive alveolar capillaries in idiopathic pulmonary fibrosis.* Am J Respir Crit Care Med, 2004. **169**(11): p. 1203-8.
58. Fell, C.D. and F.J. Martinez, *The impact of pulmonary arterial hypertension on idiopathic pulmonary fibrosis.* Chest, 2007. **131**(3): p. 641-3.
59. Renzoni, E.A., et al., *Interstitial vascularity in fibrosing alveolitis.* Am J Respir Crit Care Med, 2003. **167**(3): p. 438-43.
60. Simler, N.R., et al., *Angiogenic cytokines in patients with idiopathic interstitial pneumonia.* Thorax, 2004. **59**(7): p. 581-5.
61. Strieter, R.M., et al., *Effects of interferon-gamma 1b on biomarker expression in patients with idiopathic pulmonary fibrosis.* Am J Respir Crit Care Med, 2004. **170**(2): p. 133-40.

62. Bjoraker, J.A., et al., *Prognostic significance of histopathologic subsets in idiopathic pulmonary fibrosis.* Am J Respir Crit Care Med, 1998. **157**(1): p. 199-203.
63. Daniil, Z.D., et al., *A histologic pattern of nonspecific interstitial pneumonia is associated with a better prognosis than usual interstitial pneumonia in patients with cryptogenic fibrosing alveolitis.* Am J Respir Crit Care Med, 1999. **160**(3): p. 899-905.
64. Nicholson, A.G., et al., *The prognostic significance of the histologic pattern of interstitial pneumonia in patients presenting with the clinical entity of cryptogenic fibrosing alveolitis.* Am J Respir Crit Care Med, 2000. **162**(6): p. 2213-7.
65. Travis, W.D., et al., *Idiopathic nonspecific interstitial pneumonia: prognostic significance of cellular and fibrosing patterns: survival comparison with usual interstitial pneumonia and desquamative interstitial pneumonia.* Am J Surg Pathol, 2000. **24**(1): p. 19-33.
66. Keogh, B.A. and R.G. Crystal, *Alveolitis: the key to the interstitial lung disorders.* Thorax, 1982. **37**(1): p. 1-10.
67. Strieter, R.M., *Mechanisms of pulmonary fibrosis: conference summary.* Chest, 2001. **120**(1 Suppl): p. 77S-85S.
68. Keane, M.P. and R.M. Strieter, *The importance of balanced pro-inflammatory and anti-inflammatory mechanisms in diffuse lung disease.* Respir Res, 2002. **3**: p. 5.
69. Piguet, P.F., et al., *Expression and localization of tumor necrosis factor-alpha and its mRNA in idiopathic pulmonary fibrosis.* Am J Pathol, 1993. **143**(3): p. 651-5.
70. Wallace, W.A., et al., *A type 2 (Th2-like) pattern of immune response predominates in the pulmonary interstitium of patients with cryptogenic fibrosing alveolitis (CFA).* Clin Exp Immunol, 1995. **101**(3): p. 436-41.
71. Kolb, M., et al., *Transient expression of IL-1beta induces acute lung injury and chronic repair leading to pulmonary fibrosis.* J Clin Invest, 2001. **107**(12): p. 1529-36.
72. Adamson, I.Y., L. Young, and D.H. Bowden, *Relationship of alveolar epithelial injury and repair to the induction of pulmonary fibrosis.* Am J Pathol, 1988. **130**(2): p. 377-83.
73. Schuppan, D., et al., *Matrix as a modulator of hepatic fibrogenesis.* Semin Liver Dis, 2001. **21**(3): p. 351-72.
74. Sime, P.J., et al., *Adenovector-mediated gene transfer of active transforming growth factor-beta1 induces prolonged severe fibrosis in rat lung.* J Clin Invest, 1997. **100**(4): p. 768-76.
75. Peterson, M.W., M. Monick, and G.W. Hunninghake, *Prognostic role of eosinophils in pulmonary fibrosis.* Chest, 1987. **92**(1): p. 51-6.
76. Turner-Warwick, M. and P.L. Haslam, *The value of serial bronchoalveolar lavages in assessing the clinical progress of patients with cryptogenic fibrosing alveolitis.* Am Rev Respir Dis, 1987. **135**(1): p. 26-34.
77. Selman, M. and A. Pardo, *Idiopathic pulmonary fibrosis: an epithelial/fibroblastic cross-talk disorder.* Respir Res, 2002. **3**: p. 3.
78. Zuo, F., et al., *Gene expression analysis reveals matrilysin as a key regulator of pulmonary fibrosis in mice and humans.* Proc Natl Acad Sci U S A, 2002. **99**(9): p. 6292-7.
79. Hunninghake, G.W., et al., *Radiologic findings are strongly associated with a pathologic diagnosis of usual interstitial pneumonia.* Chest, 2003. **124**(4): p. 1215-23.

80. Noble, P.W. and R.J. Homer, *Idiopathic pulmonary fibrosis: new insights into pathogenesis.* Clin Chest Med, 2004. **25**(4): p. 749-58, vii.
81. Raghu, G. and J. Chang, *Idiopathic pulmonary fibrosis: current trends in management.* Clin Chest Med, 2004. **25**(4): p. 621-36, v.
82. Woodcock-Mitchell, J.L., et al., *Keratin species in type II pneumocytes in culture and during lung injury.* Am Rev Respir Dis, 1986. **134**(3): p. 566-71.
83. Nakao, A., et al., *Expression of cell adhesion molecules in the lungs of patients with idiopathic pulmonary fibrosis.* Chest, 1995. **108**(1): p. 233-9.
84. Corrin, B., et al., *Fine structural changes in cryptogenic fibrosing alveolitis and asbestosis.* J Pathol, 1985. **147**(2): p. 107-19.
85. Katzenstein, A.L., *Pathogenesis of "fibrosis" in interstitial pneumonia: an electron microscopic study.* Hum Pathol, 1985. **16**(10): p. 1015-24.
86. Chilosi, M., et al., *Abnormal re-epithelialization and lung remodeling in idiopathic pulmonary fibrosis: the role of deltaN-p63.* Lab Invest, 2002. **82**(10): p. 1335-45.
87. Kawanami, O., V.J. Ferrans, and R.G. Crystal, *Structure of alveolar epithelial cells in patients with fibrotic lung disorders.* Lab Invest, 1982. **46**(1): p. 39-53.
88. Sutinen, S., et al., *Ultrastructure of terminal respiratory epithelium and prognosis in chronic interstitial pneumonia.* Eur J Respir Dis, 1980. **61**(6): p. 325-36.
89. Barbas-Filho, J.V., et al., *Evidence of type II pneumocyte apoptosis in the pathogenesis of idiopathic pulmonary fibrosis (IFP)/usual interstitial pneumonia (UIP).* J Clin Pathol, 2001. **54**(2): p. 132-8.
90. Kuwano, K., et al., *P21Waf1/Cip1/Sdi1 and p53 expression in association with DNA strand breaks in idiopathic pulmonary fibrosis.* Am J Respir Crit Care Med, 1996. **154**(2 Pt 1): p. 477-83.
91. Maeyama, T., et al., *Upregulation of Fas-signalling molecules in lung epithelial cells from patients with idiopathic pulmonary fibrosis.* Eur Respir J, 2001. **17**(2): p. 180-9.
92. Kim, K.K., et al., *Alveolar epithelial cell mesenchymal transition develops in vivo during pulmonary fibrosis and is regulated by the extracellular matrix.* Proc Natl Acad Sci U S A, 2006. **103**(35): p. 13180-5.
93. Yao, H.W., et al., *TGF-beta1 induces alveolar epithelial to mesenchymal transition in vitro.* Life Sci, 2004. **76**(1): p. 29-37.
94. Schneeberger EE. Alveolar type I cells. In: The Lung: Scientific Foundations, edited by Crystal RG, West JB, Weibel ER, and Barnes PJ. Philadelphia, New York: Lippincott-Raven, 1997, p. 535–542
95. Johnson, M.D., et al., *Alveolar epithelial type I cells contain transport proteins and transport sodium, supporting an active role for type I cells in regulation of lung liquid homeostasis.* Proc Natl Acad Sci U S A, 2002. **99**(4): p. 1966-71.
96. Ridge, K.M., et al., *Differential expression of Na-K-ATPase isoforms in rat alveolar epithelial cells.* Am J Physiol, 1997. **273**(1 Pt 1): p. L246-55.
97. Mason RJ and Shannon JM. Alveolar type II cells. In: The Lung: Scientific Foundations, edited by Crystal RG, West JB, Weibel ER, and Barnes PJ. Philadelphia, New York: Lippincott- Raven, 1997, p. 543–555
98. Crouch, E. and J.R. Wright, *Surfactant proteins a and d and pulmonary host defense.* Annu Rev Physiol, 2001. **63**: p. 521-54.
99. Dobbs, L.G., et al., *Secretion of surfactant by primary cultures of alveolar type II cells isolated from rats.* Biochim Biophys Acta, 1982. **713**(1): p. 118-27.
100. Fehrenbach, H., *Alveolar epithelial type II cell: defender of the alveolus revisited.* Respir Res, 2001. **2**(1): p. 33-46.

101. Kikkawa, Y. and F. Smith, *Cellular and biochemical aspects of pulmonary surfactant in health and disease.* Lab Invest, 1983. **49**(2): p. 122-39.
102. McCormack, F.X. and J.A. Whitsett, *The pulmonary collectins, SP-A and SP-D, orchestrate innate immunity in the lung.* J Clin Invest, 2002. **109**(6): p. 707-12.
103. Goodman, B.E. and E.D. Crandall, *Dome formation in primary cultured monolayers of alveolar epithelial cells.* Am J Physiol, 1982. **243**(1): p. C96-100.
104. Mason, R.J., et al., *Transepithelial transport by pulmonary alveolar type II cells in primary culture.* Proc Natl Acad Sci U S A, 1982. **79**(19): p. 6033-7.
105. Sage, H., et al., *Granular pneumocytes in primary culture secrete several major components of the extracellular matrix.* Biochemistry, 1983. **22**(9): p. 2148-55.
106. Brightbill, H.D. and R.L. Modlin, *Toll-like receptors: molecular mechanisms of the mammalian immune response.* Immunology, 2000. **101**(1): p. 1-10.
107. Eghtesad, M., H.E. Jackson, and A.C. Cunningham, *Primary human alveolar epithelial cells can elicit the transendothelial migration of CD14+ monocytes and CD3+ lymphocytes.* Immunology, 2001. **102**(2): p. 157-64.
108. O'Brien, A.D., et al., *Role of alveolar epithelial cell intercellular adhesion molecule-1 in host defense against Klebsiella pneumoniae.* Am J Physiol, 1999. **276**(6 Pt 1): p. L961-70.
109. Rosseau, S., et al., *Monocyte migration through the alveolar epithelial barrier: adhesion molecule mechanisms and impact of chemokines.* J Immunol, 2000. **164**(1): p. 427-35.
110. Standiford, T.J., et al., *Alveolar macrophage-derived cytokines induce monocyte chemoattractant protein-1 expression from human pulmonary type II-like epithelial cells.* J Biol Chem, 1991. **266**(15): p. 9912-8.
111. Zissel, G., et al., *Human alveolar epithelial cells type II are capable of regulating T-cell activity.* J Investig Med, 2000. **48**(1): p. 66-75.
112. Adamson, I.Y. and D.H. Bowden, *The type 2 cell as progenitor of alveolar epithelial regeneration. A cytodynamic study in mice after exposure to oxygen.* Lab Invest, 1974. **30**(1): p. 35-42.
113. Adamson, I.Y. and D.H. Bowden, *Derivation of type 1 epithelium from type 2 cells in the developing rat lung.* Lab Invest, 1975. **32**(6): p. 736-45.
114. Geiser, T., *Mechanisms of alveolar epithelial repair in acute lung injury--a translational approach.* Swiss Med Wkly, 2003. **133**(43-44): p. 586-90.
115. Uhal, B.D., *Cell cycle kinetics in the alveolar epithelium.* Am J Physiol, 1997. **272**(6 Pt 1): p. L1031-45.
116. Borok, Z., et al., *Modulation of t1alpha expression with alveolar epithelial cell phenotype in vitro.* Am J Physiol, 1998. **275**(1 Pt 1): p. L155-64.
117. Danto, S.I., et al., *Reversible transdifferentiation of alveolar epithelial cells.* Am J Respir Cell Mol Biol, 1995. **12**(5): p. 497-502.
118. Dobbs, L.G., et al., *Maintenance of the differentiated type II cell phenotype by culture with an apical air surface.* Am J Physiol, 1997. **273**(2 Pt 1): p. L347-54.
119. Shannon, J.M., S.D. Jennings, and L.D. Nielsen, *Modulation of alveolar type II cell differentiated function in vitro.* Am J Physiol, 1992. **262**(4 Pt 1): p. L427-36.
120. Bowden, D.H., *Cell turnover in the lung.* Am Rev Respir Dis, 1983. **128**(2 Pt 2): p. S46-8.
121. Kalina, M., S. Riklis, and H. Blau, *Pulmonary epithelial cell proliferation in primary culture of alveolar type II cells.* Exp Lung Res, 1993. **19**(2): p. 153-75.
122. Kauffman, S.L., *Alterations in cell proliferation in mouse lung following urethane exposure. 3. Effects of chronic exposure on type 2 alveolar epithelial cell.* Am J Pathol, 1972. **68**(2): p. 317-26.

123. Evans, M.J., et al., *Transformation of alveolar type 2 cells to type 1 cells following exposure to NO2.* Exp Mol Pathol, 1975. **22**(1): p. 142-50.
124. Daly, H.E., et al., *Cell-specific gene expression reveals changes in epithelial cell populations after bleomycin treatment.* Lab Invest, 1998. **78**(4): p. 393-400.
125. Krause, D.S., *Bone marrow-derived cells and stem cells in lung repair.* Proc Am Thorac Soc, 2008. **5**(3): p. 323-7.
126. Kyono, H., et al., *Reversible lung lesions in rats due to short-term exposure to ultrafine cobalt particles.* Ind Health, 1992. **30**(3-4): p. 103-18.
127. Flecknoe, S.J., et al., *Determination of alveolar epithelial cell phenotypes in fetal sheep: evidence for the involvement of basal lung expansion.* J Physiol, 2002. **542**(Pt 1): p. 245-53.
128. McElroy, M.C. and M. Kasper, *The use of alveolar epithelial type I cell-selective markers to investigate lung injury and repair.* Eur Respir J, 2004. **24**(4): p. 664-73.
129. Rennard, S.I., P.B. Bitterman, and R.G. Crystal, *Response of the lower respiratory tract to injury. Mechanisms of repair of the parenchymal cells of the alveolar wall.* Chest, 1983. **84**(6): p. 735-9.
130. Kasper, M. and G. Haroske, *Alterations in the alveolar epithelium after injury leading to pulmonary fibrosis.* Histol Histopathol, 1996. **11**(2): p. 463-83.
131. Evans, M.J., et al., *Renewal of alveolar epithelium in the rat following exposure to NO2.* Am J Pathol, 1973. **70**(2): p. 175-98.
132. Kapanci, Y., et al., *Pathogenesis and reversibility of the pulmonary lesions of oxygen toxicity in monkeys. II. Ultrastructural and morphometric studies.* Lab Invest, 1969. **20**(1): p. 101-18.
133. Ryan, S.F., *Experimental fibrosing alveolitis.* Am Rev Respir Dis, 1972. **105**(5): p. 776-91.
134. Stephens, R.J., et al., *Early response of lung to low levels of ozone.* Am J Pathol, 1974. **74**(1): p. 31-58.
135. Fehrenbach, H., et al., *Keratinocyte growth factor-induced hyperplasia of rat alveolar type II cells in vivo is resolved by differentiation into type I cells and by apoptosis.* Eur Respir J, 1999. **14**(3): p. 534-44.
136. Guo, J., et al., *Intravenous keratinocyte growth factor protects against experimental pulmonary injury.* Am J Physiol, 1998. **275**(4 Pt 1): p. L800-5.
137. Ulich, T.R., et al., *Keratinocyte growth factor is a growth factor for type II pneumocytes in vivo.* J Clin Invest, 1994. **93**(3): p. 1298-306.
138. Ware, L.B. and M.A. Matthay, *Keratinocyte and hepatocyte growth factors in the lung: roles in lung development, inflammation, and repair.* Am J Physiol Lung Cell Mol Physiol, 2002. **282**(5): p. L924-40.
139. Danilenko, D.M., *Preclinical and early clinical development of keratinocyte growth factor, an epithelial-specific tissue growth factor.* Toxicol Pathol, 1999. **27**(1): p. 64-71.
140. Sonnenberg, E., et al., *Scatter factor/hepatocyte growth factor and its receptor, the c-met tyrosine kinase, can mediate a signal exchange between mesenchyme and epithelia during mouse development.* J Cell Biol, 1993. **123**(1): p. 223-35.
141. Aida, S., et al., *Distribution of epidermal growth factor and epidermal growth factor receptor in human lung: immunohistochemical and immunoelectron-microscopic studies.* Respiration, 1994. **61**(3): p. 161-6.
142. Raaberg, L., et al., *Epidermal growth factor transcription, translation, and signal transduction by rat type II pneumocytes in culture.* Am J Respir Cell Mol Biol, 1992. **6**(1): p. 44-9.

143. Vermeer, P.D., et al., *Segregation of receptor and ligand regulates activation of epithelial growth factor receptor.* Nature, 2003. **422**(6929): p. 322-6.
144. Leslie, C.C., et al., *Heparin-binding EGF-like growth factor is a mitogen for rat alveolar type II cells.* Am J Respir Cell Mol Biol, 1997. **16**(4): p. 379-87.
145. Lesur, O., K. Arsalane, and D. Lane, *Lung alveolar epithelial cell migration in vitro: modulators and regulation processes.* Am J Physiol, 1996. **270**(3 Pt 1): p. L311-9.
146. Vermeer, P.D., et al., *Differentiation of human airway epithelia is dependent on erbB2.* Am J Physiol Lung Cell Mol Physiol, 2006. **291**(2): p. L175-80.
147. Zhang, F., et al., *Transforming growth factor-beta antagonizes alveolar type II cell proliferation induced by keratinocyte growth factor.* Am J Respir Cell Mol Biol, 2004. **31**(6): p. 679-86.
148. Mouhieddine, O.B., et al., *Insulin-like growth factor-II (IGF-II), type 2 IGF receptor, and IGF-binding protein-2 gene expression in rat lung alveolar epithelial cells: relation to proliferation.* Endocrinology, 1994. **135**(1): p. 83-91.
149. A physician's guide to Idiopathic pulmonary fibrosis, coalition for pulmonary fibrosis
150. Thannickal, V.J., et al., *Emerging drugs for idiopathic pulmonary fibrosis.* Expert Opin Emerg Drugs, 2005. **10**(4): p. 707-27.
151. Galie, N., et al., *Sildenafil citrate therapy for pulmonary arterial hypertension.* N Engl J Med, 2005. **353**(20): p. 2148-57.
152. Ghofrani, H.A., et al., *Differences in hemodynamic and oxygenation responses to three different phosphodiesterase-5 inhibitors in patients with pulmonary arterial hypertension: a randomized prospective study.* J Am Coll Cardiol, 2004. **44**(7): p. 1488-96.
153. Schermuly, R.T., et al., *Phosphodiesterase 1 upregulation in pulmonary arterial hypertension: target for reverse-remodeling therapy.* Circulation, 2007. **115**(17): p. 2331-9.
154. Gericke, D. and P. Chandra, *Inhibition of tumor growth by nucleoside cyclic 3'-5'-monophosphates.* Hoppe Seylers Z Physiol Chem, 1969. **350**(11): p. 1469-71.
155. Keller, R. and R. Keist, *Suppression of growth of P-815 mastocytoma cells in vitro by drugs increasing cellular cyclic 3',5'-adenosine monophosphate.* Life Sci II, 1973. **12**(3): p. 97-105.
156. Ryan, W.L. and M.L. Heidrick, *Inhibition of cell growth in vitro by adenosine 3',5'-monophosphate.* Science, 1968. **162**(861): p. 1484-5.
157. Alp, S., et al., *Sildenafil improves hemodynamic parameters in COPD--an investigation of six patients.* Pulm Pharmacol Ther, 2006. **19**(6): p. 386-90.
158. Lipworth, B.J., *Phosphodiesterase-4 inhibitors for asthma and chronic obstructive pulmonary disease.* Lancet, 2005. **365**(9454): p. 167-75.
159. Collard, H.R., et al., *Sildenafil improves walk distance in idiopathic pulmonary fibrosis.* Chest, 2007. **131**(3): p. 897-9.
160. Ghofrani, H.A., et al., *Sildenafil for treatment of lung fibrosis and pulmonary hypertension: a randomised controlled trial.* Lancet, 2002. **360**(9337): p. 895-900.
161. Hemnes, A.R., A. Zaiman, and H.C. Champion, *PDE5A inhibition attenuates bleomycin-induced pulmonary fibrosis and pulmonary hypertension through inhibition of ROS generation and RhoA/Rho kinase activation.* Am J Physiol Lung Cell Mol Physiol, 2008. **294**(1): p. L24-33.
162. Beavo, J.A., *Cyclic nucleotide phosphodiesterases: functional implications of multiple isoforms.* Physiol Rev, 1995. **75**(4): p. 725-48.

163. Beavo, J.A. and D.H. Reifsnyder, *Primary sequence of cyclic nucleotide phosphodiesterase isozymes and the design of selective inhibitors.* Trends Pharmacol Sci, 1990. **11**(4): p. 150-5.
164. Conti, M. and S.L. Jin, *The molecular biology of cyclic nucleotide phosphodiesterases.* Prog Nucleic Acid Res Mol Biol, 1999. **63**: p. 1-38.
165. Manganiello, V.C. and E. Degerman, *Cyclic nucleotide phosphodiesterases (PDEs): diverse regulators of cyclic nucleotide signals and inviting molecular targets for novel therapeutic agents.* Thromb Haemost, 1999. **82**(2): p. 407-11.
166. Soderling, S.H. and J.A. Beavo, *Regulation of cAMP and cGMP signaling: new phosphodiesterases and new functions.* Curr Opin Cell Biol, 2000. **12**(2): p. 174-9.
167. Lugnier, C., *Cyclic nucleotide phosphodiesterase (PDE) superfamily: a new target for the development of specific therapeutic agents.* Pharmacol Ther, 2006. **109**(3): p. 366-98.
168. Zhang, K.Y., et al., *A glutamine switch mechanism for nucleotide selectivity by phosphodiesterases.* Mol Cell, 2004. **15**(2): p. 279-86.
169. Lincoln, T. M Cyclic GMP: Biochemistry, Physiology and Pathophysiology. Landes, Austin: 1994.
170. Geary, C.A., et al., *Role of CNP in human airways: cGMP-mediated stimulation of ciliary beat frequency.* Am J Physiol, 1995. **268**(6 Pt 1): p. L1021-8.
171. Kiemer, A.K., T. Hartung, and A.M. Vollmar, *cGMP-mediated inhibition of TNF-alpha production by the atrial natriuretic peptide in murine macrophages.* J Immunol, 2000. **165**(1): p. 175-81.
172. Niedbala, W., et al., *Nitric oxide preferentially induces type 1 T cell differentiation by selectively up-regulating IL-12 receptor beta 2 expression via cGMP.* Proc Natl Acad Sci U S A, 2002. **99**(25): p. 16186-91.
173. Ebrey, T. and Y. Koutalos, *Vertebrate photoreceptors.* Prog Retin Eye Res, 2001. **20**(1): p. 49-94.
174. Corbin, J. D., J. Kotera, V. K. Gopal, R. H. Cote and S. H. Francis: Regulation of cyclic nucleotide levels by sequestration. In: Handbook of Cell Signaling. Eds: R. Bradshaw and E. Dennis, 453-457 (2003)
175. Sager, G., *Cyclic GMP transporters.* Neurochem Int, 2004. **45**(6): p. 865-73.
176. Takio, K., et al., *Guanosine cyclic 3',5'-phosphate dependent protein kinase, a chimeric protein homologous with two separate protein families.* Biochemistry, 1984. **23**(18): p. 4207-18.
177. Walter, U., *Physiological role of cGMP and cGMP-dependent protein kinase in the cardiovascular system.* Rev Physiol Biochem Pharmacol, 1989. **113**: p. 41-88.
178. Wong, S.K. and D.L. Garbers, *Receptor guanylyl cyclases.* J Clin Invest, 1992. **90**(2): p. 299-305.
179. Torphy, T.J., *Phosphodiesterase isozymes: molecular targets for novel antiasthma agents.* Am J Respir Crit Care Med, 1998. **157**(2): p. 351-70.
180. Martins, T.J., M.C. Mumby, and J.A. Beavo, *Purification and characterization of a cyclic GMP-stimulated cyclic nucleotide phosphodiesterase from bovine tissues.* J Biol Chem, 1982. **257**(4): p. 1973-9.
181. Yamazaki, A., et al., *Cyclic GMP-specific, high affinity, noncatalytic binding sites on light-activated phosphodiesterase.* J Biol Chem, 1980. **255**(23): p. 11619-24.
182. Gillespie, P.G. and J.A. Beavo, *Characterization of a bovine cone photoreceptor phosphodiesterase purified by cyclic GMP-sepharose chromatography.* J Biol Chem, 1988. **263**(17): p. 8133-41.
183. Francis, S.H., T.M. Lincoln, and J.D. Corbin, *Characterization of a novel cGMP binding protein from rat lung.* J Biol Chem, 1980. **255**(2): p. 620-6.

184. Hamet, P. and J.F. Coquil, *Cyclic GMP binding and cyclic GMP phosphodiesterase in rat platelets.* J Cyclic Nucleotide Res, 1978. **4**(4): p. 281-90.
185. Aravind, L. and C.P. Ponting, *The GAF domain: an evolutionary link between diverse phototransducing proteins.* Trends Biochem Sci, 1997. **22**(12): p. 458-9.
186. Francis, S.H., et al., *Phosphorylation of isolated human phosphodiesterase-5 regulatory domain induces an apparent conformational change and increases cGMP binding affinity.* J Biol Chem, 2002. **277**(49): p. 47581-7.
187. Martinez, S.E., et al., *The two GAF domains in phosphodiesterase 2A have distinct roles in dimerization and in cGMP binding.* Proc Natl Acad Sci U S A, 2002. **99**(20): p. 13260-5.
188. Fawcett, L., et al., *Molecular cloning and characterization of a distinct human phosphodiesterase gene family: PDE11A.* Proc Natl Acad Sci U S A, 2000. **97**(7): p. 3702-7.
189. Soderling, S.H., S.J. Bayuga, and J.A. Beavo, *Isolation and characterization of a dual-substrate phosphodiesterase gene family: PDE10A.* Proc Natl Acad Sci U S A, 1999. **96**(12): p. 7071-6.
190. Yuasa, K., et al., *Isolation and characterization of two novel phosphodiesterase PDE11A variants showing unique structure and tissue-specific expression.* J Biol Chem, 2000. **275**(40): p. 31469-79.
191. Erneux, C., et al., *Specificity of cyclic GMP activation of a multi-substrate cyclic nucleotide phosphodiesterase from rat liver.* Eur J Biochem, 1981. **115**(3): p. 503-10.
192. Moss, J., V.C. Manganiello, and M. Vaughan, *Substrate and effector specificity of a guanosine 3':5'-monophosphate phosphodiesterase from rat liver.* J Biol Chem, 1977. **252**(15): p. 5211-5.
193. Wada, H., J.C. Osborne, Jr., and V.C. Manganiello, *Effects of pH on allosteric and catalytic properties of the guanosine cyclic 3',5'-phosphate stimulated cyclic nucleotide phosphodiesterase from calf liver.* Biochemistry, 1987. **26**(20): p. 6565-70.
194. Yamamoto, T., V.C. Manganiello, and M. Vaughan, *Purification and characterization of cyclic GMP-stimulated cyclic nucleotide phosphodiesterase from calf liver. Effects of divalent cations on activity.* J Biol Chem, 1983. **258**(20): p. 12526-33.
195. Okada, D. and S. Asakawa, *Allosteric activation of cGMP-specific, cGMP-binding phosphodiesterase (PDE5) by cGMP.* Biochemistry, 2002. **41**(30): p. 9672-9.
196. Rybalkin, S.D., et al., *PDE5 is converted to an activated state upon cGMP binding to the GAF A domain.* EMBO J, 2003. **22**(3): p. 469-78.
197. Corbin, J.D., et al., *Phosphorylation of phosphodiesterase-5 by cyclic nucleotide-dependent protein kinase alters its catalytic and allosteric cGMP-binding activities.* Eur J Biochem, 2000. **267**(9): p. 2760-7.
198. D'Amours, M.R. and R.H. Cote, *Regulation of photoreceptor phosphodiesterase catalysis by its non-catalytic cGMP-binding sites.* Biochem J, 1999. **340 (Pt 3)**: p. 863-9.
199. Yamazaki, A., et al., *Interactions between the subunits of transducin and cyclic GMP phosphodiesterase in Rana catesbiana rod photoreceptors.* J Biol Chem, 1990. **265**(20): p. 11539-48.
200. Cote, R.H., M.D. Bownds, and V.Y. Arshavsky, *cGMP binding sites on photoreceptor phosphodiesterase: role in feedback regulation of visual transduction.* Proc Natl Acad Sci U S A, 1994. **91**(11): p. 4845-9.

201. Norton, A.W., et al., *Mechanism of transducin activation of frog rod photoreceptor phosphodiesterase. Allosteric interactiona between the inhibitory gamma subunit and the noncatalytic cGMP-binding sites.* J Biol Chem, 2000. **275**(49): p. 38611-9.
202. Conti, M., *Phosphodiesterases and cyclic nucleotide signaling in endocrine cells.* Mol Endocrinol, 2000. **14**(9): p. 1317-27.
203. Stacey, P., et al., *Molecular cloning and expression of human cGMP-binding cGMP-specific phosphodiesterase (PDE5).* Biochem Biophys Res Commun, 1998. **247**(2): p. 249-54.
204. Francis, S.H. and J.D. Corbin, *Purification of cGMP-binding protein phosphodiesterase from rat lung.* Methods Enzymol, 1988. **159**: p. 722-9.
205. Thomas, M.K., S.H. Francis, and J.D. Corbin, *Characterization of a purified bovine lung cGMP-binding cGMP phosphodiesterase.* J Biol Chem, 1990. **265**(25): p. 14964-70.
206. Farrow, K.N., et al., *Hyperoxia increases phosphodiesterase 5 expression and activity in ovine fetal pulmonary artery smooth muscle cells.* Circ Res, 2008. **102**(2): p. 226-33.
207. Pauvert, O., et al., *Characterisation of cyclic nucleotide phosphodiesterase isoforms in the media layer of the main pulmonary artery.* Biochem Pharmacol, 2002. **63**(9): p. 1763-72.
208. Dent, G., et al., *Cyclic nucleotide phosphodiesterase in human bronchial epithelial cells: characterization of isoenzymes and functional effects of PDE inhibitors.* Pulm Pharmacol Ther, 1998. **11**(1): p. 47-56.
209. Toward, T.J., N. Smith, and K.J. Broadley, *Effect of phosphodiesterase-5 inhibitor, sildenafil (Viagra), in animal models of airways disease.* Am J Respir Crit Care Med, 2004. **169**(2): p. 227-34.
210. Soderling, S.H., S.J. Bayuga, and J.A. Beavo, *Identification and characterization of a novel family of cyclic nucleotide phosphodiesterases.* J Biol Chem, 1998. **273**(25): p. 15553-8.
211. Cote, R.H., *Characteristics of photoreceptor PDE (PDE6): similarities and differences to PDE5.* Int J Impot Res, 2004. **16 Suppl 1**: p. S28-33.
212. Baehr, W., M.J. Devlin, and M.L. Applebury, *Isolation and characterization of cGMP phosphodiesterase from bovine rod outer segments.* J Biol Chem, 1979. **254**(22): p. 11669-77.
213. Deterre, P., et al., *cGMP phosphodiesterase of retinal rods is regulated by two inhibitory subunits.* Proc Natl Acad Sci U S A, 1988. **85**(8): p. 2424-8.
214. Norton, A.W., et al., *Evaluation of the 17-kDa prenyl-binding protein as a regulatory protein for phototransduction in retinal photoreceptors.* J Biol Chem, 2005. **280**(2): p. 1248-56.
215. Ridge, K.D., et al., *Phototransduction: crystal clear.* Trends Biochem Sci, 2003. **28**(9): p. 479-87.
216. Muradov, H., K.K. Boyd, and N.O. Artemyev, *Analysis of PDE6 function using chimeric PDE5/6 catalytic domains.* Vision Res, 2006. **46**(6-7): p. 860-8.
217. Muradov, K.G., A.E. Granovsky, and N.O. Artemyev, *Mutation in rod PDE6 linked to congenital stationary night blindness impairs the enzyme inhibition by its gamma-subunit.* Biochemistry, 2003. **42**(11): p. 3305-10.
218. Stockman, A., et al., *The effect of sildenafil citrate (Viagra) on visual sensitivity.* J Vis, 2007. **7**(8): p. 4.
219. Arshavsky, V.Y., T.D. Lamb, and E.N. Pugh, Jr., *G proteins and phototransduction.* Annu Rev Physiol, 2002. **64**: p. 153-87.

220. Wang, H., Y. Lee, and C.C. Malbon, *PDE6 is an effector for the Wnt/Ca2+/cGMP-signalling pathway in development.* Biochem Soc Trans, 2004. **32**(Pt 5): p. 792-6.
221. Nancy, V., et al., *The delta subunit of retinal rod cGMP phosphodiesterase regulates the membrane association of Ras and Rap GTPases.* J Biol Chem, 2002. **277**(17): p. 15076-84.
222. Ionita, M.A. and S.J. Pittler, *Focus on molecules: rod cGMP phosphodiesterase type 6.* Exp Eye Res, 2007. **84**(1): p. 1-2.
223. Florio, S.K., R.K. Prusti, and J.A. Beavo, *Solubilization of membrane-bound rod phosphodiesterase by the rod phosphodiesterase recombinant delta subunit.* J Biol Chem, 1996. **271**(39): p. 24036-47.
224. Li, N., et al., *Characterization of human and mouse rod cGMP phosphodiesterase delta subunit (PDE6D) and chromosomal localization of the human gene.* Genomics, 1998. **49**(1): p. 76-82.
225. Lorenz, B., et al., *Cloning and gene structure of the rod cGMP phosphodiesterase delta subunit gene (PDED) in man and mouse.* Eur J Hum Genet, 1998. **6**(3): p. 283-90.
226. Zhang, H., et al., *Assay and functional properties of PrBP(PDEdelta), a prenyl-binding protein interacting with multiple partners.* Methods Enzymol, 2005. **403**: p. 42-56.
227. Hanzal-Bayer, M., et al., *The complex of Arl2-GTP and PDE delta: from structure to function.* EMBO J, 2002. **21**(9): p. 2095-106.
228. Van Valkenburgh, H., et al., *ADP-ribosylation factors (ARFs) and ARF-like 1 (ARL1) have both specific and shared effectors: characterizing ARL1-binding proteins.* J Biol Chem, 2001. **276**(25): p. 22826-37.
229. Marzesco, A.M., et al., *The rod cGMP phosphodiesterase delta subunit dissociates the small GTPase Rab13 from membranes.* J Biol Chem, 1998. **273**(35): p. 22340-5.
230. Wilson, S.J. and E.M. Smyth, *Internalization and recycling of the human prostacyclin receptor is modulated through its isoprenylation-dependent interaction with the delta subunit of cGMP phosphodiesterase 6.* J Biol Chem, 2006. **281**(17): p. 11780-6.
231. Madden, B.P., et al., *A potential role for sildenafil in the management of pulmonary hypertension in patients with parenchymal lung disease.* Vascul Pharmacol, 2006. **44**(5): p. 372-6.
232. Fang, X., et al., *Contribution of CFTR to apical-basolateral fluid transport in cultured human alveolar epithelial type II cells.* Am J Physiol Lung Cell Mol Physiol, 2006. **290**(2): p. L242-9.
233. Dent, G., H. Magnussen, and K.F. Rabe, *Cyclic nucleotide phosphodiesterases in the human lung.* Lung, 1994. **172**(3): p. 129-46.
234. Martina, S.D., M.S. Ismail, and K.S. Vesta, *Cilomilast: orally active selective phosphodiesterase-4 inhibitor for treatment of chronic obstructive pulmonary disease.* Ann Pharmacother, 2006. **40**(10): p. 1822-8.
235. Pullamsetti, S., et al., *Inhaled tolafentrine reverses pulmonary vascular remodeling via inhibition of smooth muscle cell migration.* Respir Res, 2005. **6**: p. 128.
236. Morin, F., et al., *Expression and role of phosphodiesterase 6 in the chicken pineal gland.* J Neurochem, 2001. **78**(1): p. 88-99.
237. Ahumada, A., et al., *Signaling of rat Frizzled-2 through phosphodiesterase and cyclic GMP.* Science, 2002. **298**(5600): p. 2006-10.
238. Kuenzi, F., et al., *Hippocampal synaptic plasticity in mice carrying the rd mutation in the gene encoding cGMP phosphodiesterase type 6 (PDE6).* Brain Res, 2003. **967**(1-2): p. 144-51.

239. Taylor, R.E., et al., *A PDE6A promoter fragment directs transcription predominantly in the photoreceptor.* Biochem Biophys Res Commun, 2001. **282**(2): p. 543-7.
240. Piriev, N.I., et al., *Rod photoreceptor cGMP-phosphodiesterase: analysis of alpha and beta subunits expressed in human kidney cells.* Proc Natl Acad Sci U S A, 1993. **90**(20): p. 9340-4.
241. Tate, R.J., V.Y. Arshavsky, and N.J. Pyne, *The identification of the inhibitory gamma-subunits of the type 6 retinal cyclic guanosine monophosphate phosphodiesterase in non-retinal tissues: differential processing of mRNA transcripts.* Genomics, 2002. **79**(4): p. 582-6.
242. Ballard, S.A., et al., *Effects of sildenafil on the relaxation of human corpus cavernosum tissue in vitro and on the activities of cyclic nucleotide phosphodiesterase isozymes.* J Urol, 1998. **159**(6): p. 2164-71.
243. Murray, F., M.R. MacLean, and N.J. Pyne, *An assessment of the role of the inhibitory gamma subunit of the retinal cyclic GMP phosphodiesterase and its effect on the p42/p44 mitogen-activated protein kinase pathway in animal and cellular models of pulmonary hypertension.* Br J Pharmacol, 2003. **138**(7): p. 1313-9.
244. Wan, K.F., et al., *The inhibitory gamma subunit of the type 6 retinal cyclic guanosine monophosphate phosphodiesterase is a novel intermediate regulating p42/p44 mitogen-activated protein kinase signaling in human embryonic kidney 293 cells.* J Biol Chem, 2001. **276**(41): p. 37802-8.
245. Wan, K.F., et al., *The inhibitory gamma subunit of the type 6 retinal cGMP phosphodiesterase functions to link c-Src and G-protein-coupled receptor kinase 2 in a signaling unit that regulates p42/p44 mitogen-activated protein kinase by epidermal growth factor.* J Biol Chem, 2003. **278**(20): p. 18658-63.
246. Frame, M., et al., *The gamma subunit of the rod photoreceptor cGMP phosphodiesterase can modulate the proteolysis of two cGMP binding cGMP-specific phosphodiesterases (PDE6 and PDE5) by caspase-3.* Cell Signal, 2001. **13**(10): p. 735-41.
247. Ma, L. and H.Y. Wang, *Mitogen-activated protein kinase p38 regulates the Wnt/cyclic GMP/Ca2+ non-canonical pathway.* J Biol Chem, 2007. **282**(39): p. 28980-90.
248. Brown, R.L. and L. Stryer, *Expression in bacteria of functional inhibitory subunit of retinal rod cGMP phosphodiesterase.* Proc Natl Acad Sci U S A, 1989. **86**(13): p. 4922-6.
249. Piriev, N.I., et al., *Expression of cone photoreceptor cGMP-phosphodiesterase alpha' subunit in Chinese hamster ovary, 293 human embryonic kidney, and Y79 retinoblastoma cells.* Mol Vis, 2003. **9**: p. 80-6.
250. Qin, N. and W. Baehr, *Expression of mouse rod photoreceptor cGMP phosphodiesterase gamma subunit in bacteria.* FEBS Lett, 1993. **321**(1): p. 6-10.
251. Qin, N. and W. Baehr, *Expression and mutagenesis of mouse rod photoreceptor cGMP phosphodiesterase.* J Biol Chem, 1994. **269**(5): p. 3265-71.
252. Qin, N., S.J. Pittler, and W. Baehr, *In vitro isoprenylation and membrane association of mouse rod photoreceptor cGMP phosphodiesterase alpha and beta subunits expressed in bacteria.* J Biol Chem, 1992. **267**(12): p. 8458-63.
253. Stroop, S.D., H. Charbonneau, and J.A. Beavo, *Direct photolabeling of the cGMP-stimulated cyclic nucleotide phosphodiesterase.* J Biol Chem, 1989. **264**(23): p. 13718-25.
254. Hurwitz, R.L., et al., *cGMP phosphodiesterase in rod and cone outer segments of the retina.* J Biol Chem, 1985. **260**(1): p. 568-73.

255. Dryja, T.P., et al., *Frequency of mutations in the gene encoding the alpha subunit of rod cGMP-phosphodiesterase in autosomal recessive retinitis pigmentosa.* Invest Ophthalmol Vis Sci, 1999. **40**(8): p. 1859-65.
256. Lipkin, V.M., et al., *Beta-subunit of bovine rod photoreceptor cGMP phosphodiesterase. Comparison with the phosphodiesterase family.* J Biol Chem, 1990. **265**(22): p. 12955-9.
257. Zhang, F.L. and P.J. Casey, *Protein prenylation: molecular mechanisms and functional consequences.* Annu Rev Biochem, 1996. **65**: p. 241-69.
258. Chiu, T., C. Santiskulvong, and E. Rozengurt, *ANG II stimulates PKC-dependent ERK activation, DNA synthesis, and cell division in intestinal epithelial cells.* Am J Physiol Gastrointest Liver Physiol, 2003. **285**(1): p. G1-11.
259. Hecquet, C., et al., *Activation and role of MAP kinase-dependent pathways in retinal pigment epithelial cells: ERK and RPE cell proliferation.* Invest Ophthalmol Vis Sci, 2002. **43**(9): p. 3091-8.
260. Kuemmerle, J.F., *IGF-I elicits growth of human intestinal smooth muscle cells by activation of PI3K, PDK-1, and p70S6 kinase.* Am J Physiol Gastrointest Liver Physiol, 2003. **284**(3): p. G411-22.
261. Thrane, E.V., et al., *Persistent versus transient map kinase (ERK) activation in the proliferation of lung epithelial type 2 cells.* Exp Lung Res, 2001. **27**(4): p. 387-400.
262. Sanchez-Esteban, J., et al., *Mechanical stretch induces fetal type II cell differentiation via an epidermal growth factor receptor-extracellular-regulated protein kinase signaling pathway.* Am J Respir Cell Mol Biol, 2004. **30**(1): p. 76-83.
263. Chen, D., et al., *Osmotic shock inhibits insulin signaling by maintaining Akt/protein kinase B in an inactive dephosphorylated state.* Mol Cell Biol, 1999. **19**(7): p. 4684-94.
264. Wang, D. and H.S. Sul, *Insulin stimulation of the fatty acid synthase promoter is mediated by the phosphatidylinositol 3-kinase pathway. Involvement of protein kinase B/Akt.* J Biol Chem, 1998. **273**(39): p. 25420-6.
265. Lu, Y., et al., *Activated Akt protects the lung from oxidant-induced injury and delays death of mice.* J Exp Med, 2001. **193**(4): p. 545-49.
266. Zhang, H., et al., *Deletion of PrBP/delta impedes transport of GRK1 and PDE6 catalytic subunits to photoreceptor outer segments.* Proc Natl Acad Sci U S A, 2007. **104**(21): p. 8857-62.
267. Cook, T.A., et al., *The delta subunit of type 6 phosphodiesterase reduces light-induced cGMP hydrolysis in rod outer segments.* J Biol Chem, 2001. **276**(7): p. 5248-55.
268. Laties, A. and E. Zrenner, *Viagra (sildenafil citrate) and ophthalmology.* Prog Retin Eye Res, 2002. **21**(5): p. 485-506.
269. Pentia, D.C., et al., *Purification of PDE6 isozymes from mammalian retina.* Methods Mol Biol, 2005. **307**: p. 125-40.
270. Usuki, J. and Y. Fukuda, *Evolution of three patterns of intra-alveolar fibrosis produced by bleomycin in rats.* Pathol Int, 1995. **45**(8): p. 552-64.
271. Chua, F., J. Gauldie, and G.J. Laurent, *Pulmonary fibrosis: searching for model answers.* Am J Respir Cell Mol Biol, 2005. **33**(1): p. 9-13.
272. Gillespie, P.G. and J.A. Beavo, *Inhibition and stimulation of photoreceptor phosphodiesterases by dipyridamole and M&B 22,948.* Mol Pharmacol, 1989. **36**(5): p. 773-81.

273. Turko, I.V., et al., *Inhibition of cyclic GMP-binding cyclic GMP-specific phosphodiesterase (Type 5) by sildenafil and related compounds.* Mol Pharmacol, 1999. **56**(1): p. 124-30.
274. Gresser, U. and C.H. Gleiter, *Erectile dysfunction: comparison of efficacy and side effects of the PDE-5 inhibitors sildenafil, vardenafil and tadalafil--review of the literature.* Eur J Med Res, 2002. **7**(10): p. 435-46.
275. Zhang, X., Q. Feng, and R.H. Cote, *Efficacy and selectivity of phosphodiesterase-targeted drugs in inhibiting photoreceptor phosphodiesterase (PDE6) in retinal photoreceptors.* Invest Ophthalmol Vis Sci, 2005. **46**(9): p. 3060-6.
276. Behn, D. and M.J. Potter, *Sildenafil-mediated reduction in retinal function in heterozygous mice lacking the gamma-subunit of phosphodiesterase.* Invest Ophthalmol Vis Sci, 2001. **42**(2): p. 523-7.
277. Foresta, C., et al., *Expression of the PDE5 enzyme on human retinal tissue: new aspects of PDE5 inhibitors ocular side effects.* Eye, 2008. **22**(1): p. 144-9.
278. Corbin, J.D., et al., *High lung PDE5: a strong basis for treating pulmonary hypertension with PDE5 inhibitors.* Biochem Biophys Res Commun, 2005. **334**(3): p. 930-8.
279. Wharton, J., et al., *Antiproliferative effects of phosphodiesterase type 5 inhibition in human pulmonary artery cells.* Am J Respir Crit Care Med, 2005. **172**(1): p. 105-13.
280. McAllister-Lucas, L.M., et al., *The structure of a bovine lung cGMP-binding, cGMP-specific phosphodiesterase deduced from a cDNA clone.* J Biol Chem, 1993. **268**(30): p. 22863-73.
281. Beltman, J., et al., *Characterization of cyclic nucleotide phosphodiesterases with cyclic GMP analogs: topology of the catalytic domains.* Mol Pharmacol, 1995. **47**(2): p. 330-9.
282. Francis, S.H., et al., *Zinc interactions and conserved motifs of the cGMP-binding cGMP-specific phosphodiesterase suggest that it is a zinc hydrolase.* J Biol Chem, 1994. **269**(36): p. 22477-80.
283. He, F., et al., *Multiple zinc binding sites in retinal rod cGMP phosphodiesterase, PDE6alpha beta.* J Biol Chem, 2000. **275**(27): p. 20572-7.
284. Lochhead, A., et al., *The regulation of the cGMP-binding cGMP phosphodiesterase by proteins that are immunologically related to gamma subunit of the photoreceptor cGMP phosphodiesterase.* J Biol Chem, 1997. **272**(29): p. 18397-403.
285. Tate, R.J., et al., *The gamma-subunit of the rod photoreceptor cGMP-binding cGMP-specific PDE is expressed in mouse lung.* Cell Biochem Biophys, 1998. **29**(1-2): p. 133-44.
286. Martinez, S.E., J.A. Beavo, and W.G. Hol, *GAF domains: two-billion-year-old molecular switches that bind cyclic nucleotides.* Mol Interv, 2002. **2**(5): p. 317-23.
287. Pittler, S.J. and W. Baehr, *Identification of a nonsense mutation in the rod photoreceptor cGMP phosphodiesterase beta-subunit gene of the rd mouse.* Proc Natl Acad Sci U S A, 1991. **88**(19): p. 8322-6.
288. Bowes, C., et al., *Localization of a retroviral element within the rd gene coding for the beta subunit of cGMP phosphodiesterase.* Proc Natl Acad Sci U S A, 1993. **90**(7): p. 2955-9.
289. Wimer, R.E., et al., *The mouse gene retinal degeneration (rd) may reduce the number of neurons present in the adult hippocampal dentate gyrus.* Brain Res, 1991. **547**(2): p. 275-8.

290. Pittler, S.J., et al., *Functional analysis of the rod photoreceptor cGMP phosphodiesterase alpha-subunit gene promoter: Nrl and Crx are required for full transcriptional activity.* J Biol Chem, 2004. **279**(19): p. 19800-7.
291. Lerner, L.E., et al., *Nrl and Sp nuclear proteins mediate transcription of rod-specific cGMP-phosphodiesterase beta-subunit gene: involvement of multiple response elements.* J Biol Chem, 2001. **276**(37): p. 34999-5007.
292. Lerner, L.E., et al., *The rod cGMP-phosphodiesterase beta-subunit promoter is a specific target for Sp4 and is not activated by other Sp proteins or CRX.* J Biol Chem, 2002. **277**(29): p. 25877-83.
293. Mears, A.J., et al., *Nrl is required for rod photoreceptor development.* Nat Genet, 2001. **29**(4): p. 447-52.
294. Daniele, L.L., et al., *Cone-like morphological, molecular, and electrophysiological features of the photoreceptors of the Nrl knockout mouse.* Invest Ophthalmol Vis Sci, 2005. **46**(6): p. 2156-67.
295. Anant, J.S., et al., *In vivo differential prenylation of retinal cyclic GMP phosphodiesterase catalytic subunits.* J Biol Chem, 1992. **267**(2): p. 687-90.
296. Paglia, M.J., H. Mou, and R.H. Cote, *Regulation of photoreceptor phosphodiesterase (PDE6) by phosphorylation of its inhibitory gamma subunit re-evaluated.* J Biol Chem, 2002. **277**(7): p. 5017-23.
297. Schermuly, R.T., et al., *Reversal of experimental pulmonary hypertension by PDGF inhibition.* J Clin Invest, 2005. **115**(10): p. 2811-21.
298. Weissmann, N., et al., *Hypoxia-induced pulmonary hypertension: different impact of iloprost, sildenafil, and nitric oxide.* Respir Med, 2007. **101**(10): p. 2125-32.
299. Fellrath, J.M. and R.M. du Bois, *Idiopathic pulmonary fibrosis/cryptogenic fibrosing alveolitis.* Clin Exp Med, 2003. **3**(2): p. 65-83.
300. Maher, T.M., A.U. Wells, and G.J. Laurent, *Idiopathic pulmonary fibrosis: multiple causes and multiple mechanisms?* Eur Respir J, 2007. **30**(5): p. 835-9.
301. Bender, A.T. and J.A. Beavo, *Cyclic nucleotide phosphodiesterases: molecular regulation to clinical use.* Pharmacol Rev, 2006. **58**(3): p. 488-520.
302. Omori, K. and J. Kotera, *Overview of PDEs and their regulation.* Circ Res, 2007. **100**(3): p. 309-27.
303. Shuman, S., *Recombination mediated by vaccinia virus DNA topoisomerase I in Escherichia coli is sequence specific.* Proc Natl Acad Sci U S A, 1991. **88**(22): p. 10104-8.
304. Shuman, S., *Novel approach to molecular cloning and polynucleotide synthesis using vaccinia DNA topoisomerase.* J Biol Chem, 1994. **269**(51): p. 32678-84.